Examination of Cadmium-Induced Heat Shock Protein Gene Expression in *Xenopus laevis* A6 Kidney Epithelial Cells

by

Jessica Woolfson

A thesis
presented to the University of Waterloo
in fulfillment of the
thesis requirement for the degree of
Master of Science
in
Biology

Waterloo, Ontario, Canada, 2008

Author's Declaration Page

I hereby declare that I am the sole author of this thesis. This is a true copy of the thesis, including any required final revisions, as accepted by my examiners.

I understand that my thesis may be made electronically available to the public.

Abstract

Cadmium is a highly toxic chemical and has been classified by the International Agency for Research on Cancer as a human carcinogen. Cadmium is abundant in the environment, at specific work places, and in food and water. Toxicological responses to cadmium exposure include respiratory diseases, neurological disorders and kidney damage. The present study examined the effects of cadmium on heat shock protein (HSP) accumulation in *Xenopus laevis* A6 kidney epithelial cells. HSPs are molecular chaperones involved in protein folding and translocation. In response to environmental stress these proteins bind to unfolded protein and inhibit their aggregation. Stress-inducible *hsp* gene transcription is mediated by the heat shock promoter element (HSE), which interacts with heat shock transcription factor (HSF). In the present study, *hsp30* and *hsp70* mRNA and protein were induced by heat shock, as determined by northern and western blot analysis. Exposure of A6 cells to cadmium chloride also induced the expression of *hsp* genes. For example, northern and western blot analysis revealed that exposure of A6 cells to cadmium chloride induced the accumulation of *hsp30* and *hsp70* mRNA and their respective proteins. Western blot analysis also revealed that A6 cells recovering from a cadmium chloride treatment retained relatively high levels of HSP30 and HSP70 protein accumulation over 24 h after the removal of the stress. Treatments combining a mild heat shock and cadmium chloride resulted in a synergistic increase in *hsp30* and *hsp70* gene expression at mRNA and protein levels. Further experiments in which two stressors were combined revealed that synergistic effects occurred with varying cadmium concentrations and different temperatures. Immunocytochemistry and confocal microscopy were used to confirm the results attained from western blot analysis. Further, this technique allowed the determination of intracellular localization of HSP30 in A6 cells and the examination of cellular morphology and

cytoskeletal structure during cadmium chloride treatments. A 2 h heat shock at 33ºC resulted in the accumulation of HSP30 in the cytoplasm, whereas a 2 h heat shock at 35ºC resulted in some HSP30 accumulation in the peripheral region of the nucleus. This is in contrast to cells treated with cadmium chloride, where HSP30 accumulation was restricted to the cytoplasm. A 14 h 50 μM cadmium chloride treatment resulted in the accumulation of HSP30 in approximately 10% of cells. The proportion of cells displaying HSP30 accumulation increased to 80% and 95% in cells treated with 100 μM and 200 μM, respectively. HSP30 accumulation frequently occurred in large granular structures. High concentrations of cadmium chloride resulted in cell membrane ruffling at areas of cell-cell contact, as well as actin disorganization. This study characterized the pattern of *hsp* gene expression, accumulation and localization under various cadmium chloride conditions. These results suggest that *hsp30* and *hsp70* gene expression can be used as potential biomolecular markers for cadmium exposure.

Acknowledgements

What a long, strange trip it's been. First and foremost I want to thank my supervisor Dr. John Heikkila for giving me this opportunity. I came into this Masters with no previous background in molecular biology and John has been patient, understanding and incredibly informative. His relaxed supervisory approach and accommodating nature has made him a pleasure to work for. I have learned so much in the past two years and I am grateful for all that he has taught me. I'd like to thank my committee members, Dr. Bernie Duncker and Dr. Heidi Engelhardt, for their time and helpful advice and feedback. I'd especially like to thank Dale Weber for coming to my rescue nearly every time I used the confocal microscope. His assistance and permanent positive demeanour were always appreciated. Most importantly I want to thank my labmates Julie Gauley, Janine Voyer, Jordan Young and Shantel Walcott for their friendship and constant entertainment. Thank you for helping me maintain my sanity and making my Masters an enjoyable experience. I will always remember and cherish the good times I had at Club Heikkila. Finally, I want to thank my friends and family for their unwavering unconditional love and encouragement.

I dedicate this work to Makoto Kawano for always trying to save the world. I'm sorry so many trees had to die for this thesis.

Table of Contents

List of Figures

1 Introduction

Organisms are equipped with mechanisms to cope with changes in their external and internal environment, to enable adaptation and survival. Stress causes modifications in the pattern of gene expression, specifically resulting in the increased expression of selected genes. These genes include those that encode stress inducible proteins known as the heat shock proteins (HSPs).

1.1 Heat Shock Proteins

Ferruccio Ritossa was the first to report that a transient increase in temperature activates the expression of HSPs as a cellular protective response in *Drosophila* in 1962 (Ritossa, 1962). Since then a number of different HSP families have been discovered and characterized in a variety of organisms. HSPs are highly conserved, which suggests they play a crucial role in cellular processes (Kregel, 2002). They are also ubiquitous and have been found in all organisms, from bacteria and yeast to humans. HSPs are categorized into families by their molecular weight and function. These families include the small heat shock proteins (sHSPs), HSP40, HSP60, HSP70, HSP90 and HSP110. Some HSPs are constitutively expressed, whereas others are stress-inducible. HSPs serve as molecular chaperones by binding to denatured proteins and aiding in their refolding to the native functional states (Palleros *et al.*, 1991; Wang and Spector 2000). They also prevent the aggregation of other proteins during stress and assist in the degradation of damaged proteins (Fernando and Heikkila, 2000; Abdulle *et al.*, 2002).

1.2 The Heat Shock Response

The term "heat shock response" is somewhat misleading, since the expression of HSPs has been documented as a result of exposure to a number of different stressors other than heat shock. Environmental stress conditions include heat, cold, heavy metals, oxidants, dehydration and toxic agents including sodium arsenite, ethanol and hydrogen peroxide (Darasch *et al.*, 1988; Nowack *et al.*, 1990; Muller *et al.*, 2004; Gauley and Heikkila, 2006). HSPs are also induced by pathophysiological states, such as aging, infections, and hypoxia (Ciocca *et al.*, 1993; Giffard *et al.*, 2004; Njemini *et al.*, 2007). Exposure to stress causes proteins to denature, misfold or unfold. The unfolding of proteins exposes hydrophobic areas, leading to aggregation. The heat shock response is therefore essential to maintain proper protein structure and thus cellular function.

The mechanism by which a cell detects stress is unclear; however, it is thought that the presence of non-native or misfolded proteins triggers the heat shock response. *Hsp* genes were activated when denatured proteins were injected into frog oocytes (Ananthan *et al.*, 1986). Inducible HSP expression is regulated by heat shock transcription factors (HSF). There are several members of the HSF family that have been found in vertebrates. HSF1 is the functional vertebrate homologue of the HSF found in yeast and is activated by a number of different stressors (Rabindran *et al.*, 1991; Sarge *et al.*, 1993). HSF2 is not activated in response to stress, but rather in response to developmental conditions (Schuetz *et al.*, 1991; Goodson *et al.*, 1995). HSF3 is a unique avian HSF, which has been shown to respond to heat (Nakai *et al.*, 1995), and HSF4 is functionally distinct and exhibits tissue-specific expression (Nakai *et al.*, 1997). HSF1 is highly conserved and is regulated both at the level of DNA binding and the level of transcriptional activation (Newton *et al.*, 1996; Pirrkala *et al.,* 2001). HSF1 preexists in unstressed cells as inactive monomers either in the cytosol or nucleus, where it is unable to bind

DNA (Mercier *et al.*, 1990; Sarge *et al.*, 1993; Shi *et al.*, 1998). This suppression is partially regulated by hydrophobic sequences within HSF1 itself, as well as by the constitutively expressed heat shock cognate 70 (HSC70), HSP70 and HSP90 (Ali *et al.*, 1998; Bharadwaj *et al.*, 1998; Farkas *et al.*, 1998; Voellmy, 2004). These chaperones have been shown to have a role in maintaining HSF1 in its inert state; however, it has yet to be confirmed how these interactions maintain this monomeric repression (Morimoto, 1998). The HSP90-containing complex may interact with hydrophobic repeat regions or sequence elements at the N-terminal, but not with the regulatory domain of monomeric HSF1 (Voellmy, 2004). It has been suggested that during stress, proteins become denatured and HSP70 and HSP90 are recruited to other areas of the cell for their chaperone abilities. This relieves the repression of the HSF1 monomers allowing them to form an active trimer (Morimoto, 1998; Zou *et al.*, 1998). Activation of HSF1 results in the relocalization of HSF1 into the nucleus where it is able to bind to a regulatory DNA motif known as the heat shock element (HSE), which is located in the 5' promoter region of *hsp* genes (Ovsenek and Heikkila, 1990; Gordon et al, 1997; Morimoto, 1998). Phosphorylation occurs on serine and threonine residues, and transcription of HSPs is facilitated by RNA polymerase II, resulting in the accumulation of HSPs (Sarge *et al.*, 1993; Ali *et al.*, 1998; Morimoto, 1998). HSP70, which has been shown to directly interact with the HSF1 activation domain, functions as a negative regulator (Shi *et al.*, 1998). Elevated synthesis and accumulation of HSP70 leads to the binding of HSP70 to the HSF1 activation domain, and results in the repression of further heat shock-induced transcription. Shi and colleagues (1998) indicated that HSP70 chaperone function is required for direct binding to HSF1. During attenuation of the heat shock response, the transcriptional activity of HSF1 is repressed by the direct binding of HSP70, Hdj-1 and HSF binding protein 1 (HSBP1) (Satyal *et al.*, 1998; Shi *et al.*, 1998). This causes the HSF1 trimer to

dissociate into the inactive HSF1 monomers. Attenuation also occurs if cells are heated for an extended period, resulting in the loss of HSF1's DNA-binding and transcriptional properties (Bharadwaj *et al.*, 1998).

1.3 *Hsp* Gene Regulation

HSPs are expressed in a characteristic pattern of induction and repression that depends on the cell type, development stage and intensity and duration of stress (Heikkila *et al.*, 1987a; Darasch *et al.*, 1988; Lang *et al.*, 1999; Lang *et al.*, 2000). *Hsp* genes are temporarily inducible as well as subjected to developmental regulation (Bienz, 1984b). Inducible genes are triggered in response to stress, which activates HSF1 and results in the transcription of *hsp* genes. Regulation of *hsp* gene expression occurs primarily at the transcriptional level, with mediation occurring at the levels of mRNA synthesis and stability (Bienz, 1984; Lindquist 1986). However, expression is controlled at multiple levels, which also includes translational efficiency (Kim and Jang, 2002). *Hsp* message is preferentially translated by a cell under stress, while synthesis of other proteins may be repressed (Schlesinger, 1990; Ovelgönne *et al.*, 1995). Messenger RNAs from heat shock genes have structures that allow for their selective translation, including a lack of introns, and regions conferring translational efficiency and increased stability (Schlesinger, 1990). HSP expression is autoregulated, such that high levels of HSPs inhibit further expression (Shi *et al.*, 1998). Some *hsp* genes are constitutively activated or can be in a repressed state, likely due to changes in chromatin structure (Bienz 1984a; Heikkila, 2004). Development can also regulate gene specific transcription factors (Bienz 1984b).

1.4 Small Heat Shock Proteins

1.4.1 Structure of sHSPs

Small heat shock proteins (sHSPs) range in size from 12 to 43 kDa and include α-crystallin (Wistow, 1985; MacRae, 2000). Structural homology between family members is quite low compared to other HSP families (Singh *et al.*, 1996; Ganea, 2001). sHSPs share a conserved region of 80-100 amino acids at the C-terminal region, also known as the α-crystallin domain (MacRae, 2000; Ganea, 2001). The α-crystallin domain is highly conserved between species and consists of β-pleated sheet conformation. It plays a role in binding unfolded proteins during stress as well as potentially binding nucleotides and cytoskeletal proteins (Djabali *et al.*, 1997; Singh *et al.*, 2006). This region is flanked by an N-terminal hydrophobic region and a short, flexible C-terminal extension (Singh *et al.*, 1996; Haslbeck, 2002). The N-terminal domain of sHSPs is poorly conserved, with the exception of a conserved WDPF sequence, which contains two α-helices and may play a role in oligomeric formation (Lambert, 1999; Ganea , 2001). C-terminal extensions are variable in sequence and length, but are common in polar properties between sHSPs and are essential for chaperone functions (MacRae, 2000; Fernando and Heikkila, 2000). sHSPs also contain hydrophobic sites, which have been proposed to play a role in the binding of target proteins during stress (Smulders and de Jong, 1997; Kundu *et al.*, 2007). A common feature of sHSPs is their organization into large oligomeric structures. These globular complexes are believed to be crucial for their regulation and chaperone function (Leroux *et al.*, 1997; Ehrnsperger *et al.*, 1997; Ehrnsperger *et al.*, 1999). During development and after the removal of stress, sHSPs are phosphorylated. This causes a change in secondary structure and oligomers to down-size, thereby limiting chaperone action of sHSPs (Lambert *et al.*, 1999; Fernando *et al.*, 2003).

1.4.2 Expression of sHSPs

Expression of sHSPs depends on development, cell type, growth cycle and oncogenic status of the cell, as well as the type, duration and intensity of stimuli (Welch *et al.*, 1985; Haslbeck, 2002). sHSPs accumulate in different organs and tissues, and levels vary in a stage-, tissue- and stress-specific manner (Ciocca *et al.*, 1993). For example, Hsp25 is most abundant in lens, heart, stomach, colon, lung and bladder in rodents (Klemenz *et al.*, 1993), whereas Hsp27 is detected in muscle, nervous, connective tissue and female reproductive tract in human (Ciocca *et al.*, 1983). Developmental or tissue-specific controls in gene expression may be regulated at the level of chromatin structure or organization (Heikkila, 2004). Intracellular localization of sHSPs changes according to the physiological state of the cells and to the type and intensity of the stressor (Beaulieu *et al.,* 1989; Adhikari *et al.,* 2004; Gellalchew and Heikkila, 2005; Manwell and Heikkila, 2007). Expression of the sHSPs, Hsp27 and α-crystallin, increase in various types of cancer and overexpression of sHSPs have been observed in several neurodegenerative disorders (Hitotsumatsu *et al.*, 1996; Renkawek *et al.*, 1999; Wilhelmus *et al.*, 2006). The variable distribution of the sHSPs demonstrates that they are a group of dynamic proteins, which are able to form large aggregates or complexes.

1.4.3 Function of sHSPs

sHSPs have diverse roles, including chaperone capabilities and protecting cells from stress. sHSPs form complexes with unfolded proteins and stabilize these proteins under stress conditions, thereby suppressing aggregation of denatured proteins (Ehrnsperger *et al.*, 1997; Leroux *et al.*, 1997). To date, chaperone activity of sHSPs have been found to be independent of ATP binding and hydrolysis (Haslbeck, 2002). sHSP monomers oligomerize as a prerequisite for

chaperone function and functional efficiency depends on sHSPs ability to bind protein substrates (Bova *et al.*, 1999). The sHSPs are effective chaperones since they are able to selectively bind non-native proteins in large quantities per oligomeric sHSP complex (Haslbeck, 2002). sHSPs bind denatured proteins and hold them in a folding-competent state until normal conditions are restored (Haslbeck, 2002). In *Xenopus*, HSP30 is phosphorylated once the stress has been removed, directing the release of HSP30 from denatured proteins, thus playing a role in the cellular recovery from stress (Fernando *et al.*, 2003). sHSPs also cooperate with other HSPs, such as HSP70 in presence of ATP to refold proteins into their native states (Ehrnsperger *et al.*, 1997). *Xenopus* HSP30 has been shown to function as a molecular chaperone by inhibiting heat-induced aggregation of citrate synthase *in vitro* (Fernando and Heikkila, 2000). Studies indicate that the carboxyl region is required to inhibit stress induced aggregation and to maintain secondary structure for chaperone function (Fernando and Heikkila, 2000; Fernando *et al.*, 2002). Mutations in α-crystallin impair flexibility and decrease chaperone function and are also associated with congenital cataracts and cardiovascular disease (Lentze *et al.*, 2003; Wang *et al.*, 2003; Singh *et al.*, 2006; Kundu *et al.*, 2007).

sHSPs also have a number of other roles, which include stabilizing actin filaments, maintaining the integrity of the cytoskeleton and preserving mitochondrial membrane potential (Djabali *et al.*, 1997; Préville *et al.*, 1999). sHSPs have also been implicated in actin capping and decapping, cellular differentiation, prevention of apoptosis and the acquisition of thermotolerance (Phang *et al.*, 1999; Arrigo, 2000; Haslbeck, 2002). Over-expression of *Xenopus* HSP30 in *E. coli* cells conferred greater survival at increased temperatures (Fernando and Heikkila, 2000). sHSP expression and phosphorylation may also be involved in cellular signal transduction (Ciocca *et al.*, 1993; Fernando *et al.*, 2003).

1.5 Heat Shock Protein 70

1.5.1 Structure of HSP70

The 70-kDa heat shock protein family is extremely well conserved in different species (Bienz, 1984a; Heikkila et al, 1997). Functional properties are conserved, although HSP70 is synthesized in response to varying stimuli (Darasch *et al.*, 1988; Briant *et al.*, 1997; Ali *et al.*, 1997; Hallare *et al.*, 2005). HSP70 is highly inducible and is synthesized in response to multiple stressors, HSC70 is constitutively produced (Yu *et al.*, 1994; Ali *et al.*, 1996a). The HSP70 gene consists of 2440 base pairs and contains at least two regulatory elements in the 5` region that interact with HSF1 (Wu *et al.*, 1986). HSP70 proteins display highly conserved amino acid sequences and domain structures. The HSP70 molecule is composed of an ATP-binding domain at the N-terminal end, plus a region with protease sensitive sites (Daugaard *et al.,* 2007; Goloubinoff and De Los Rios, 2007). At the C-terminal end there is a peptide binding domain, which contains an EEVD-motif enabling HSP70 binding to co-chaperones and other HSPs (Freeman *et al.*, 1995). The substrate-binding site has a high affinity for polypeptides with a hydrophobic core, and binds a seven-residue peptide between β-sheet and α-helical subdomains (Rüdiger *et al.*, 1997). A notable member of the HSP70 is Grp78 or immunoglobulin-binding protein (BiP), which contains a highly conserved endoplasmic reticulum (ER) retention signal (the KDEL sequence) at the C-terminal end (Munro and Pelham, 1986; 1987).

1.5.2 Expression of HSP70

Like other members of the HSP family, HSP70 is regulated at the transcriptional, post-transcriptional and translational levels (Ali *et al.*, 1997). Although production of HSP70 protein usually depends on the synthesis and accumulation of *hsp70* mRNA (Heikkila *et al.*, 1985),

message accumulation doesn't always result in an increase in protein production (Bruce *et al.*, 1993). *Hsp70* gene expression is dependent on the stage of development and displays tissue-specific patterns of accumulation (Heikkila *et al.*, 1985; 1987; Ali *et al.*, 1997). In *Xenopus laevis, Hsp70* mRNA is absent in oocytes and is not heat inducible until gastrulation (Bienz, 1984; Heikkila *et al.*, 1985; Davis and King, 1989). It is also localized to specific tissues during stress. For example, exposure of *Xenopus laevis* to hyperthermic conditions resulted in *hsp70* mRNA and protein accumulation in the heart at lower temperatures than in muscle, spleen, eye or liver (Ali *et al.*, 1997). Tissue-specific expression may be caused by varying sensitivity to stress than what is present in other tissues and differences in the relative levels of *hsp70* mRNA between tissues may be reflective of their specialized cell environment (Ali *et al.*, 1997; Heikkila *et al.*, 1997). HSP70 proteins are also expressed in a cell type and cell cycle dependent manner during normal conditions (Daugaard *et al.*, 2007). Like any cell modulator, expression of HSP70 needs to be tightly regulated, since over-expression of the protein can be problematic. HSP70 has been found to be abundantly expressed in malignant tumours (Jäättelä, 1995; Vargas-Roig *et al.*,1998; Kregel, 2002).

1.5.3 Function of HSP70

The main role of HSP70 is to control protein quality and regulate protein structures within the cell. These functions vary between stress-inducible HSP70 and constitutively expressed family members. The main roles of stress-inducible HSP70 are to prevent aggregation and to catalyze the refolding of unfolded proteins (Freeman and Morimoto, 1996; Nollen and Morimoto, 2002). HSP70 binds and releases extended sections of hydrophobic amino acids exposed by incorrectly folded proteins, in an ATP-dependent manner (Freeman and Morimoto,

1996; Freeman *et al.*, 1995). Stress-inducible HSP70 thereby functions as a chaperone, which allows cells to cope with potentially detrimental aggregations of denatured proteins during stress. HSP70 is induced by a number of different stressors, including heat, hypoxia, reactive oxygen species and toxic compounds (Darasch *et al.*, 1988; Giffard *et al.*, 2004; Han *et al.*, 2007). The expression of inducible HSP70 has been shown to enhance the survival of cells exposed to heat, although the mechanism is unclear (Heikkila *et al.*, 1985; Phang *et al.*, 1999). Thermotolerance has been shown to correlate with the synthesis of HSP70 and is associated with a high survival rate in *Xenopus* embryos (Heikkila *et al.*, 1985). The loss of thermotolerance, usually occurring several days after the heat stress, is associated with increased HSP70 degradation (Heikkila *et al.*, 1985; Phang *et al.*, 1999). The induction of HSP70 is also correlated with acquired thermotolerance to other stressors, such as UV radiation, acidosis and energy depletion (Weitzel *et al.*, 1985; Barbe *et al.*, 1988; Samelman, 2000).

HSP70 has roles in controlling physiological processes in the cell, which include vesicular trafficking, differentiation and signalling for growth (Goloubinoff and De Los Rios, 2007). HSP70 has also been reported to play a role in preventing cell death, by interacting with factors that inhibit caspase-dependent apoptosis (Mosser *et al.*, 1997). Under non-stressed conditions, specific HSP70s have roles in the import of cytoplasmic proteins into the mitochondria or ER. BiP, for example, facilitates the transport of newly synthesized proteins into the ER lumen and plays a role in their subsequent folding (Zimmerman *et al.*, 2006). Cytosolic HSP70 may interact with growing polypeptide chains as they emerge from the ribosome to assist its exit and prevent aggregation (Beckmann *et al.*, 1990; Georgopoulos and Welch, 1993). Further housekeeping roles of HSP70 include protein translocation, degradation of unstable

proteins, control of regulatory proteins, prevention of aggregation and disassembly of clathrin-coated vesicles (Daugaard *et al.,* 2007).

1.6 *Xenopus laevis* as a Model Organism

The South African clawed frog, *Xenopus laevis*, represents an excellent model to evaluate amphibian development on account of its rapid and well characterized development. Their eggs are easily obtainable in large quantities and can be fertilized *in vitro*. The large size of oocytes and eggs make them suitable for microinjection studies (Heikkila, 1990). *Xenopus laevis* is relatively inexpensive and easily maintained in the laboratory. They are also a valuable bioindicator for environmental studies and have been used often as an investigation tool. Studies have used *Xenopus* to evaluate reproductive and developmental toxicity (Sunderman *et al.*, 1991; Herkovits *et al.,* 1998; Lienesch *et al.*, 2000; Mouchet *et al.*, 2006; Mouchet *et al.*, 2007).

A *Xenopus laevis* A6 kidney epithelial cultured cell line was derived from the renal uriniferous tubules of adult male *Xenopus* (Rafferty, 1969). This cell line is well established, with logarithmic growth until the culture is confluent (Rafferty, 1969). *Hsp* gene expression has been examined in *Xenopus laevis* A6 cells and embryos during development, and to a variety of stressors (Darasch *et al.*, 1988; Lang *et al.*, 1999; Heikkila 2003; Heikkila 2004).

1.6.1 HSP30 in *Xenopus laevis*

To date, sixteen HSP30 polypeptides have been detected in *Xenopus laevis* and five *Xenopus hsp30* genes (A-E) have been cloned and sequenced (Darasch *et al.*, 1988; Krone *et al.*, 1992; Tam and Heikkila, 1995; Heikkila *et al.*, 1997; Ohan *et al.,* 1998a). *Hsp30*A contains an insertion in the coding region and *hsp30*B appears to be a pseudogene, and therefore both are not

representative of the *hsp30* gene family (Bienz, 1984a). *Hsp30*C has a high level of sequence similarity with previously published *hsp30* DNA, compared to the *hsp30*D gene. Both *hsp30C* and *hsp30D* are intronless genes that encode 24-kDa proteins (Heikkila *et al.,* 1997). In contrast, only a portion of the *hsp30*E gene has been isolated (Krone *et al.,* 1992). *Hsp30C* genes are developmentally regulated in *Xenopus* embryos. *Hsp30C* mRNA is not detectable in heat shocked oocytes (Davis and King, 1989), but is detected in relatively low levels at the late blastula stage (Ohan and Heikkila, 1995). Heat shock-induced accumulation of *hsp30C* mRNA and protein was first observed in early and midtailbud embryos, with enrichment in certain tissues (Lang *et al.*, 1999). *Hsp30C* mRNA is constitutively expressed in the cement gland of early and midtailbud stage embryos, possibly to prevent apoptosis (Lang *et al.,* 1999; Heikkila, 2003). HSP30C protein synthesis was not detectable in early embryonic stages, but was heat-inducible from the late tailbud stage (Tam and Heikkila, 1995). *Hsp30* mRNA and HSP30 protein are not constitutively expressed in *Xenopus laevis* cultured cells, although they are induced by heat shock, sodium arsenite, herbimycin A and hydrogen peroxide (Darasch *et al.*, 1988; Briant *et al.*, 1997; Muller *et al.,* 2004).

HSP30 proteins form high molecular weight complexes that are capable of acting as molecular chaperones in *Xenopus* A6 kidney epithelial cells (Ohan *et al.,* 1998b). HSP30 exists as multimeric complexes with molecular mass of 350-510 kDa consisting of monomers of approximately 24 kDa (Ohan *et al.*, 1998b; Ganea *et al.,* 2001). It also forms aggregates that combine upon heat shock to produce much larger structures known as heat shock granules (Ohan *et al.,* 1998b). HSP30C in *Xenopus* holds other proteins in a folding-competent state to protect them from aggregating (Abdulle *et al.*, 2002). HSP30C inhibits heat-induced aggregation of citrate synthase and luciferase (Fernando and Heikkila, 2000; Abdulle *et al.,* 2002). The

chaperone capability of HSP30C is dependent on the C-terminal end (Fernando and Heikkila, 2000; Abdulle *et al.*, 2002). Current models suggest that sHSPs bind and hold misfolded proteins so that other HSPs, such as HSP70, can refold them in an ATP-dependent manner (Abdulle *et al.*, 2002). Phosphorylation has been found to occur following removal of heat stress, during the period when cells recover from damage (Fernando *et al.,* 2003). Phosphorylation has been shown to compromise the ability of HSP30C to prevent stress-induced aggregation of citrate synthase or luciferase in vitro, by resulting in protein structural changes. This ultimately destabilizes HSP30C multimeric complexes, leading to a decrease in HSP30C affinity for target protein binding and a subsequent loss of chaperone functions (Fernando *et al.,* 2003).

1.6.2 HSP70 in *Xenopus laevis*

Hsp70 genes (A-D) have been isolated and sequenced in *Xenopus laevis* (Heikkila *et al.*, 1997). These genes are intronless and share a high level of similarity with *Drosophila hsp70* at the mRNA and protein level. They also contain the HSE in the 5' region, as well as a TATA and CCAAT box (Heikkila *et al.*, 1997). Two *Hsc70* cDNA clones have also been isolated and sequenced in *Xenopus* (Ali *et al.*, 1996a; 1996b) The *hsc* gene contains an ATP-binding domain, which is conserved between rat *hsc70*, and a more divergent carboxyl region (Ali *et al.*, 1996a). Both *hsp70* and *hsc70* contain the EEVD motif and a putative nuclear localization signal, which likely plays a role in translocation into the nucleus (Ali et al., 1996a; Heikkila *et al.*, 1997).

Hsp70 mRNA is first detected in heat shocked embryos during the postblastula stages (Heikkila *et al.*, 1987a; Lang *et al.*, 2000). Accumulation increases in a development-dependent manner to the midtailbud stage, then decreases at the late tailbud stage (Lang *et al.*, 2000). Heat shock also results in preferential enrichment of *hsp70* mRNA in certain tissues, such as the heart,

somites, cement gland, spinal cord and proctodeum in heat shocked tailbud embryos (Lang *et al.*, 2000). Tissue-specific enhancement is detected following heat shock, and other stressors, such as zinc chloride and sodium arsenite, can also induce a similar *hsp70* mRNA response (Lang *et al.*, 2000). *Hsc70* mRNA, on the other hand, is not enhanced via heat shock and is detected constitutively in embryos, with levels increasing in the later stages of development (Ali *et al.*, 1996a; Lang *et al.*, 2000). Basal levels of *hsc70* mRNA are high in adult frog spleen and testis and moderate in the eye, heart, liver and brain (Ali *et al.*, 1996a). BiP was detected constitutively in *Xenopus* unfertilized eggs, cleavage and blastula stage embryos. Heat shock enhanced BiP accumulation at the gastrula stage, with relative levels higher in selective tissues (Miskovic and Heikkila, 1999).

Hsp70 mRNA and protein are also stress inducible in the *Xenopus* A6 kidney epithelial cells. Treatments of elevated temperature, sodium arsenite, herbimycin A, hydrogen peroxide and ethanol resulted in enhanced accumulation of *hsp70* mRNA and protein (Darasch *et al.*, 1988; Briant *et al.*, 1997; Muller *et al.*, 2004; Gauley and Heikkila, 2006). *Hsp70* mRNA and HSP70 protein accumulation increased in *Xenopus* adult heart tissue following a mild hyperthermia (Ali *et al.*, 1997).

1.7 Cadmium

Cadmium is a teratogenic and carcinogenic that occurs naturally in the environment and is also released anthropogenically (Vogiatzis and Loumbourdis, 1997; Waalkes et al., 1999; Fang et al., 2002). It is an industrial and environmental pollutant that exerts a large number of adverse effects on ecosystems and organism health (Mouchet *et al.*, 2007). It is extracted during the production of other metals and emitted during the burning of fossil fuels (Cao *et al.*, 2007;

Mendez-Armenta and Rios, 2007). Cadmium is used in metal plating, mining, ceramics and the production of chemical stabilizers (Martins *et al.*, 2004). It is persistent in the environment, has no biological role and is not an essential metal (Jin *et al.*, 1998). Cadmium exposure can occur through contaminated food or water, polluted air or inhalation of tobacco smoke (Waisberg *et al.*, 2003). Cadmium accumulates in the major organs, but primarily in the kidney, liver and reproductive tissues, such as the gonads and uterus (Lohiya, 1976; Vogiatzis and Loumbourdis, 1997; Barbier *et al.*, 2004; Mouchet *et al.*, 2006). It has been shown that cadmium contamination of freshwater can exert a number of negative acute and chronic effects, which include renal impairment, cellular damage and apoptosis (Uriu *et al.*, 2000; Audry *et al.*, 2004; Agnello *et al.*, 2007; Mouchet *et al.*, 2007).

1.7.1 Effect of Cadmium on Cells

Heavy metals can enter the cell by active ion transport or diffusion (Faurskov and Bjerregaard, 2002). In aquatic organisms, cadmium can enter dermally via skin and gills, or can be passed onto progeny during reproduction (Pederson and Bjerregaard, 2000; Fort *et al.*, 2001). Uptake has been shown to be concentration-dependent due to an increase in active transepithelial ion transport (Bjerregaard, 2007). Cadmium exposure produces reactive oxygen species (ROS) and results in the formation of denatured or abnormal proteins (Waisberg *et al.*, 2003; Wätjen and Beyersmann, 2004). Cellular damage, such as DNA adducts, DNA strand breaks, chromosomal aberrations and the presence of micronuclei also occur following cadmium exposure (Mouchet *et al.*, 2007). The relative amount of DNA damage is dependent on both the concentration of cadmium and the length of exposure (Mouchet *et al.*, 2007). Cadmium not only induces DNA damage, but also interferes with DNA repair processes and enhances genotoxicity

(Mendez-Armenta and Rios, 2007). Additionally, cadmium exposure also affects cellular calcium homeostasis and calcium-mediated functions in kidney cells by increasing intracellular calcium (Faurskov and Bjerregaard, 2002; Bjerregaard, 2007). Changes in cell morphology are also observed, including an alteration of cell shape, a loss of cell-cell attachment and monolayer integrity, as well as disruption of actin filament distribution when treated with cadmium (Bonham *et al.*, 2003; Bjerregaard, 2007).

1.7.2 Impact of Cadmium on Gene Expression

Like other stressors, cadmium alters the expression of cellular genes in response to chemical-induced changes (Othumpangat *et al.*, 2005). Cadmium modulates cellular signal transduction pathways by enhancing protein phosphorylation and activating transcriptional and translational factors (Waisberg *et al.*, 2003). In particular, cadmium affects the regulation of the expression of genes involved in stress response, apoptosis, signal transduction and carcinogenesis (Cao *et al.*, 2006; Liu *et al.*, 2006). Cadmium triggers stress responses in various signalling cascades and by modifying transcription factor activity to deregulate gene expression (Cao *et al.*, 2006; Xie and Shaikh, 2006). This includes the upregulation of stress response genes that encode for metallothioneins (MT), anti-oxidant defences and HSP expression (Bonham *et al.*, 1993; Liu *et al.*, 2006; Mouchet *et al.*, 2006). MTs sequester and detoxify heavy metals, thereby limiting the genotoxic effects of cadmium on the cell (Mouchet *et al.*, 2006). MTs are detected in renal epithelial cells in cells treated with cadmium, and are predominantly regulated at the transcriptional level (Choudhuri *et al.*, 1993; Bonham *et al.*, 2003). Cadmium also effects expression of genes regulating translation (Cao *et al.*, 2006). For example, elongation initiation

factor 4E (eIF4E), a rate-limiting factor required for translation, is a cellular target for cadmium (Yokouchi *et al.*, 2007).

1.7.3 Effect of Cadmium on Organism

Cadmium is toxic to organisms, especially in larvae and during early stages of development (Herkovits *et al.*, 1998; Mouchet *et al.*, 2007). Lethal concentrations of cadmium can cause immediate death, whereas sublethal concentrations may increase the risk of DNA damage and vulnerability to predation or unsuccessful fertilization (Mouchet *et al.*, 2007). Histological and histochemical alterations occur in the livers and kidneys of frogs exposed to cadmium (Loumbourdis , 2005). Cadmium exposure also affects oocyte development and all stages of oogenesis in *Xenopus* (Lienesch *et al.*, 2000). It affects embryo viability and results in malformations, including visceral edema, skeletal kinking of the notochord, craniofacial defects, ruptured pigmented retina. Further, cadmium exposure leads to a loss of weight, ovary health, sperm count and fertilization rates in adult frogs (Lienesch *et al.*, 2000; Fort *et al.*, 2001). Both reproductive and developmental toxicity is transgenerational and can be passed on to progeny (Fort *et al.*, 2001). Cadmium has also been shown to result in greater toxicity, via cardiac and head edema, in a dose-dependent way when aggravated by extreme temperatures in zebrafish (Hallare *et al.*, 2005).

1.8 Objectives

Cadmium chloride has been shown to induce *hsp70* and *hsp110* accumulation in *Xenopus laevis* A6 cells when treated with 200 μM for 5 h (Gauley and Heikkila, 2006). However, the effect of cadmium on *hsp* gene expression has yet to be fully characterized in this species or cell line. The objectives for this study were as follows:

- To determine the patterns of cadmium chloride-induced *hsp30* and *hsp70* gene expression in *Xenopus laevis* A6 kidney epithelial cells.
- To examine the effects of recovery from cadmium chloride exposure on the accumulation of HSP30 and HSP70 protein.
- To examine the combined effect of cadmium exposure with a mild heat shock on the *hsp30* and *hsp70* mRNA and their respective proteins in *Xenopus laevis* A6 cells.
- To monitor the cadmium-induced accumulation and intracellular localization of HSP30 in *Xenopus laevis* A6 cells using laser scanning confocal microscopy.
- To examine the effects of cadmium chloride on cell morphology and cytoskeleton organization in *Xenopus laevis* A6 cells.

2 Experimental Procedures

2.1 *Xenopus laevis* A6 Cell Treatments

Xenopus laevis A6 kidney epithelial cells were acquired from American Type Culture Collection (ATCC; Rockville, Maryland). A6 cells were cultured in 55% (w/v) Leibovitz (L)-15 media (Sigma; Oakville, Ontario) supplemented with 10% (v/v) fetal bovine serum (100 U/ml) (Sigma) and 1% penicillin/streptomycin (100 µg/ml) (Sigma) and grown at 22˚C in T75 cm^2 flasks. When cells were confluent, they were washed with 2 ml of versene [0.02% (w/v) KCl, 0.8% (w/v) NaCl, 0.02% (w/v) KH_2PO_4, 0.115% (w/v) Na_2HPO_4, 0.02% (w/v) sodium ethlenediaminetetraacetic acid (Na_2EDTA), pH 7.2] for 2 min and then treated with 0.5 ml of 1X trypsin (Sigma) in 100% Hank's balanced salt solution (HBSS; Sigma) until cells began to detach. Non-adherent cells were re-suspended in fresh media and aliquoted evenly into additional culture flasks. Cell treatments were performed once cells reached 90-100% confluence, with a minimum of 48 h between cell splitting and experimentation.

Cadmium chloride treatments of A6 cells were performed at 22˚C using dilutions from a 100 mM cadmium chloride stock solution made from 99.99% pure cadmium chloride (Sigma). Flasks of A6 cells were subjected to heat stress using a temperature regulated water bath (VWR; Cornelius, Oregon). Following treatment, cells were washed using 2 ml of 65% HBSS, with a subsequent addition of 1 ml 100% HBSS. Cells were harvested using a rubber scraper and transferred to 1.5 ml microcentrifuge tubes. Cells were pelleted in an Eppendorf 5415D microcentrifuge (Brinkmann Instruments Ltd; Mississauga, Ontario) for 1 min at 13,200 rpm. The supernatant was removed and cells were stored at -80˚C until protein or RNA isolation.

2.2 Production of *hsp* Antisense Riboprobes

2.2.1 *Hsp30C* Template Generation

The entire open reading frame of the *hsp30C* gene was previously inserted into a pRSET expression vector (Invitrogen; Carlsbad, California) in our laboratory (Fernando and Heikkila, 2000). Plasmids were transformed into *Escherichia coli* DH5α cells. Colonies were used to inoculate bacteria in 5 ml LB broth [1% w/v tryptone-peptone, 0.5% (w/v) yeast extract, 1% (w/v) NaCl, pH 7.5] supplemented with 100 μg/ml ampicillin (Bioshop; Burlington, Ontario) in 15 mL Falcon tubes. Cells were grown overnight in a shaker waterbath at 37˚C for 14-16 h.

2.2.2 *Hsp70* Template Generation

The coding region of *hsp70* genomic DNA was previously isolated (Lang *et al.*, 2000) and inserted into the plasmid pSP72 (Promega; Napean, Ontario). Plasmids containing the *hsp70* insert were inoculated into 15 mL Falcon tubes and grown overnight in 5 mL of LB broth, containing 100 μg/ml ampicillin (Bioshop) at 37˚C.

2.2.3 Isolation of Plasmid DNA

Cells were centrifuged at 5,000 rpm for 5 min at 4 ºC in an Eppendorf Centrifuge 5810R (Brinkmann Instruments Ltd) in a swinging-bucket rotor. Pelleted cells were resuspended in 200 μl of ice-cold alkaline lysis solution I [50 mM glucose, 25 mM Tris (pH 8.0), 10mM EDTA (pH 8.0)], vortexed and transferred to a microcentrifuge tube. Cells were then lysed with 200 μl frehsly prepared alkaline lysis solution II [0.2 N NaOh, 1% (w/v) SDS], mixed via inversion and stored on ice. Next, 200 μl of ice-cold alakline lysis solution III [3M potassium acetate, 5 M glacial acetic acid) was added and dispersed through the bacterial lysate by inverting the tube

several times. Samples were then stored on ice for 5 min. Samples were then centrifuged at 14,000 rpm for 5 min at 4 ˚C and supernatants were transferred to fresh tubes. RNase A (µg/mL; Bioshop) was added and samples were incubated at 37 ˚C for 1 h to digest any remaining RNA. A solution of 600 µl phenol and chlorofrom (1:1) was added, vortexed for 30 sec and centrifuged at 14,000 rpm for 3 min at 4 ˚C. The top layer was removed and transferred to a fresh tube. A 600 µl solution of chloroform and isoamyl alcohol (25:1) was added, mixed via vortexing for 30 sec and then centrifuged at 14,000 rpm for 3 min at 4 ˚C. The supernatant was transferred to a fresh tube and nucleic acids were precipitated by adding 600 µl of ice-cold isopropanol. The solution was mixed by vortexing and allowed to stand at room temperature for 2 min. The precipitated nucleic acids were collected by centrifugation at 13,200 rpm at room temperature. The supernatant was removed, 1 ml of cold, filtered 70% (v/v) ethanol was added and DNA was recovered by centrifugation at 13,200 rpm for 2 min at room temperature. The supernatant was removed and the tube was opened and stored at room temperature for 5 min until the ethanol had evaporated. The nucleic acid was dissolved in 50 µl MilliQ water, quantified using a NanoDrop ND-1000 UV-Vis Spectrophotometer (NanoDrop Technologies) and stored at –20 ˚C. Gel electrophoreses [1% agarose (Bioshop), 1X tris-acetate EDTA buffer (TAE, Millipore; Bedford, Massachusetts), 1 µl ethidium bromide (Sigma)] was performed, using 1X TAE running buffer, to ensure plasmid DNA was recovered. 2 µg of plasmid DNA, supplemented with 2 µl 6X loading dye (MBI Fermentas; Burlington, Ontario) was run with a 1 kB ladder (MBI Fermentas).

2.2.4 Restriction Enzyme Digestion

Restriction enzyme *Pvu*II or *Mlu*NI (10 U/µl; Roche Molecular Biochemicals; Mississauga, Ontario) with buffer M or buffer A (Roche Molecular Biochemicals), for *hsp30* and

hsp70, respectively, were added to 40 µl plasmid DNA and incubated for 2 h at 37 ˚C. The cut plasmid sample (50 µl) was run on a 1% agarose gel [1X TAE, 1 µl ethidium bromide] for 1 h at 100 V. A UV lamp was used to visualize the band of interest, which was cut out using a razor blade.

2.2.5 Extraction of DNA from Agarose Gel

DNA was extracted using a Montage DNA Gel Extraction Kit (Millipore). The gel slice was placed in a Montage gel nebulizer and centrifuged for 10 min at 5,000 x g. The purified DNA was then precipitated by adding 1/10 volume of 3M sodium acetate (pH 5.2) and 2.5x 100% cold, filtered ethanol. The sample was stored at –20 ˚C for 30 min and then centrifuged at 14,000 rpm for 5 min at 4 ˚C. The supernatant was removed and 1 ml of 70% cold, filtered ethanol was added to the pellet. The sample was centrifuged at 14,000 rpm for 5 min at 4 ˚C and the supernatant was removed. Another 1 ml of 70% ethanol was added and the sample was centrifuged again at 14,000 rpm for 5 min at 4 ˚C. The supernatant was removed and the pellet was resuspended in 12 µl diethyl pyrocarbonate-treated (DEPC; Sigma) water.

2.2.6 *In Vitro* Transcription

In vitro transcription was used to synthesize a digoxigenin (DIG)-labelled riboprobe. Ingredients were brought to room temperature (except for RNA polymerase and RNA inhibitors) and mixed in a microcentrifuge tube in the following order: 4 µl DIG-rNTPs [10 µM rCTP, 10 µM rGTP, 10 µM rATP, 10 µM rUTP (Promega), 10 µM DIG-11 UTP (Roche Molecular Biochemicals)], 5.5 µl of linearized DNA template, 4 µl 100 mM dithiothreitol (DTT) (final 20 mM; Promega), 0.5 µl RNase inhibitor (MBI Fermentas), 4 µl 5 X transcription buffer (final 1X;

MBI Fermentas) and 2 µl SP6 RNA polymerase (MBI Fermentas). Transcription reactions were incubated for 2 h at 37 ˚C followed by the addition of 1 µl of RNase-free DNase I (Roche Molecular Biochemicals) for 10 min at 37 ˚C to digest any remaining DNA template. Then, 1 µl was removed for analysis by electrophoresis to determine transcript integrity. Transcripts were precipitated from the remainder of the sample with 10 µl 3M sodium acetate (pH 5.2), 80 µl TES [10 mM Tris-Hcl (pH 7.4), 5 mM EDTA (pH 8.0), 1% (w/v) SDS] and 220 µl of ice-cold, 100% filtered ethanol. The sample was mixed via vortexing and incubated at –80 ˚C for 30 min. After precipitation, transcribed riboprobes were pelleted by centrifugation at 14,000 rpm for 10 min at 4 ˚C. The supernatant was removed and the pelleted riboprobe was re-suspended in 20 µl DEPC-treated water and stored at –80 ˚C until use for northern hybridization analysis.

2.3 RNA Isolation and Northern Hybridization

2.3.1 RNA Isolation from A6 Cells

RNA was isolated from A6 cells using the QIAGEN RNeasy Mini Kit (QIAGEN; Mississauga, Ontario) according to the manufacturers protocol in RNeasy Mini Handbook (3rd edition, 2001). Pelleted cells stored at –80 ˚C were lysed with 600 µl Buffer RLT containing 1% (v/v) β-mercaptoethanol, vortexed and homogenized by 5 passages of the lysate through a 20 ½ inch-gauge needle, fitted to a sterile syring. An equal volume of 70 % cold, filtered ethanol was added to the homogenized lysate and mixed via pipetting. Samples were applied in 600 µl aliquots to RNeasy mini columns held in 2 ml collection tubes and centrifuged at 13,200 rpm for 15 sec in an Eppendorf 5415 D microcentrifuge (Brinkmann Instruments Ltd). The flow through was discarded and 700 µl of Buffer RW1 was added to the RNeasy column, followed by a 15 sec 13,200 rpm centrifugation. The RNeasy column was transferred to a new 2 ml collection tube

and 500 µl Buffer RPE was added to the columns, and centrifuged for 15 sec at 13,200 rpm. The eluent was discarded and another 500 µl Buffer RPE was added and centrifuged for 2 min at 13,200 rpm. The RNeasy column was then transferred to a new 1.5 ml Eppendorf tubes. RNA was eluted by two 30 µl aliquots of DEPC-treated water, followed by centrifugation at 13,200 rpm for 1 min each. RNA was stored at –80 ˚C.

2.3.2 RNA Quantification

RNA samples were quantified using a NanoDrop ND-1000 UV-Vis Spectrophotometer (NanoDrop Technologies). RNA quantity was measured three times and the average was taken. RNA integrity was assessed by electrophoresis of 2 µg samples on a 1.2% (w/v) formaldehyde/agarose gel [1.2% (w/v) agarose (Bioshop), 10% (v/v) 10X MOPS (0.2 M 3-morpholino propane sulfonic acid, pH 7.0 (Bioshop)); 3 M sodium acetate, pH 5.2, 0.5M EDTA, pH 8.0 and 16% (v/v) formaldehyde]. RNA samples were denatured for 10 min at 68 ˚C in solution of 1 µl 10X MOPS, 1.6 µl formaldehyde (Bioshop), 5 µl formamide (EMD Biosciences; Gibbston, New Jersey) 2 µl 10X loading dye [0.2% (w/v) bromophenol blue, 1 mM EDTA (pH 8.0) and 50% (v/v) glycerol] and 1 µl ethidium bromide. Samples were cooled on ice for 5 min, loaded onto a 1.2% formaldehyde agarose gel and electrophoresed at 90 V for 1 h to confirm RNA quality and equal loading.

2.3.3 Northern Hybridization

Gel electrophoresis was performed using 10 µg of isolated RNA in a 1.2% formaldehyde agarose gel, as described above, with the exception that ethidium bromide was not included in the loading buffer (Sambrook and Russell 2001). The gel was electrophoresed for 3 h at 70 V

and then soaked in 0.05 NaOH for 20 min to ensure RNA denaturation. Gels were rinsed with DEPC-treated water then soaked twice for 20 min each in 20X SSC [3M sodium chloride, 300 mM sodium citrate (pH 7.0)].

RNA was transferred overnight by capillary action onto a positively charged nylon membrane (Roche Molecular Biochemicals). For transfer, gels were inverted onto Whatman filter paper (VWR International; West Chester, Pennsylvania) wick, presoaked in 20X SSC, set on a Plexiglass support over a Pyrex® dish filled with 500 ml 20X SSC. Nylon membrane was laid directly on top of the gel and covered with two pieces of presoaked filter paper and a 4 inch stack of cut paper towels and approximately 500 g of weight. After transfer RNA was crosslinked to the membrane using a UV Crosslinker (UltraLum Inc; Claremont, California) at 12,000 microJ/CM^2.

Equal loading and the success of the transfer was determined by staining the membrane with 1X Blot Stain Blue Reversible Northern Blot Staining Solution (Sigma) (Herrin and Schmidt, 1988). The membrane was pre-soaked in 10% (v/v) glacial acetic acid for 5 min prior to addition of the blot stain. DEPC-treated water was used to destain the membrane in order to visualize the individual RNA bands. The image was scanned using a Hewlett Packard ScanJet 3300C.

The membrane was transferred to a hybridization bag (Kapak SealPAK pouches; KAPAK; Minneapolis, Minnesota) and incubated in a Boekel Scientific Shake'N'Bake Hybridization Oven (VWR International) at 68 ˚C for 4 h in 50 mL pre-hybridization buffer [50% (v/v) formamide, 5X SSC, 0.02% SDS, 0.01% N-lauryl sarcosine, 2% blocking reagent (Roche Molecular Biochemicals)]. The membrane was then incubated overnight in 50 ml of

hybridization buffer containing either the DIG-labeled *hsp30* riboprobe or the DIG-labeled *hsp70* riboprobe.

Stringency washes in decreasing concentrations of SSC were performed to remove any unbound probe. The first two washes (5 min each) occurred in 2X SSC (with 0.1% (w/v) SDS) at room temperature. This was followed by a 15 min wash in 0.5X SSC (with 0.1% (w/v) SDS) at 68 ˚C. Finally, the membrane was washed in 0.1X SSC (with 0.1% (w/v) SDS) for 15 min at 68 ˚C . The membrane was equilibrated at room temperature for 1 min in washing buffer [100 mM 10X maleic acid (pH 7.5), 0.3% (v/v) Tween 20 (Sigma)]. Incubation for 30 min at room temperature in blocking solution [2% (w/v) blocking reagent, 10% (v/v) 10X maleic acid buffer (pH 7.5)] was used to prevent non-specific binding of the secondary antibody. The membrane was then incubated for another 30 min at room temperature in blocking solution containing a 1:8000 dilution of secondary antibody anti-DIG-AP-conjugated Fab fragments (Roche Molecular Biochemicals). The membrane was washed twice for 15 min each in washing buffer at room temperature to remove any excess unbound antibody. The membrane was equilibrated for 2 min in detection buffer [0.1M Tris-HCl (pH 9.5), 0.1M NaCl]. The membrane was placed in a new Kapak bag and chemiluminescent reagent CDP-Star (Roche Molecular Biochemicals) was applied and incubated for 10 min in the dark. Signal detection was visualized using a DNP chemiluminescent imager (DNR BioImaging Systems Ltd.; Kirkland, Quebec) for 2-10 min.

2.4 Protein Isolation and Western Immunoblotting

2.4.1 Polyclonal Antibodies

A polyclonal anti-HSP30 *Xenopus* antibody was previously made in our laboratory using the entire open reading from of the *hsp30C* gene (Fernando and Heikkila, 2000). Previous studies

suggest that the anti-HSP30 antibody binds to all HSP30 family members in *Xenopus laevis.* A polyclonal anti-HSP70 antibody was commercially made against a C-terminal peptide fragment, specific to the stress-inducible HSP70B (Abgent; San Diego, California). The anti-HSP70 antibody will recognize all stress-inducible HSP70 family members but not HSC70 or BiP in *Xenopus laevis.*

2.4.2 Protein Isolation

Protein was isolated from A6 cell pellets using 500 µl lysis buffer at pH 7.4 [160 mM sucrose, 1.6 mM ethylene glycol-bis N,N,N',N'-tetraacetic acid (EGTA; Bioshop), 0.8 mM EDTA, 32 mM NaCl, 24 mM N-Z-hydroxylethylpiperazine-N'-2 ethane sulfonic acid (HEPES; Bioshop), 1% (w/v) SDS] containing protease inhibitors [100 µg/ml phenylmethyl-sufonyl fluoride (PMSF; Bioshop), 1 µg/ml aprotinin (Sigma), 0.5 µg/ml leupeptin (Sigma)]. Samples were mixed via vortexing, sonicated (output control 4.5, 65% duty cycle for 15 pulses) using a Branson sonifier (Branson Sonic Power Co., Danbury, Connecticut) and then centrifuged at 14,000 rpm for 1 h at 4˚C in an Eppendorf Centrifuge 5810R. The supernatant containing the protein sample was isolated and kept at -20˚C until use.

2.4.3 Protein Quantification

Protein concentrations were determined by means of a bicinchoninic acid (BCA) protein assay, according to the manufaturer's protocol (Pierce; Rockford, Illinois). A standard series of bovine serum albumin (BSA; G Biosciences; St. Louis, Missouri) dilutions, ranging from 0 to 2 mg/ml were prepared in MilliQ water from a 2 mg/ml stock. Protein samples were aliquoted and diluted in MilliQ water at concentration of 1:2. Standards and samples were loaded in triplicate onto a polystyrene 96 well assay plate in 10 µl aliquots with the addition of 80 µl of BCA reagent

A and reagent B (50:1; Pierce). Samples were mixed via pipetting and plates were incubated for 30 min at 37 °C. Reactions were analyzed with a Versamax Tunable microplate reader (Molecular Devices, Sunnyvale, California), and the plate was read at 562 nm. BSA standards were used to construct a standard curve using Microsoft Excel, which was used to determine the protein concentration of each sample.

2.4.4 Immunoblot Analysis

Immunoblot analysis was performed using 20-40 μg of protein and sodium dodecyl sulfate-polyacrylamide gel electrophoresis (SDS-PAGE). Gels were run on a BioRad Mini Protean III system (BioRad; Mississauga, Ontario). Separating gels [12% (v/v) acrylamide, 0.32% (v/v) n'n;-bis methylene acrylamide, 0.375 M Tris (pH 8.8), 1% (w/v) SDS, 0.2% (w/v) ammonium persulfate (APS), 0.14% (v/v) n,n,n'n'-tetramethylethylenediamine (TEMED)] were prepared, poured and allowed to polymerize for 30 min with 100% ethanol layered on top. Ethanol was poured off and stacking gel [4% (v/v) acrylamide, 0.11% (v/v) n'n'-bis methylene acrylamide, 0.125 M Tris (pH 6.8), 1% (w/v) SDS, 0.4% (w/v) APS, 0.21 % (v/v) TEMED] was prepared, poured and allowed to polymerize for 30 min.

Protein samples (20-40 μg) were aliquoted and loading buffer [0.0625M Tris (pH 6.8), 10% (v/v) glycerol, 2% (w/v) SDS, 5% (v/v) β-mercaptoethanol, 0.00125% (w/v) bromophenol blue] was added, to a final concentration of 1X. Samples were denatured via boiling for 10 min, cooled on ice for 5 min and pulse-centrifuged prior to loading. Gels were electrophoresed with 1X running buffer [25mM Tris, 0.2M glycine, 1 mM SDS] at 90 V until samples reached the separating gel, at which time the voltage was turned up to 160-170 V until the dye front reached the bottom of the gel.

Pure nitrocellulose transfer blot membranes (BioRad) and filter paper (BioRad) were cut to 5.5 cm x 8.5 cm, and membranes were incubated for 30 min in transfer buffer [25 mM Tris, 192 mM glycine, 20% (v/v) methanol]. After electrophoresis, the stacking gel was cut away and the remainder of the gel was soaked in transfer buffer for 15 min. Protein was transferred to the nitrocellulose membrane with a Trans-Blot Semi-Dry Transfer Cell (BioRad) at 20 volts for 20 min. Blots were then stained with Ponceau-S stain [0.19% (w/v) Ponceau-S, 5% (v/v) acetic acid] for 20 min to determine the success of the transfer and equal loading. The membrane was destained with MilliQ water and then scanned with a Hewlett Packard ScanJet 3300C. The membrane was incubated in 5% blocking solution [20 mM Tris (pH 7.5), 0.1% Tween 20 (Sigma), 300 mM NaCl, 5% (w/v) Nestle® Carnation skim milk powder] for 1 h to prevent non-specific binding. The membrane was then incubated for 1 h in blocking solution containing the primary polyclonal antibody. The antibodies used were either rabbit polyclonal anti-HSP30, anti-HSP70 (Abgent) or anti-actin antibodies at a dilution of 1:5000; 1:200 and 1:200, respectively. Excess unbound antibody was removed by rinsing the membrane with 1X Tris-Buffered Saline with Tween (TBS- T) [20 mM Tris, 300 mM NaCl, (pH 7.5), 0.1% Tween 20 (Sigma)]. The membrane was washed with fresh TBS-T for 15 min, followed by two 10 min washes. The membrane was then incubated for 1 h with blocking solution containing the secondary antibody conjugate, AP-conjugated goat-anti-rabbit (BioRad) at a 1:3000 dilution). The membrane was rinsed with TBS-T and then washed with fresh TBS-T for 15 min, followed by two 5 min washes. The membrane was incubated in alkaline phosphatase detection buffer [alkaline phosphatase buffer (100 mM Tris base, 100 mM NaCl, 50 mM $MgCl_2$ (pH 9.5)), 0.3% 4-nitro blue tetrazolium (NBT; Roche Molecular Biochemicals), 0.17% 5-bromo-4-chloro-3-indolyl-

phosphate, toluidine salt (BCIP; Roche Moelcular Biochemicals)] until the bands were visible. Images were scanned using a Hewlett Packard ScanJet 3300C.

2.5 Densitometric Analysis

Densitometry was performed using ImageJ (1.38) software on individual blots. Experiments were repeated in triplicate, and the average densitometric values were expressed as a percentage of the maximum hybridization band. The data were graphed with standard error, represented as vertical error bars. Two-tailed, unpaired T-tests were performed for some experiments to determine if statistically significant differences existed between the sample with the maximum binding and another treatment. Confidence levels used were 95% ($p < 0.05$) and 99% ($p < 0.001$).

2.6 Confocal Laser Scanning Microscopy

Xenopus laevis A6 cells were grown on 22x22 mm, base-washed [48% distilled water, 50% mL 100% filtered ethanol and 2% 10M NaOH], flame sterilized glass coverslips at 22ºC. Cells were treated once they were confluent, approximately 48 h after seeding, with the direct addition of cadmium chloride to the media and/or incubation in a hot water bath (VWR). Following treatment, cells were washed twice (2 min each) with 1X phosphate buffered saline (PBS), containing magnesium and chloride [8% NaCl, 0.2% KCl, 0.2% KH_2PO_4, 2.1% $Na_2HPO_4 \cdot 10H_2O$, 1 mM $MgCl_2$, 1 mM $CaCl_2$] and fixed in 3.7% (w/v) paraformaldehyde in PBS for 15 min. Cells were washed three times for 5 min each in PBS and then permeablized in 0.3% (v/v) Triton X-100 (Sigma) in PBS for 10 min. Cells were washed again in PBS (3 x 2 min) and then incubated for 1 h in 3.7% (w/v) bovine serum albumin (BSA) fraction V (Sigma) in PBS,

filter sterilized using a 0.4 μm filter (Pall Filtration Corporation, Mississauga, Ontario). Indirect labeling was performed using a 1:500 dilution of rabbit anti-*Xenopus* HSP30 polyclonal antibody in 3.7% BSA fraction V for 1 h. Cells were washed with PBS (3 x 2 min) to remove any unbound antibody. Secondary antibody incubation occurred for 30 min, using a mouse anti-rabbit IgG antibody conjugated with Alexa-488 (Invitrogen) at a 1:2000 dilution in 3.7% BSA fraction V in PBS. Cells were washed with PBS (3 x 3 min) and then incubated with rhodamine-tetramethylrhodamine-5-isothiocyanate (TRITC; 300 U of rhodamine phalloidin in 1.5 mL 100% methanol, Invitrogen Molecular Probes) at a 1:60 dilution for 15 min to visualize the actin cytoskeleton. Coverslips were washed again in PBS (3 x 3 min), dried and mounted on a microscope slide with Vectashield (Vector Laboratories Inc; Burlingame, California) containing 4,6-diamidino-2-phenylindole (DAPI) to stain the nucleic acids. After a 10 min incubation with DAPI, excess Vectashield mounting medium was removed and coverslips were sealed to slides using clear nailpolish. Slides were kept at 4°C until use.

Slides were imaged using a Zeiss Axiovert 200 confocal microscope with LSM 510 META software (Carl Zeiss Canada Ltd., Mississauga, Ontario) according to the manufacturer's instructions. Slides were mounted using oil emmersion (Zeiss) and observed using Plan-Neofluar 40x / 1.3 numerical apenture (NA) oil differential interference contrast (DIC) and Plan-Apochromat 63x / 1.4 NA oil DIC objectives. Individual channels were used to detect TRITC (red), DAPI (blue) and HSP30 (green) separately, and then images were merged.

3. Results

3.1. Characterization of *hsp* mRNA and HSP protein accumulation in A6 cells in response to elevated temperature.

Initial studies used Northern hybridization analysis to examine the effect of heat shock on *hsp30* and *hsp70* mRNA accumulation in *Xenopus laevis* A6 cells. Cells were maintained at 22ºC or subjected to a heat shock at 30, 33, or 35ºC for 1 or 2 h. *Hsp30* and *hsp70* mRNA were not detected in control cells or in cells treated with a 30ºC heat shock, but accumulation was detected at temperatures of 33ºC and 35ºC (Figure 1). Both *hsp30* and *hsp70* mRNA accumulation increased with increasing temperature, as well as with duration of the heat shock.

The next phase of this study utilized Western blot analysis to determine the effects of heat shock on HSP30 and HSP70 protein accumulation in A6 cells. Cells were maintained at 22ºC or exposed to a 1 or 2 h heat shock at 30ºC, 33ºC or 35ºC, with a 2 h recovery period at 22ºC. HSP30 or HSP70 protein was not detectable in control cells (Figure 2). Whereas a 30ºC heat shock failed to elicit a detectable heat shock response, treatment of cells at increased temperatures (33ºC and 35ºC) resulted in the accumulation of both HSP30 and HSP70 protein. Subsequent longer durations of heat shock (2 h versus 1 h) yielded greater accumulations of both HSP30 and HSP70 protein.

Immunocytochemistry and LSCM were used to examine intracellular localization and accumulation of HSP30 protein in A6 cells. Cells were maintained at 22ºC or heat shocked at 30, 33, or 35ºC for 2 h, followed by a 2 h recovery period at 22ºC. Whereas HSP30 protein was not detectable in control cells (Figure 3, A-C), or in cells treated at 30ºC (Figure 3, D-F), temperatures of 33ºC or higher resulted in the accumulation of HSP30 (Figure 3, G-L). In cells treated at 33ºC (Figure 3, G-I), HSP30 protein was localized to the cytoplasm whereas

Figure 1. Effect of heat shock on *hsp30* and *hsp70* mRNA accumulation in A6 cells. Cells were maintained at 22ºC (C) or subjected to a 1 or 2 h heat shock at 30ºC, 33ºC or 35ºC. Cells were harvested and total RNA was isolated and quantified. Total RNA (10 μg) was analyzed via northern hybridization analysis using antisense *hsp30* and *hsp70* riboprobes. The lower panel shows a reversible blot stain to confirm equal loading and quality of transfer.

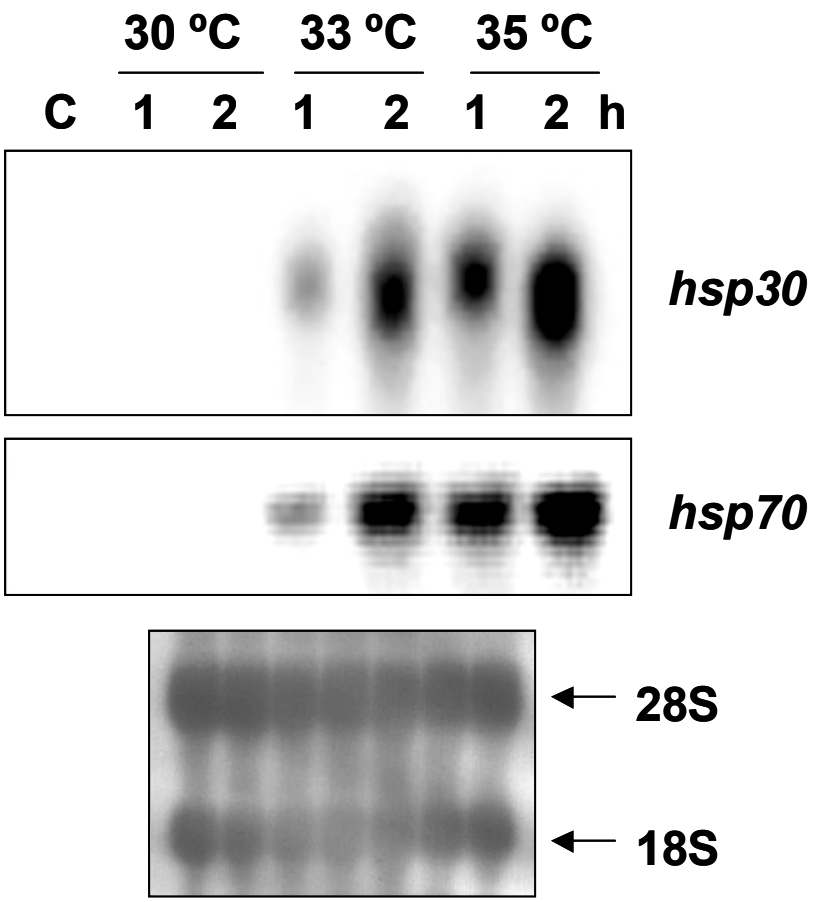
30 ºC
33 ºC
35 ºC
C 1 2 1 2 1 2 h
hsp30
hsp70
28S
18S

Figure 2. Effect of heat shock on HSP30 and HSP70 protein accumulation in A6 cells. Cells were maintained at 22ºC (C) or exposed to a 1 or 2 h heat shock at 30, 33 or 35ºC with a 2 h recovery period at 22ºC. Protein was isolated and quantified. Total protein (20-40 μg) was analyzed using immunoblotting with HSP30 and HSP70 polyclonal antibodies. A Ponceau-S stain shows equal loading and quality of transfer.

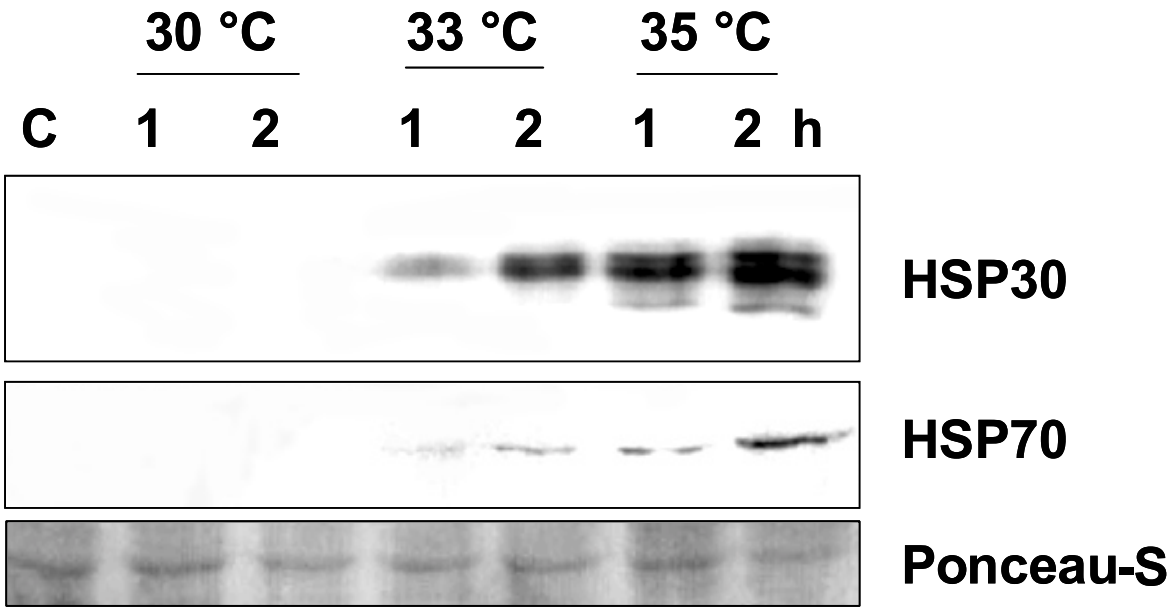
30 °C
33 °C
35 °C
C
1
2
1
2
1
2
h
HSP30
HSP70
Ponceau-S

Figure 3. The effect of heat shock on the intracellular localization of HSP30 in A6 cells using LSCM. A6 cells were grown on glass coverslips in L-15 media (A-L). Cells (A-C) were maintained at 22ºC or were heat shocked at 30ºC (D-F), 33ºC (G-I) or 35ºC (J-L) for 2 h, followed by a recovery for 2 h at 22 ºC. Actin and nuclei were directly detected by staining with TRITC (red) and DAPI (blue), respectively. HSP30 was indirectly detected with an anti-HSP30 antibody and Alexa-488 secondary antibody conjugate (green). Columns, from left to right, indicate fluorescence detection channels for actin, HSP30 and merged images of all three channels. Temperatures greater than 30ºC resulted in the accumulation of HSP30. Cells treated at 33ºC display HSP30 accumulation in the cytoplasm only, whereas at 35ºC, HSP30 also accumulated in the peripheral region of the nucleus (white arrow). Cells treated at 35ºC also displayed some membrane ruffling (white asterisks). The 10 μM white scale bar is indicated.

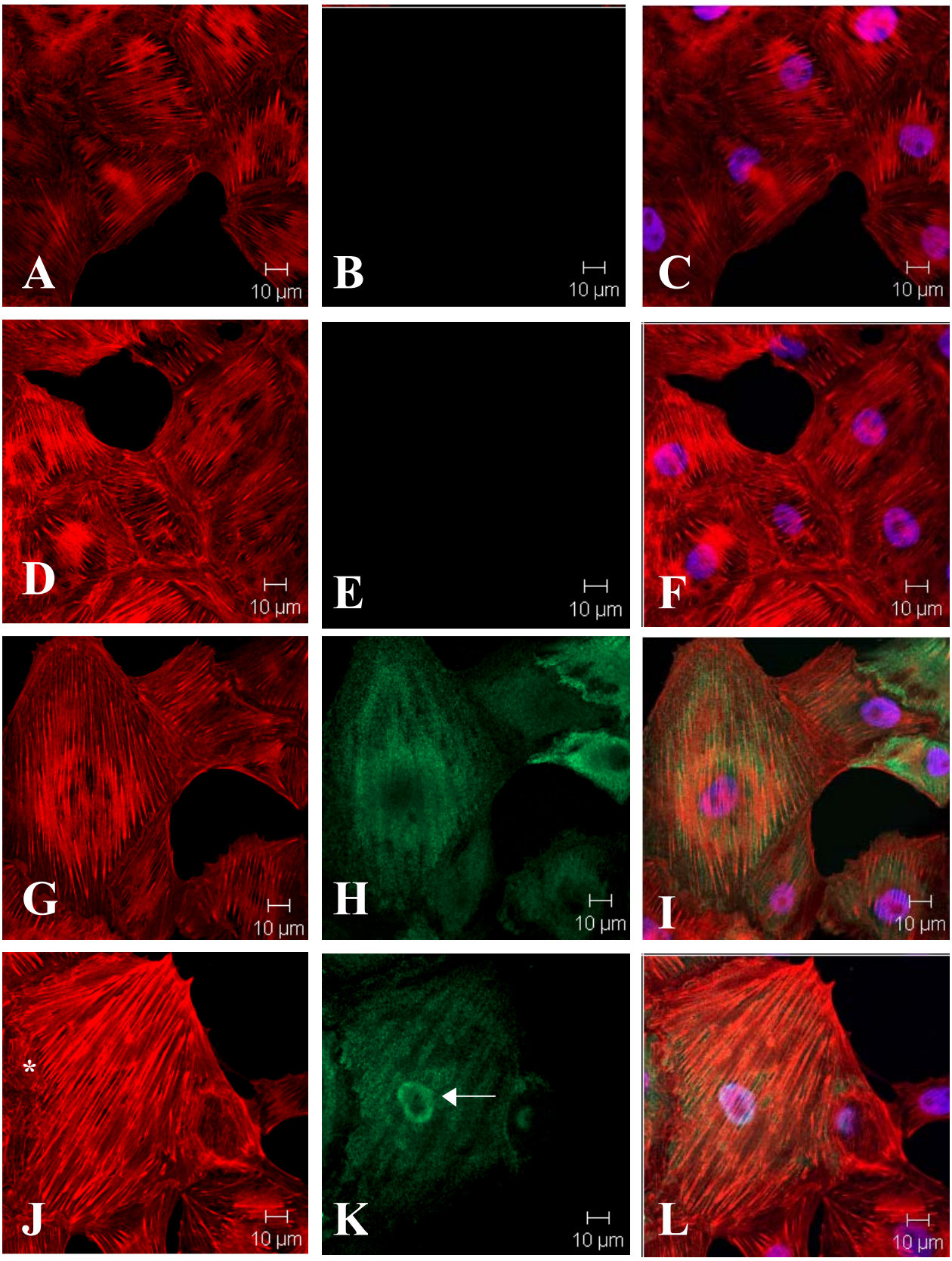
A
10 µm
B
10 µm
C
10 µm
D
10 µm
E
10 µm
F
10 µm
G
10 µm
H
10 µm
I
10 µm
*
J
10 µm
K
10 µm
L
10 µm

incubation of cells at 35ºC (Figure 3, J-L) resulted in HSP30 accumulation at the nuclear periphery (Figure 3, white arrow). Incubation of cells at 30ºC or 33ºC did not disrupt actin organization, whereas cells treated at 35ºC displayed some ruffled edges in areas of cell-cell contact (Figure 3, white asterisk).

3.2. Characterization of *hsp30* and *hsp70* mRNA and protein accumulation in response to cadmium chloride.

The effects of cadmium chloride on *hsp30* and *hsp70* mRNA accumulation in *Xenopus laevis* A6 cells were examined by Northern hybridization analysis, coupled with densitometry. Cells were maintained at 22ºC or treated with cadmium chloride (10 – 400 μM) for 5 h. Control A6 cells did not display *hsp30* or *hsp70* mRNA accumulation, nor did cells treated with low (10-50 μM) cadmium chloride concentrations (Figure 4 and 5). *Hsp30* transcript accumulation was detected following a 100 μM and 200 μM treatment, at approximately 8% and 67%, respectively, of the maximum signal observed at 400 μM. *Hsp70* message was also detected following a 100 μM and 200 μM treatment, but at approximately 50% and 72%, respectively, of the maximum signal at 400 μM.

This study also evaluated the effect of cadmium chloride on HSP30 and HSP70 protein accumulation in A6 cells via western blotting and densitometric analysis. Cells were maintained at 22ºC or treated with cadmium chloride (10 – 400 μM) for 14 h. As shown in Figure 6, HSP30 and HSP70 protein were not detectable in A6 control cells. Immunoblot analysis also revealed that cadmium chloride treatment increased the relative levels of HSP30 and HSP70 in cells treated with 100 μM or greater concentrations of cadmium chloride (Figure 6 and 7). Both HSP30 and HSP70 protein reached a maximal level of accumulation with a 200 μM cadmium

Figure 4. Effect of cadmium chloride on the accumulation of *hsp30* and *hsp70* mRNA in A6 kidney epithelial cells. A6 cells were maintained at 22ºC (C) or exposed to varying concentrations of cadmium chloride (10 – 400 μM) for 5 h. Cells were harvested and total RNA was isolated and quantified. Ten μg of total RNA was analyzed by northern hybridization analysis using *hsp30* and *hsp70* antisense riboprobes. The bottom panel shows a reversible blot stain to confirm equal loading and quality of transfer.

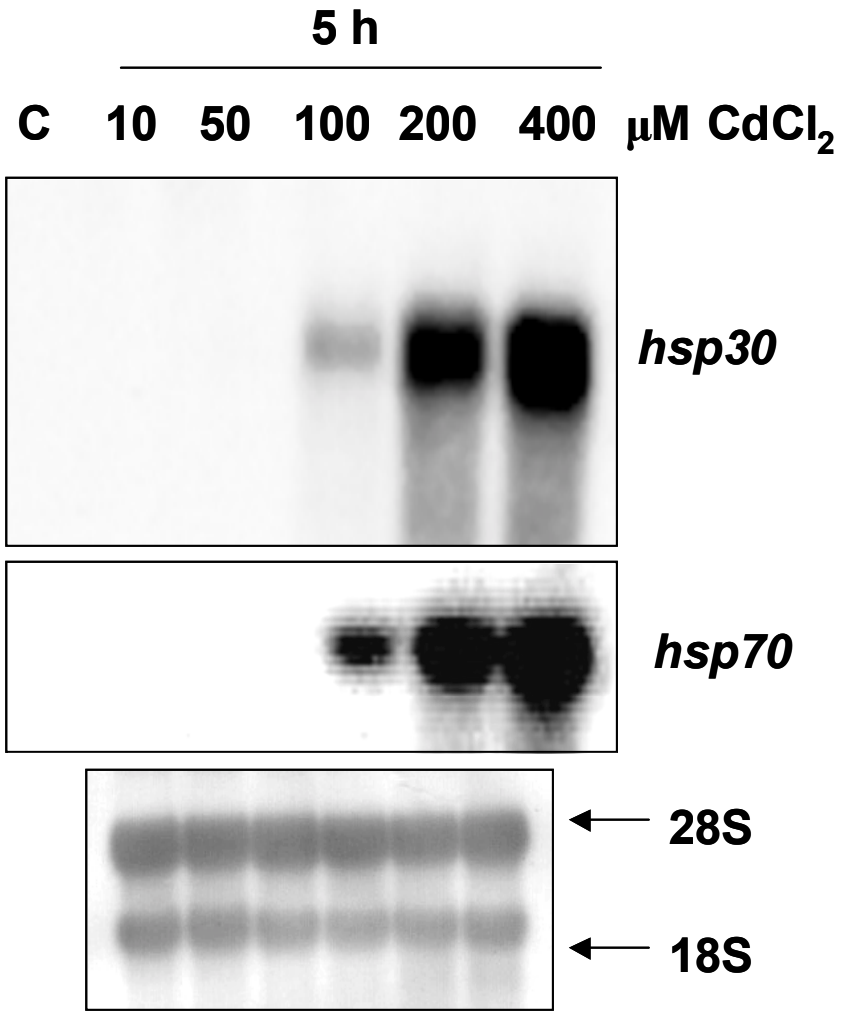
5 h
C 10 50 100 200 400 μM CdCl2
hsp30
hsp70
28S
18S

Figure 5. Densitometric analysis of cadmium chloride-induced accumulation of *hsp30* and *hsp70* mRNA in A6 cells. ImageJ (1.38) software was used for densitometric analysis of *hsp30* (solid bars) and *hsp70* (open bars) mRNA bands on northern blot images. The data were expressed as a percentage of the maximum hybridization band (at 400 μM) and then graphed with standard error represented as vertical error bars.

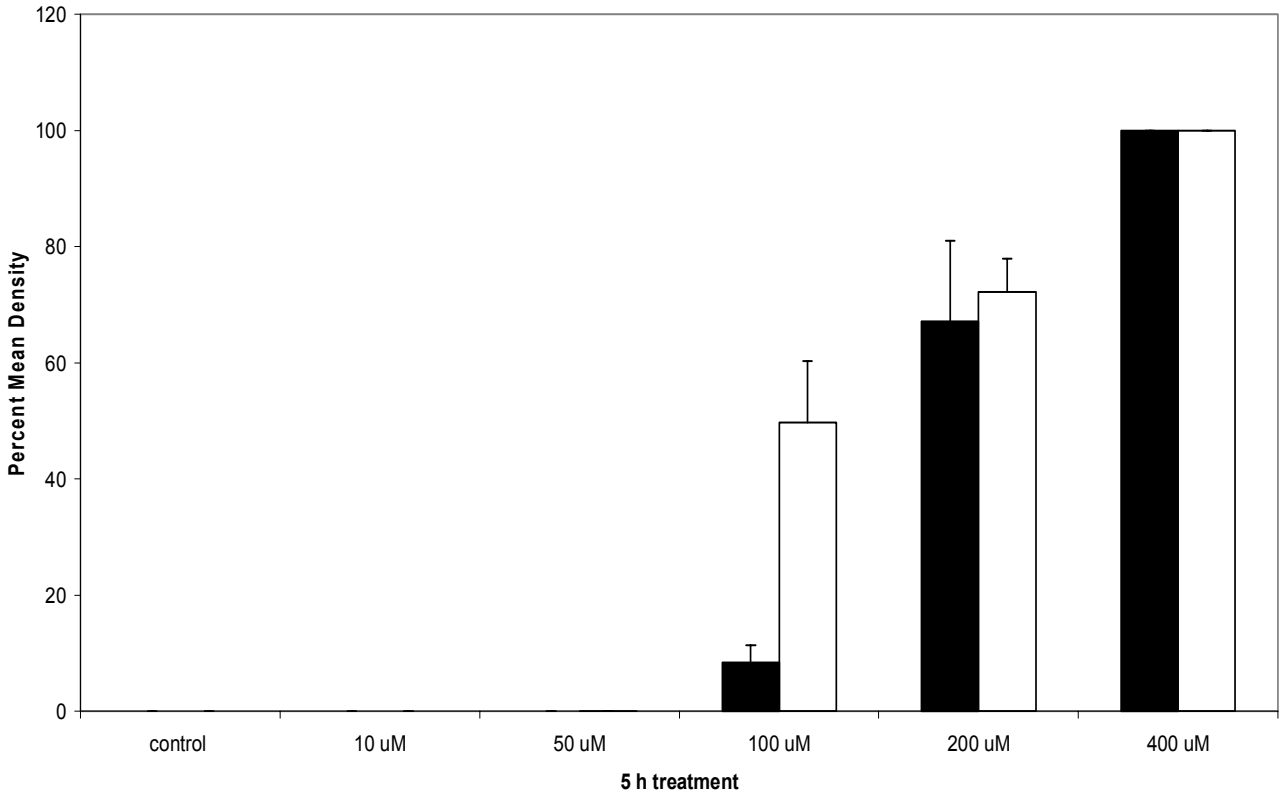
120
100
80
60
40
20
0
Percent Mean Density
control
10 uM
50 uM
100 uM
200 uM
400 uM
5 h treatment

Figure 6. Cadmium-induced HSP30 and HSP70 protein accumulation in A6 cells. Cells were maintained at 22ºC (C) or exposed to various concentrations of cadmium chloride (10-400 μM) for 14h. Cells were harvested and total protein was isolated. Total protein (20 μg for HSP30 and actin and 40 μg HSP70, respectively) was analyzed via immunoblotting. Polyclonal primary HSP30, HSP70 and actin antibodies were used to detect protein accumulation. A Ponceau-S reversible blot stain is shown (bottom panel) to confirm equal loading and quality of transfer.

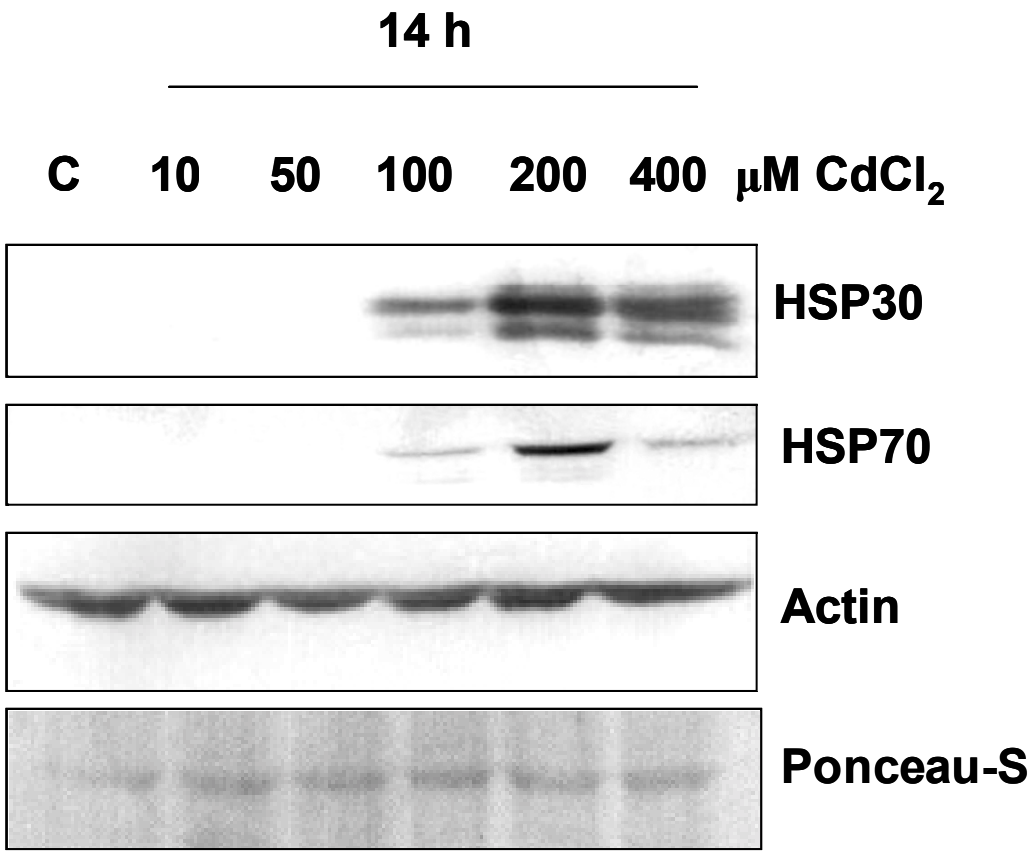
14 h
C
10
50
100
200
400
μM CdCl2
HSP30
HSP70
Actin
Ponceau-S

Figure 7. Densitometric analysis of cadmium-induced HSP30 and HSP70 protein accumulation in A6 cells. ImageJ (1.38) software was used for densitometric analysis of HSP30 (solid bars) and HSP70 (open bars) protein bands on immunoblot images. The data were expressed as a percentage of the maximum binding within each blot. Vertical error bars represent standard error.

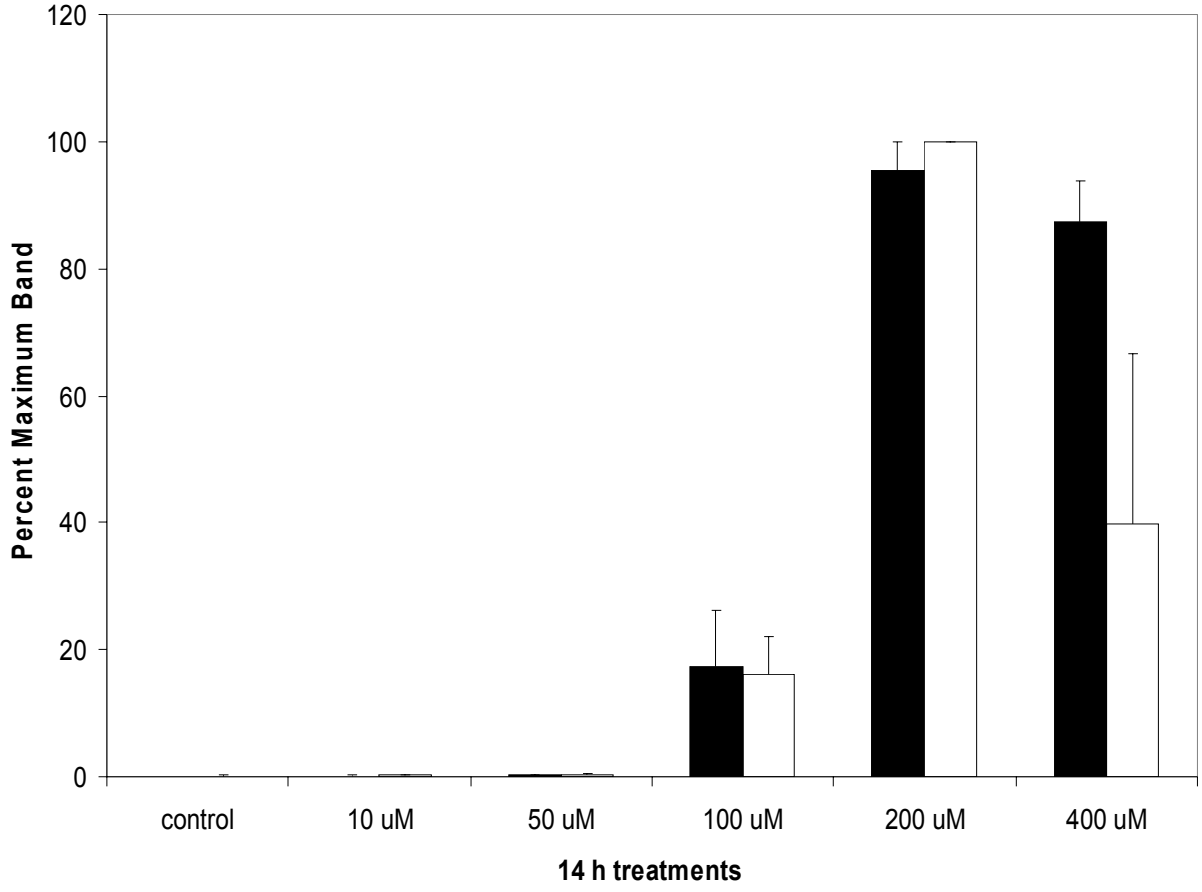
120
100
80
60
40
20
0
Percent Maximum Band
control
10 uM
50 uM
100 uM
200 uM
400 uM
14 h treatments

chloride treatment for 14 h. Relative levels of HSP30 and HSP70 protein decreased 8% and 60%, respectively, as the cadmium chloride concentration increased to 400 μM. Actin was detected in control cells and its levels remained fairly constant throughout all treatments.

The effects of cadmium chloride on HSP30 protein localization and accumulation in A6 cells were then examined by immunocytochemistry and LSCM. Cells were grown on coverslips and either maintained at 22ºC, or treated with 50, 100 or 200 μM cadmium chloride for 14 h. HSP30 accumulation was not detected in control cells (Figure 8, A-C), but was present at low levels in approximately 10% of cells treated with 50 μM cadmium chloride (Figure 8, D-F; Figure 9 A-L). A6 cells treated with 100 μM cadmium chloride displayed an increase in the relative abundance of HSP30 protein within the cytoplasm compared to cells treated with 50 μM cadmium chloride (Figure 10, A-L). Incubation of cells in the presence of 100 μM cadmium chloride also resulted in enhanced HSP30 accumulation in an average of 80% of cells (Figure 8, G-I; Figure 10, A-L). HSP30 staining occurred in large granular structures in cells treated with 50 or 100 μM (Figure 8-10, white arrows). The relative level of HSP30 further increased with increased cadmium chloride concentrations. An average of 95% of cells treated with 200 μM cadmium chloride showed the presence of HSP30 protein (Figure 8, J-L). Treatment of A6 cells with 200 μM cadmium chloride also resulted in the disruption of stress fibers (Figure 8, white asterisks) and resulted in cell aggregates (Figure 8, J-L).

3.3. Time course of *hsp30* and *hsp70* mRNA accumulation in A6 cells treated with cadmium chloride.

Northern hybridization and densitometric analysis were used to characterize a time course of *hsp30* and *hsp70* transcript accumulation in A6 cells treated with cadmium

Figure 8. Cadmium chloride-induced HSP30 accumulation in A6 cells using LSCM. Cells were grown on glass coverslips in L-15 media at 22 ºC. Cells were maintained at 22ºC (A-C) or treated with either 50 μM (D-F), 100 μM (G-I) or 200 μM (J-L) cadmium chloride for 14 h at 22ºC . Actin was directly stained using TRITC (red) and the nucleus was directly stained using DAPI (blue). HSP30 was detected indirectly via an anti-HSP30 antibody and Alexa-488 secondary antibody conjugate (green). From left to right the columns indicate fluorescence detection channels for actin, HSP30 and merged images (containing all three channels). HSP30 was not detected in control cells (A-C) and present in low levels in approximately 10% of cells treated with 50 μM (D-F). Treatments with 100 μM resulted in an increased accumulation of HSP30 in the cytoplasm and of a larger proportion of cells (approximately 80%) (G-I). HSP30 staining occurred in large granule structures (white arrows). Cells treated with 200 μM cadmium chloride displayed an even greater increase in HSP30 accumulation, and the presence of HSP30 in approximately 95% of cells. Treatment with 200 μM also caused the disruption of actin fibers (white asterisks) and resulted in cell aggregation (J-L). The 10 μM white scale bar is indicated.

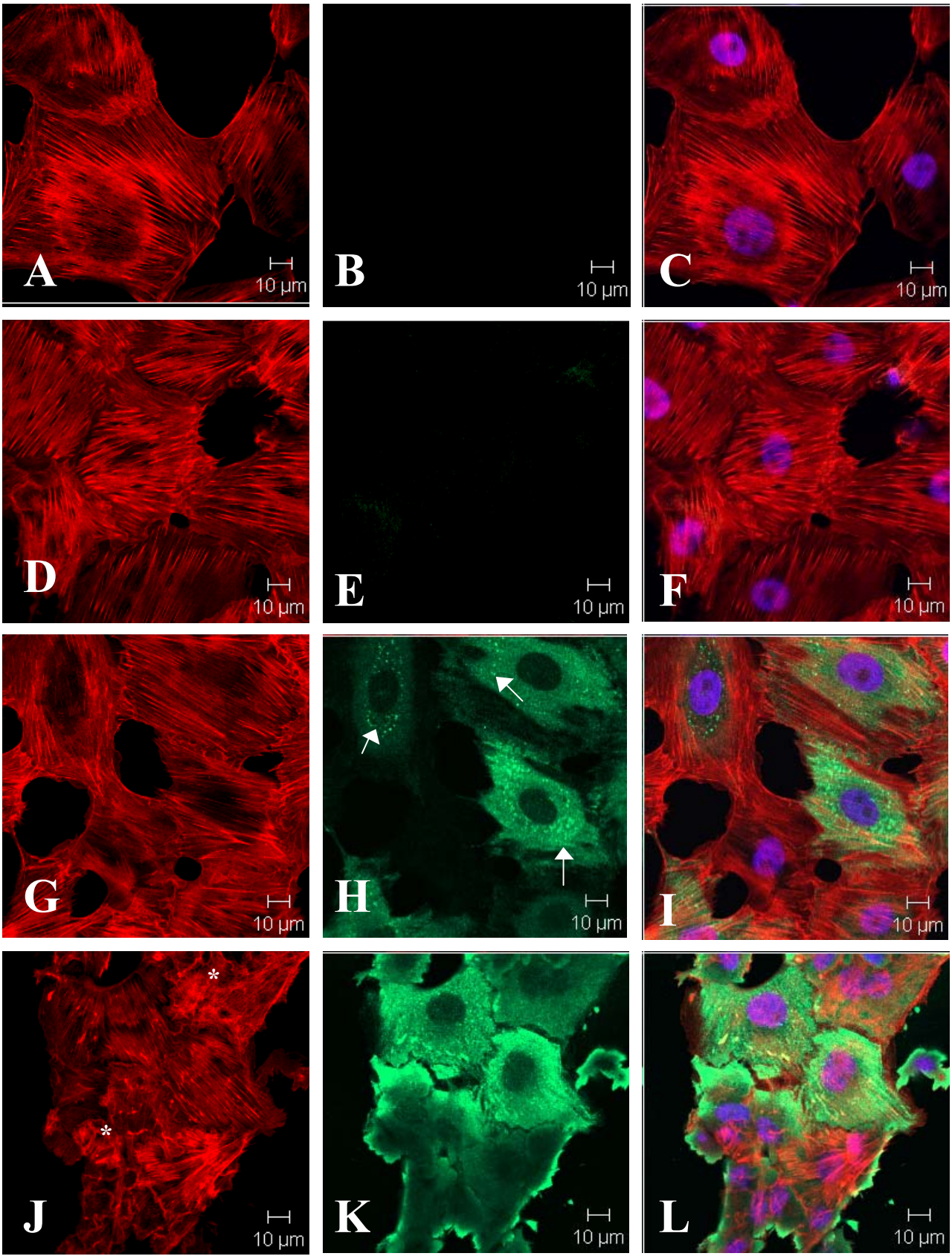
A
10 µm
B
10 µm
C
10 µm
D
10 µm
E
10 µm
F
10 µm
G
10 µm
H
10 µm
I
10 µm
J
10 µm
K
10 µm
L
10 µm

Figure 9. Detailed analysis of HSP30 accumulation in A6 cells following a 14 h 50 µM cadmium chloride treatment. A6 cells were grown on glass coverslips at 22ºC in L-15 media, supplemented with 50 µM cadmium chloride (A-L). TRITC (red) and DAPI (blue) stains were used to directly detect actin and the nuclei, respectively. HSP30 was detected using an anti-HSP30 antibody and Alex-488 secondary antibody conjugate (green). From left to right, the columns indicate fluorescence detection channels for actin, HSP30 and merged channels. Images A-C were taken using a Plan-Neofluar 40x / 1.3 NA oil DIC objective and show the relative proportion of cells (approximately 10%) that accumulate HSP30 following the 14 h cadmium treatment. All other images (D-L) were taken using a Plan-Apochromat 63x / 1.4 NA oil DIC objective, with increasing magnification. HSP30 accumulation occurs in only some cells when treated with 50 µM cadmium chloride for 14 h (A-F). Zoomed in images reveal that HSP30 is restricted to the cytoplasm, with the occurrence of large granules (white arrows) (G-L). The 10 µM white scale bar is indicated.

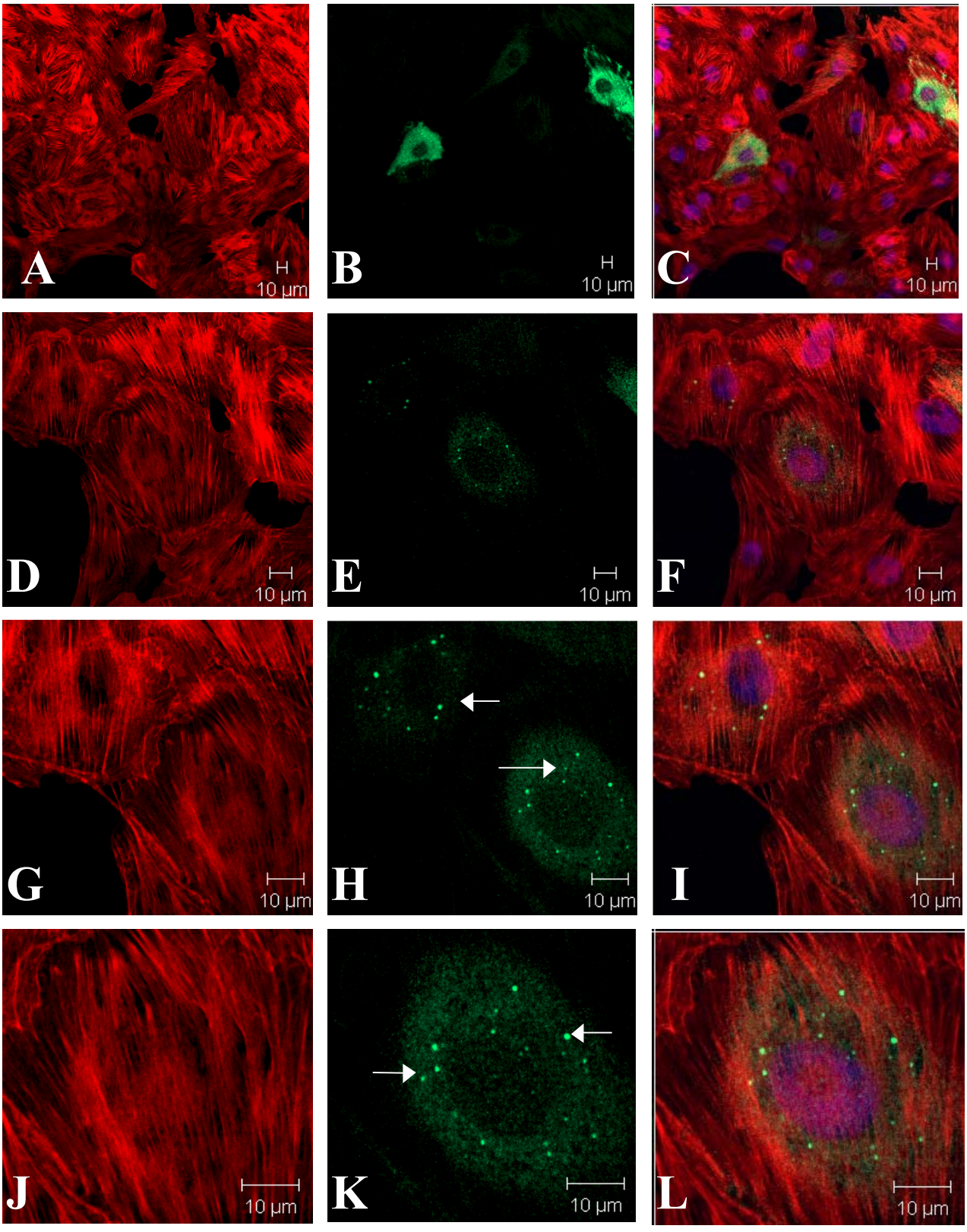
A
H
10 µm
B
H
10 µm
C
H
10 µm
D
10 µm
E
10 µm
F
10 µm
G
10 µm
H
10 µm
I
10 µm
J
10 µm
K
10 µm
L
10 µm

Figure 10. Detailed analysis HSP30 accumulation in A6 cells following a 14 h 100 µM cadmium chloride treatment. A6 cells were grown on glass coverslips at 22 °C in L-15 media, supplemented with 100 µM cadmium chloride (A-L). Actin (red) and the nuclei (blue) were directly stained using TRITC and DAPI, respectively. HSP30 was detected using an anti-HSP30 antibody and Alexa-488 secondary antibody conjugate (green). From left to right, the columns indicate fluorescence detection channels for actin, HSP30 and all three merged channels. Images A-C were taken using a Plan-Neofluar 40x / 1.3 NA oil DIC objective to show the relative proportion of cells that accumulate HSP30 following the 14 h 100 µM cadmium treatment. All other images (D-L) were taken using a Plan-Apochromat 63x / 1.4 NA oil DIC objective, with increasing magnification. HSP30 accumulation occurs in approximately 80% of cells treated with 100 µM cadmium chloride for 14h (A-C). Higher magnification revealed that HSP30 accumulation occurs in the cytoplasm, with some formation of large granule structures (white arrow) (D-L). The 10 µM white scale bar is indicated.

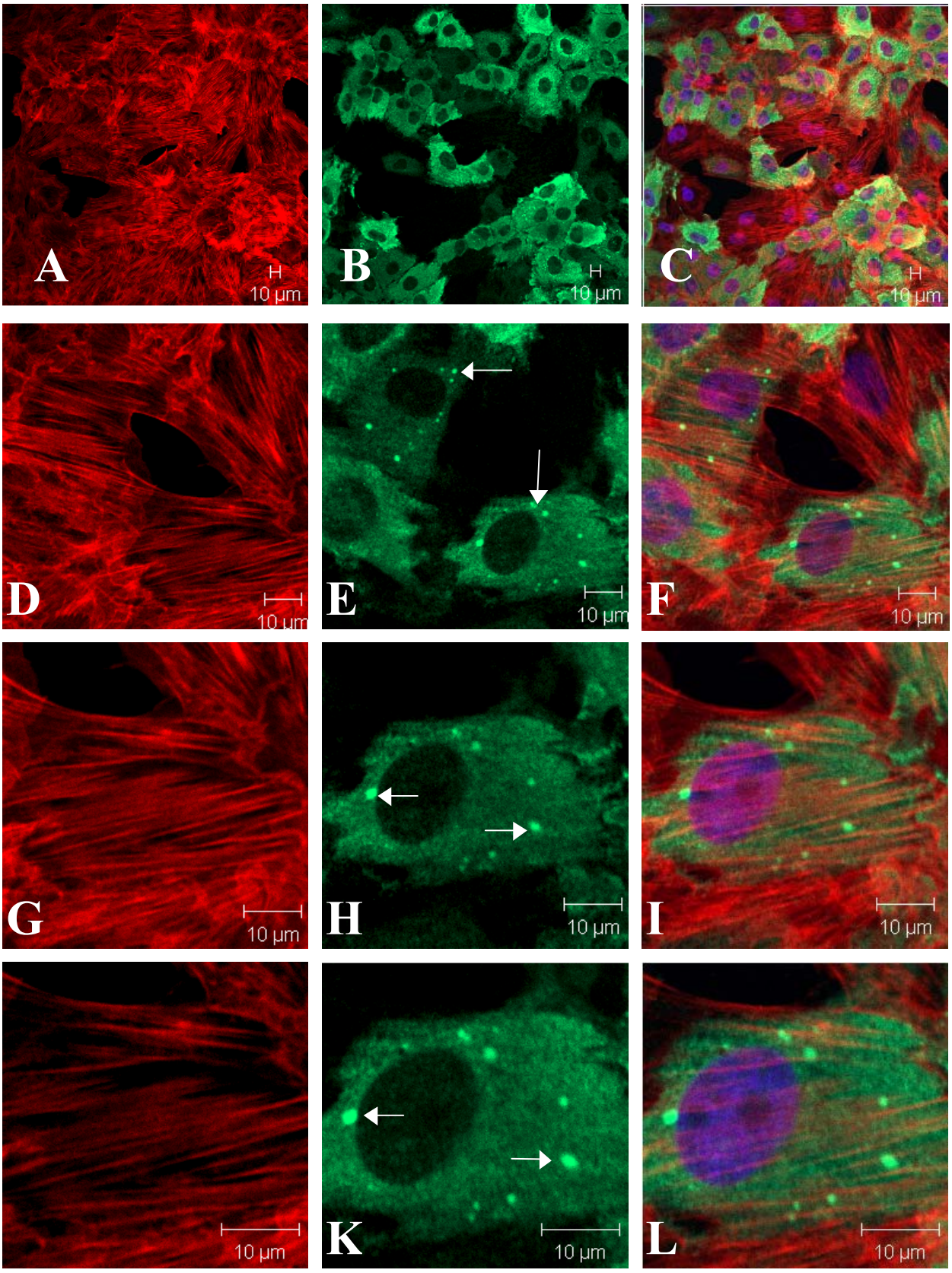
A
H
10 µm
B
H
10 µm
C
H
10 µm
D
10 µm
E
10 µm
F
10 µm
G
10 µm
H
10 µm
I
10 µm
10 µm
K
10 µm
L
10 µm

chloride. Cells were maintained at 22ºC or treated with 200 μM of cadmium chloride for 2 - 24 h. *Hsp30* and *hsp70* mRNA were not detected in control A6 cells, or in cells exposed to cadmium for 2 h (Figure 11 and 12). *Hsp30* mRNA accumulation was first detectable at 4 h (2% of the maximum signal), whereas *hsp70* mRNA accumulation was first detectable at 3 h (14% of the maximum signal). The relative levels of *hsp30* transcript increased with increasing duration of treatment, to a maximum observed at 16 h, and a decline to 65% of peak values by 24 h. *Hsp70* transcript accumulation followed a similar pattern of expression, but with maximal accumulation observed at 8 h, and a subsequent decrease to 64% of peak values by 24 h.

A time course of *hsp30* and *hsp70* gene expression was also characterized at the protein level in A6 cells by using Western blot and densitometric analysis. Cells were maintained at 22ºC or treated with 200 μM for 5 - 24 h. HSP30 protein accumulation was first detected in low amounts (2% of maximum band) at 5 h, whereas HSP70 protein accumulation was not visibly detectable until 8 h (24% of maximum band) (Figure 13 and 14). Treatment of A6 cells for 14 or 16 h resulted in a maximal accumulation of HSP70 and HSP30, respectively. During prolonged cadmium chloride exposure (24 h) HSP30 protein levels declined by less than 1%, whereas HSP70 protein levels declined by approximately 50% from their respective maximum bands. Actin accumulation was detected in the control cells and levels decreased slightly with duration of treatment.

3.4. Heat shock protein accumulation during recovery from cadmium chloride exposure in A6 cells.

The relative levels of HSP30 and HSP70 during recovery from cadmium exposure were analyzed via Western blotting and densitometry. Cells were treated with 200 μM cadmium

Figure 11. Time course of *hsp30* and *hsp70* mRNA accumulation in A6 cells treated with cadmium chloride. A6 cells were maintained at 22ºC (C) exposed to 200 μM of cadmium chloride for various durations of time (2-24 h). RNA was isolated and quantified after treatment. Total RNA (10 μg) was analyzed by northern blot hybridization using *hsp30* and *hsp70* antisense riboprobes. A reversible blot stain (bottom panel) verifies equal sample loading and efficient transfer.

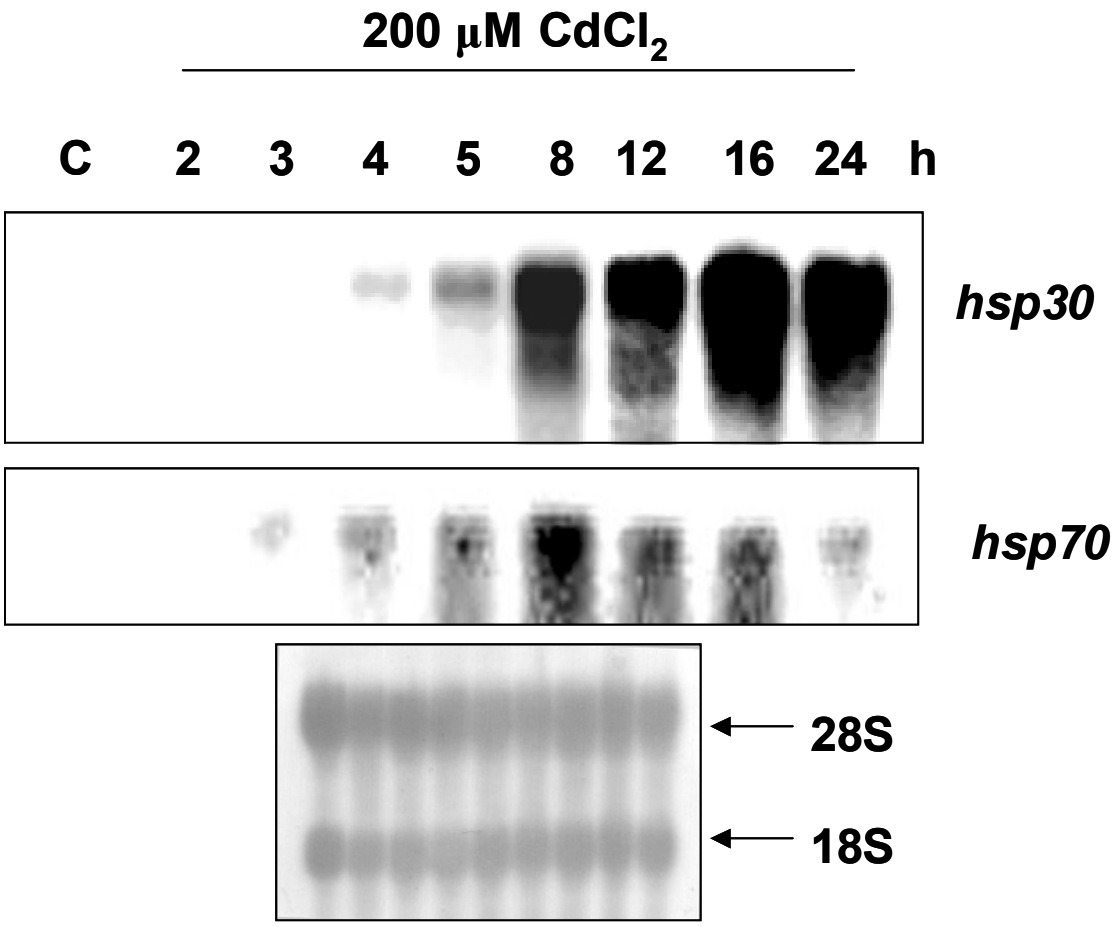
200 μM CdCl2
C 2 3 4 5 8 12 16 24 h
hsp30
hsp70
28S
18S

Figure 12. Time course of cadmium-induced accumulation of *hsp30* and *hsp70* mRNA in A6 cells. ImageJ (1.38) software was used for densitometric analysis of *hsp30* (solid bars) and *hsp70* (open bars) mRNA bands on northern blot images. The data were expressed as a percentage of the maximum band at 16 h and 8 h, for *hsp30* and *hsp70,* respectively. Vertical error bars represent standard error.

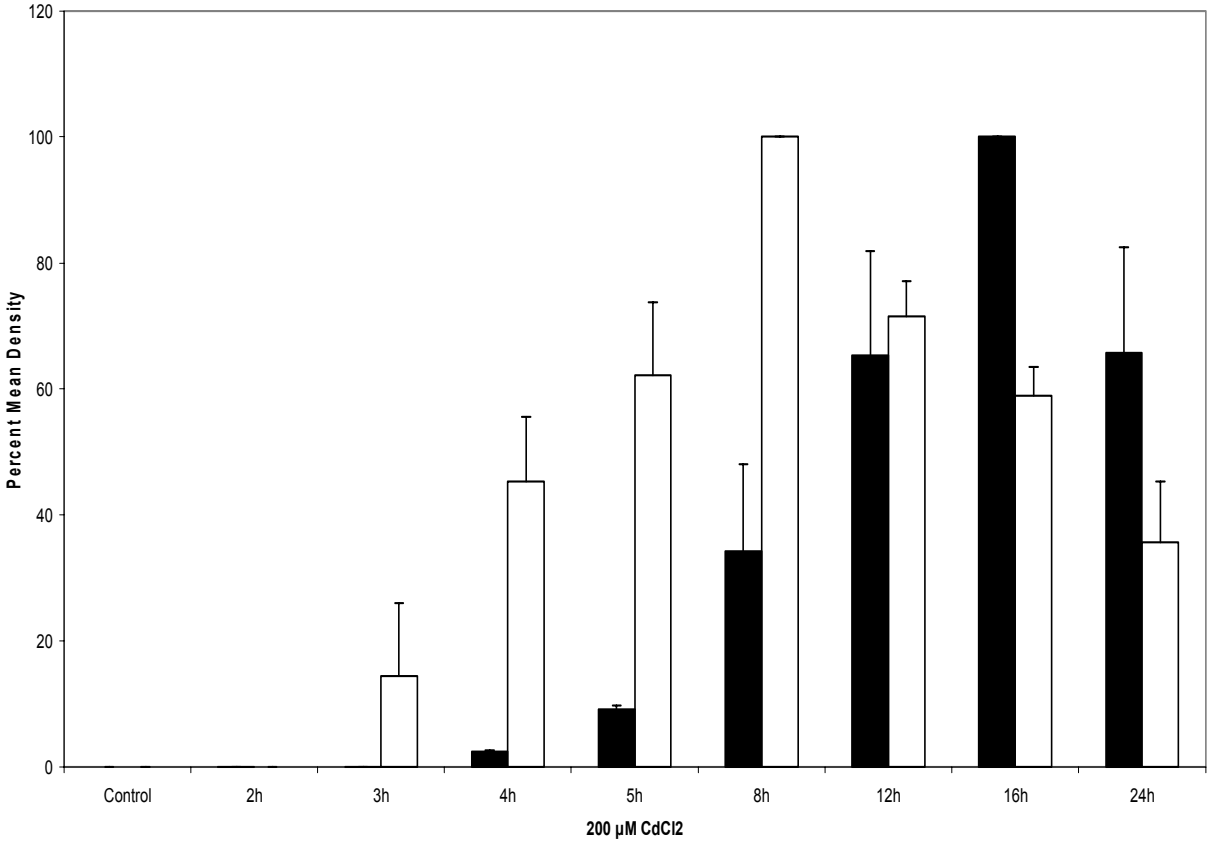
120
100
80
60
40
20
0
Percent Mean Density
Control
2h
3h
4h
5h
8h
12h
16h
24h
200 µM CdCl2

Figure 13. Time course of cadmium-induced HSP30 and HSP70 protein accumulation in A6 cells. Cells were maintained at 22ºC (C) or treated with 200 μM cadmium chloride for various lengths of time (5-24 h). Total protein was isolated and 20-40 μg were analyzed by immuoblotting using polyclonal HSP30, HSP70 and actin antibodies

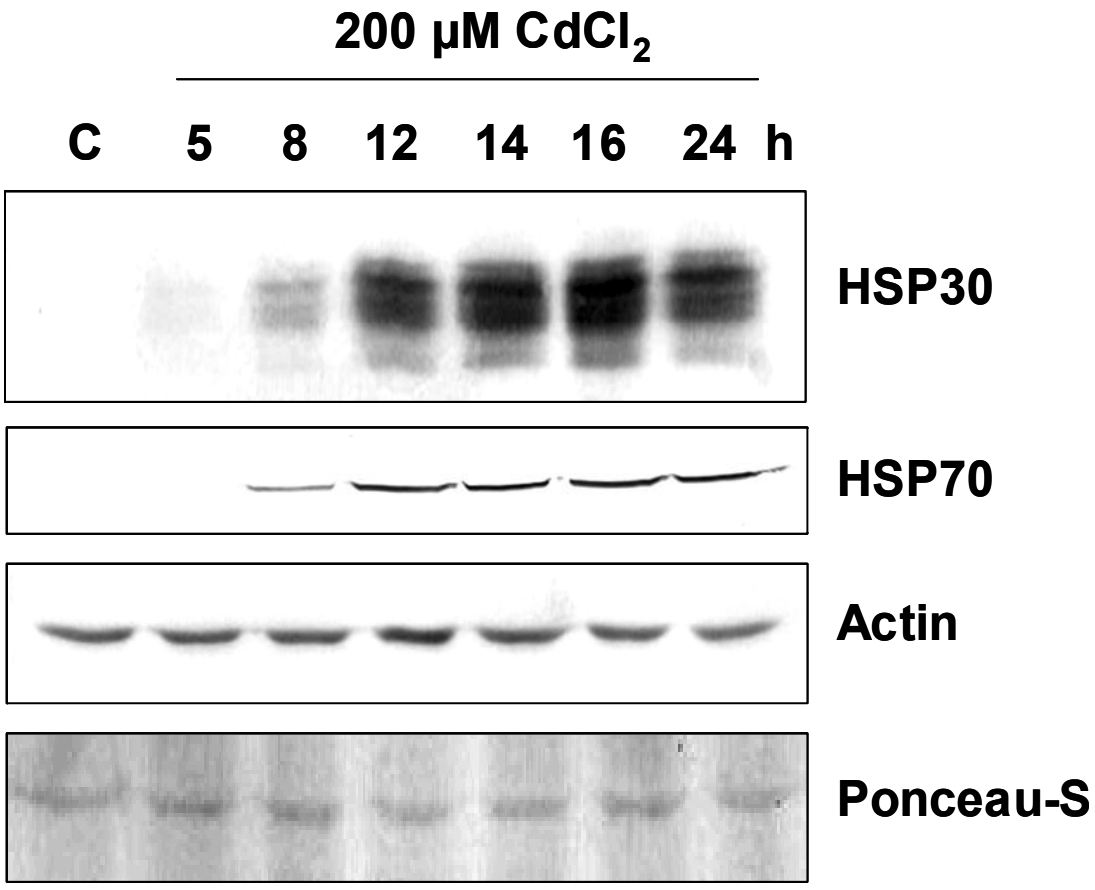
200 μM $CdCl_2$
C 5 8 12 14 16 24 h
HSP30
HSP70
Actin
Ponceau-S

Figure 14. Time course of cadmium-induced HSP30 and HSP70 accumulation. ImageJ (1.38) software was used for densitometric analysis of protein on western blot images. HSP30 (solid bars) and HSP70 (open bars) data were expressed as a percentage of the maximum hybridization within each blot and then graphed with the standard error, represented as vertical error bars.

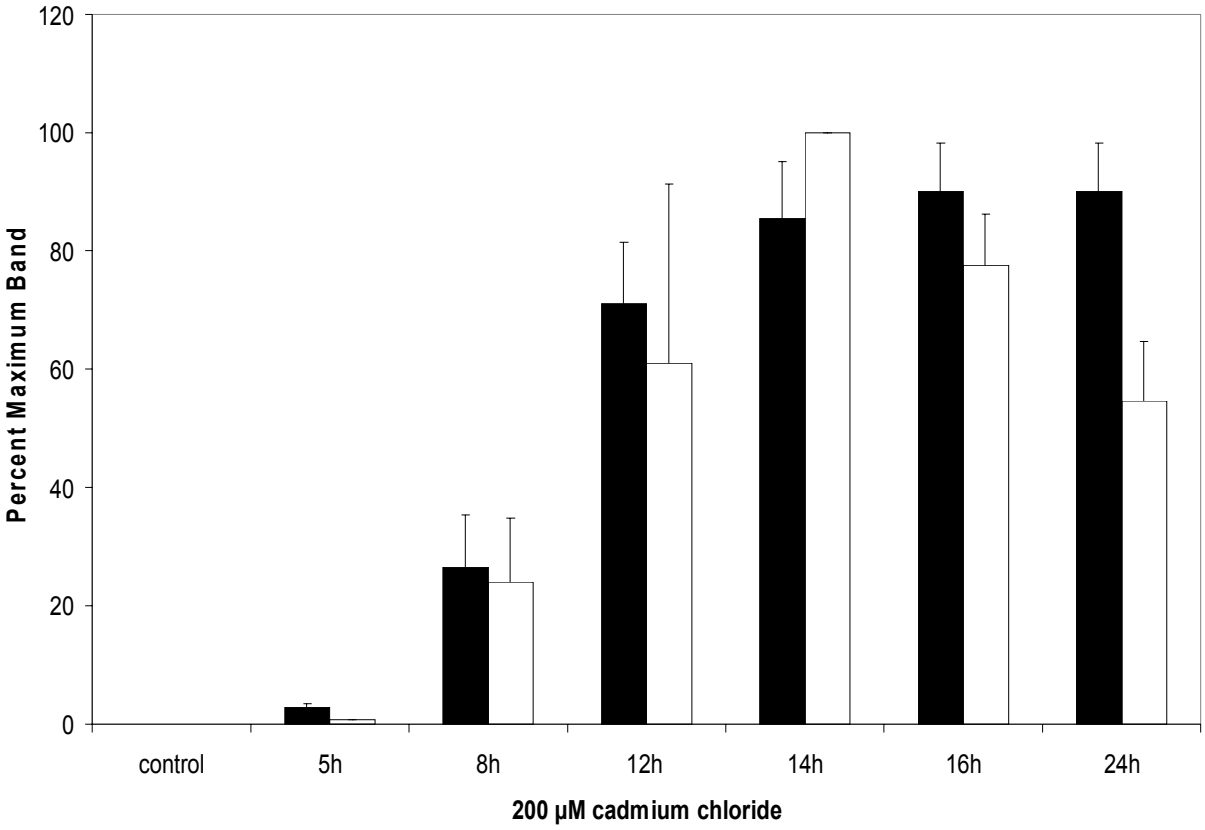
120
100
80
60
40
20
0
Percent Maximum Band
control
5h
8h
12h
14h
16h
24h
200 µM cadmium chloride

chloride for 8 h, and then allowed to recover from the stress for 0 - 72 h. HSP30 and HSP70 protein accumulation was detected following an 8 h cadmium chloride treatment, at 22% and 55% of the maximum signal, respectively (Figure 15 and 16). Maximum levels of HSP30 and HSP70 accumulation occurred 12 h after the removal of the cadmium chloride stressor. HSP30 and HSP70 accumulation levels subsequently decreased as the duration of recovery increased. HSP30 accumulation was significantly lower after a 48 and 72 h recovery period, when compared to maximum accumulation at 12 h ($p < 0.05$). HSP70 accumulation also decreased with longer recovery times after the 12 h maximum, with significant differences observed at 24 ($p < 0.05$), 48 ($p < 0.001$) and 72 h ($p < 0.001$). HSP70 accumulation was nearly undetectable in recovery periods longer than 24 h, with HSP70 protein levels decreasing 99% relative to the maximum signal at 12 h of recovery. In contrast, HSP30 accumulation remained visible on the blot at approximately 53% of the maximum signal.

3.5. Characterization of *hsp30* and *hsp70* gene expression in A6 cells after a mild heat shock plus cadmium treatment.

Studies, using Northern hybridization analysis with densitometry, examined the effect of a mild heat shock plus cadmium chloride treatments on *hsp30* and *hsp70* mRNA accumulation *Xenopus laevis* A6 cells. Cells were either maintained at 22ºC, treated with heat shock at 30ºC or 200 µM cadmium chloride, or subjected to a combination of the two stressors for 5 h. *Hsp30* and *hsp70* mRNA were not detectable in control A6 cells or following a 30ºC heat shock for 5 h (Figure 17 and 18). Treatment of cells with 200 µM for 5 h induced the accumulation of the

Figure 15. HSP30 and HSP70 protein accumulation in A6 cells during recovery from cadmium exposure. Cells were maintained at 22ºC (C) or subjected to an 8 h 200 μM cadmium chloride treatment and then allowed to recovery for 0-72 h. The media containing cadmium was removed and fresh media was added to the cells. Total protein was isolated and 20-40μg was analyzed by immuoblotting using HSP30 and HSP70 polyclonal antibodies. A Ponceau-S reversible blot stain (bottom panel) reveals equal loading and quality of protein transfer.

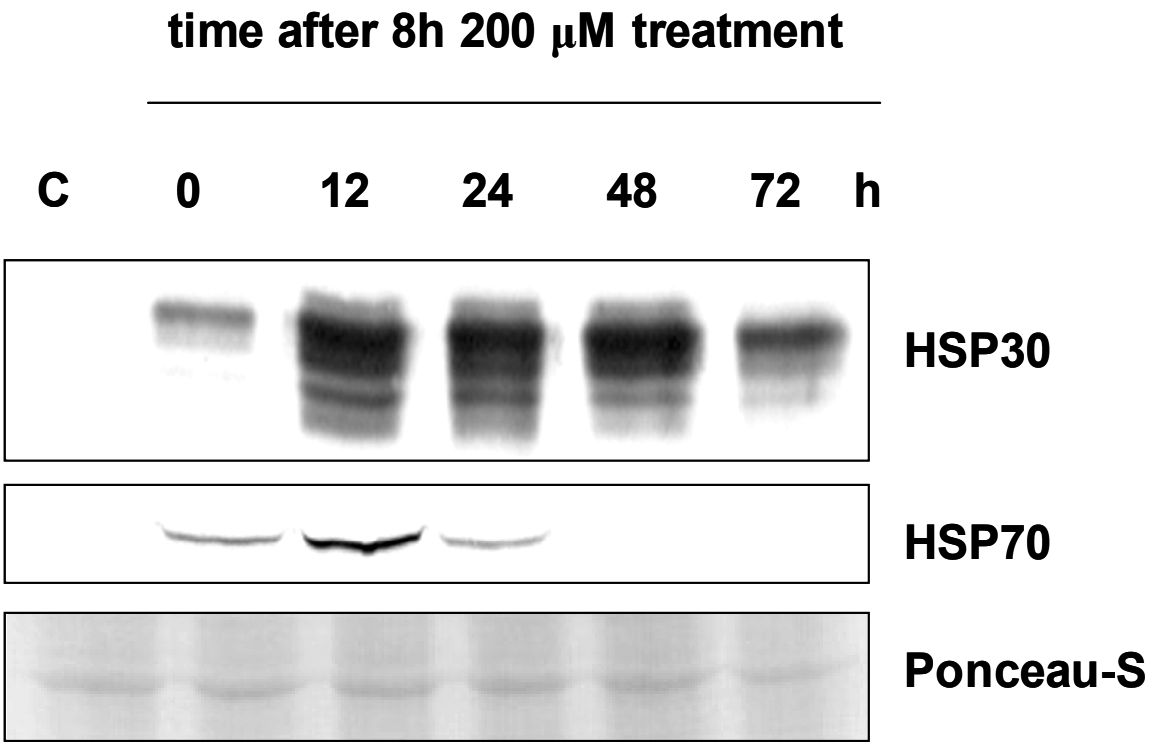
time after 8h 200 μM treatment
C
0
12
24
48
72
h
HSP30
HSP70
Ponceau-S

Figure 16. HSP30 and HSP70 protein accumulation levels in A6 cells during recovery from a cadmium treatment. ImageJ software (1.38) was used to perform densitometric analysis of protein bands from western blots. HSP30 (solid bars) and HSP70 (open bars) data were expressed as a percentage of the maximum hybridization within each blot. Vertical error bars represent standard error. Significant differences are denoted between HSP30 at 12 h and longer recovery times (*, $p < 0.05$), as well as between HSP70 at 12 h and longer recovery times (Δ, $p < 0.05$, Δ Δ $p < 0.001$).

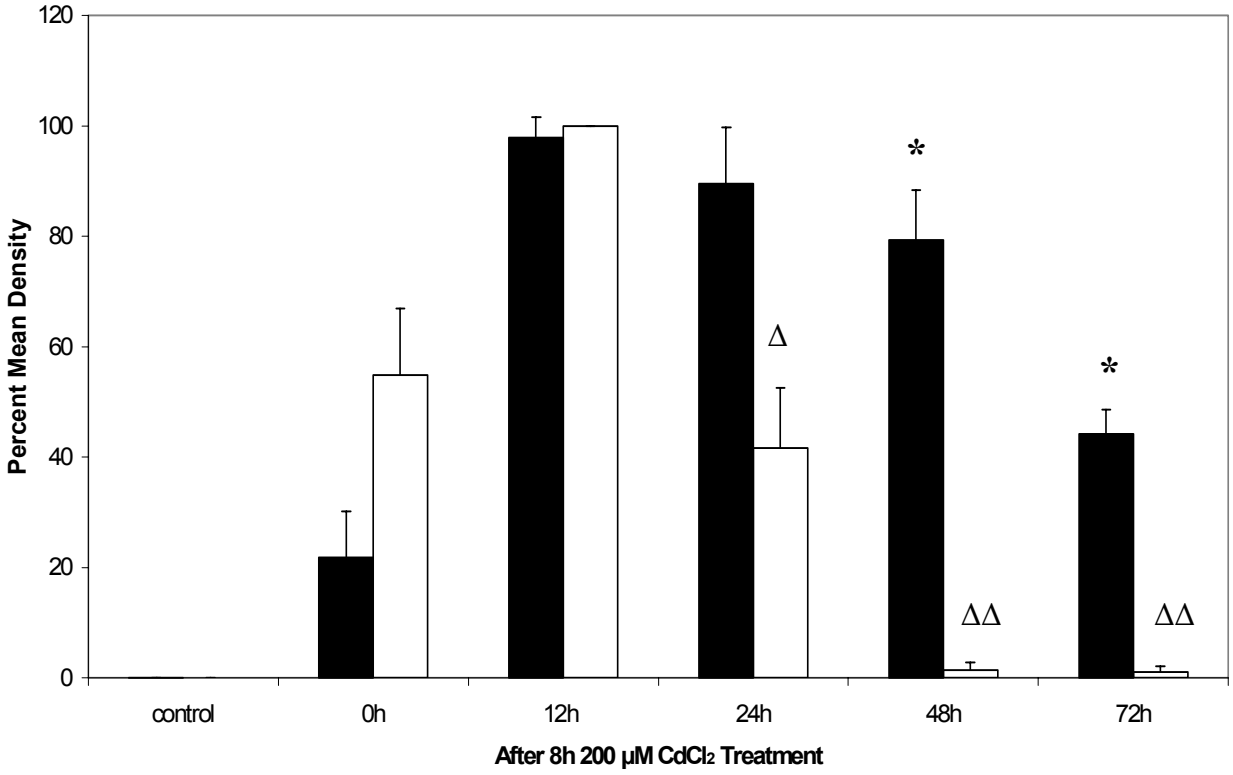
120
100
80
60
40
20
0
Percent Mean Density
*
Δ
*
ΔΔ
ΔΔ
control
0h
12h
24h
48h
72h
After 8h 200 µM CdCl2 Treatment

Figure 17. Accumulation of *hsp30* and *hsp70* mRNA in A6 cells after a mild heat shock plus cadmium treatment. Cells were maintained at 22ºC (C), or treated with either a heat shock at 30ºC, 200 μM of cadmium chloride or a combination of the two stressors for 5 h. Total RNA (10 μg) was analyzed by northern blot hybridization using *hsp30* and *hsp70* antisense riboprobes. The bottom panel shows a reversible blot stain to confirm equal loading and quality of transfer.

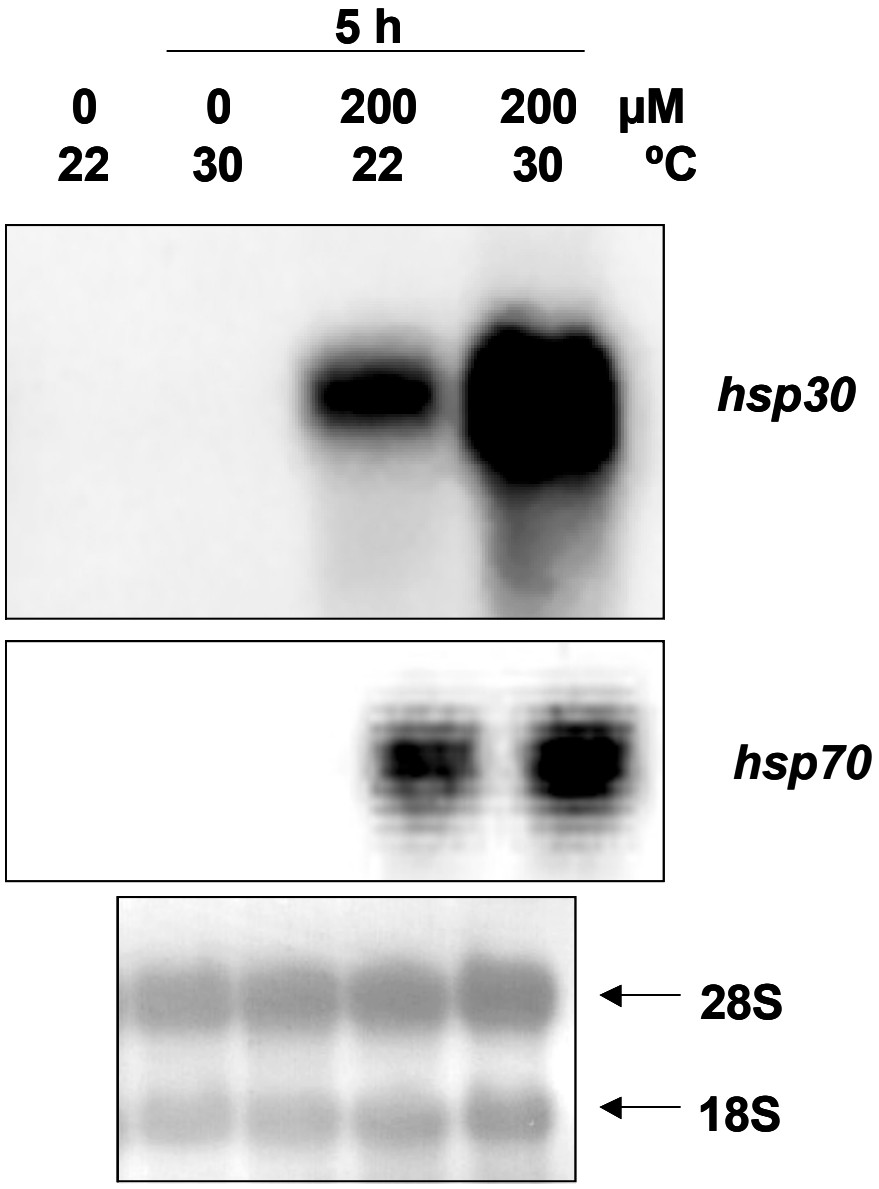
5 h
0
0
200
200
μM
22
30
22
30
°C
hsp30
hsp70
28S
18S

Figure 18. Densitometric analysis of *hsp30* and *hsp70* mRNA induction by a combination of stressors in A6 cells. ImageJ (1.38) software was used to perform densitometric analysis of *hsp30* (solid bars) and *hsp70* (open bars) mRNA bands on northern blot images. Results are expressed as a percentage of the maximum hybridization within the blot. Vertical error bars represent the standard error. Significant differences between individual stressors and combined treatment are annoted for *hsp30* (**, $p < 0.001$) and *hsp70* (Δ, $p < 0.05$; $\Delta\ \Delta$, $p < 0.001$)

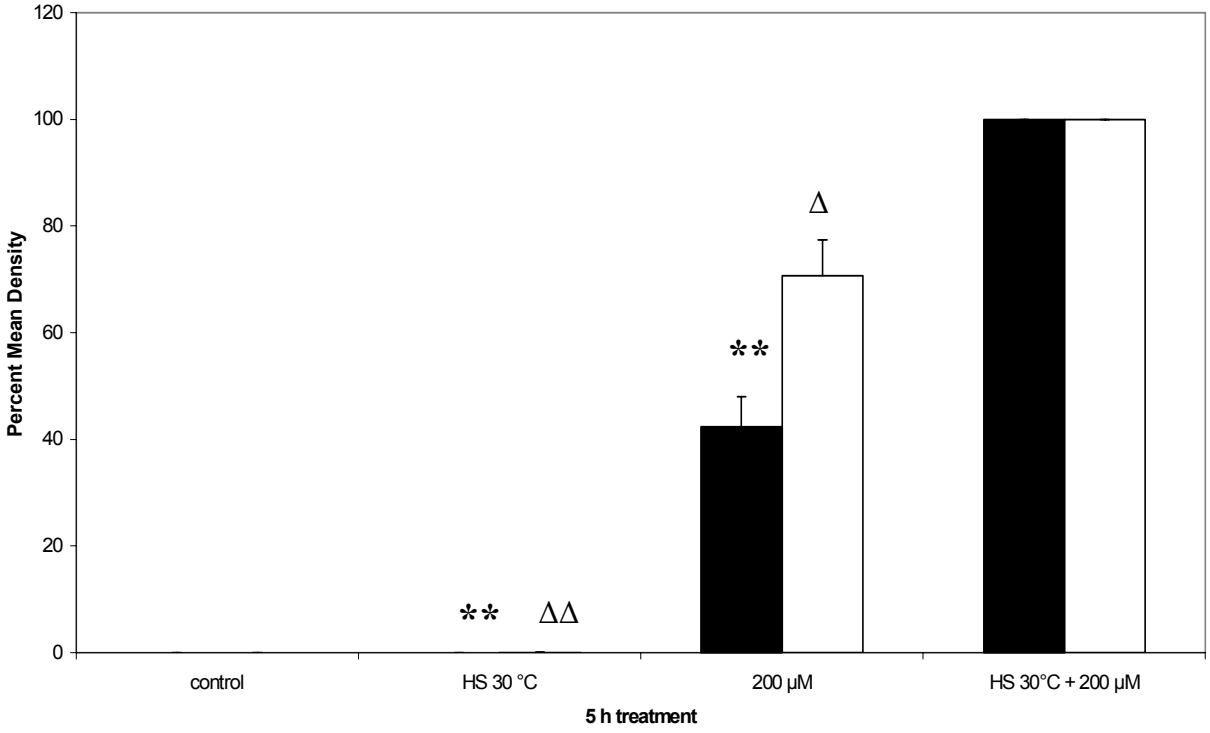
120
100
80
60
40
20
0
Percent Mean Density
**
ΔΔ
**
Δ
control
HS 30 °C
200 µM
HS 30°C + 200 µM
5 h treatment

hsp30 message (42% of the maximum band) and the *hsp70* message (71% of the maximum band). Cells that were exposed to a combination of the two stressors displayed over a 2-fold increase in *hsp30* mRNA compared to the cadmium chloride treatment alone, whereas a *hsp70* mRNA accumulation increased 1.4-fold. Analysis revealed significant differences between cells treated with a single stressor (either heat shock or cadmium) and *hsp30* ($p < 0.001$, $p < 0.001$, respectively) and *hsp70* ($p < 0.001$, $p < 0.05$, respectively) transcript accumulation in cells treated with both stressors

The effect of heat shock plus cadmium on the relative levels of HSP30 and HSP70 in A6 cells was examined using Western blot analysis and densitometry. Cells that were maintained at 22ºC or incubated at 30ºC for 5 h did not result in the accumulation of HSP30 and HSP70 protein (Figure 19 and 20). Treatment of A6 cells with 200 μM cadmium chloride for 5 h resulted in a small accumulation of HSP30 (8% of the maximum band), whereas HSP70 protein was not detectable. Cells treated with 200 μM cadmium chloride plus a mild heat shock at 30ºC for 5 h resulted in an enhanced increase in the relative levels of both HSPs. Compared to A6 cells treated with one stressor alone, 200 μM cadmium chloride plus a heat shock at 30ºC significantly increased the accumulation of HSP30 and HSP70 protein ($p < 0.001$). Actin accumulation was detected in control cells and its relative levels remained relatively constant, with a slight decrease observed in the more intense treatments.

Further experiments, using western blot and densitometric analysis, were performed to determine if similar effects of a mild heat shock plus cadmium treatment held true for lower cadmium chloride concentrations. HSP30 and HSP70 protein were not detected in cells treated with a 30ºC heat shock or 10, 25, 50 or 100 μM cadmium chloride for 5 h (Figure 21 and 22). Treatment of A6 cells with 10 μM cadmium chloride plus a 30ºC heat shock for 5 h resulted in a

Figure 19. Effect of heat shock plus cadmium chloride on HSP30 and HSP70 protein accumulation in A6 cells. Cells were maintained at 22ºC (C) or treated with a 30ºC heat shock, 200 μM cadmium chloride or a combination of the two stressors for 5 h. Total protein was isolated and quantified and 20-40 μg was analyzed by immunoblotting using HSP30, HSP70 and actin antibodies. A Ponceau-S reversible stain confirms equal loading and efficient transfer.

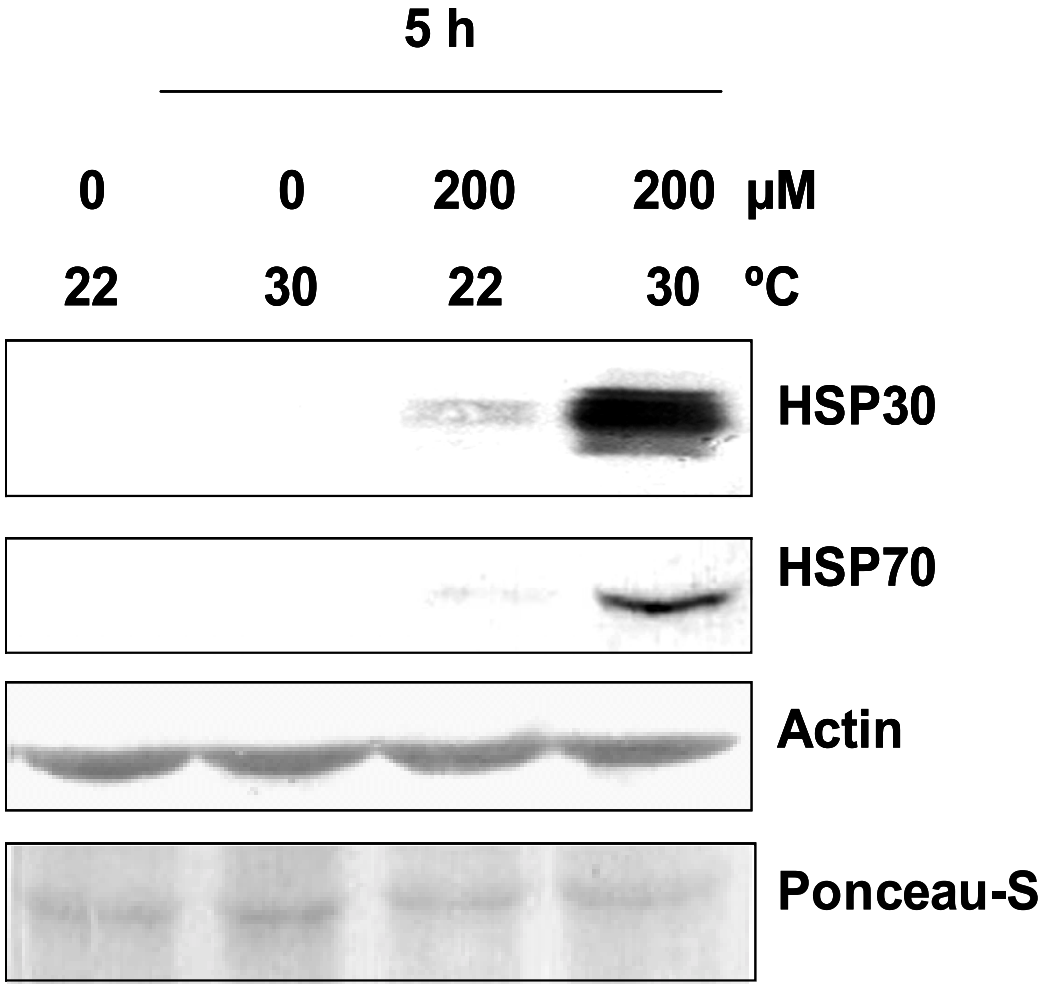
5 h
0
0
200
200 µM
22
30
22
30 °C
HSP30
HSP70
Actin
Ponceau-S

Figure 20. Accumulation of HSP30 and HSP70 protein after treatment with a mild heat plus cadmium exposure in A6 cells. ImageJ (1.38) software was used to perform densitometric analysis of protein bands from western blots. Data for HSP30 (solid bars) and HSP70 (open bars) were expressed as a percentage of the maximum hybridization within each blot and then graphed with the standard error, represented as vertical error bars. Significant differences between individual stressors and combined treatment are annoted for HSP30 (**, $p < 0.001$) and HSP70 ($\Delta\Delta$, $p < 0.001$).

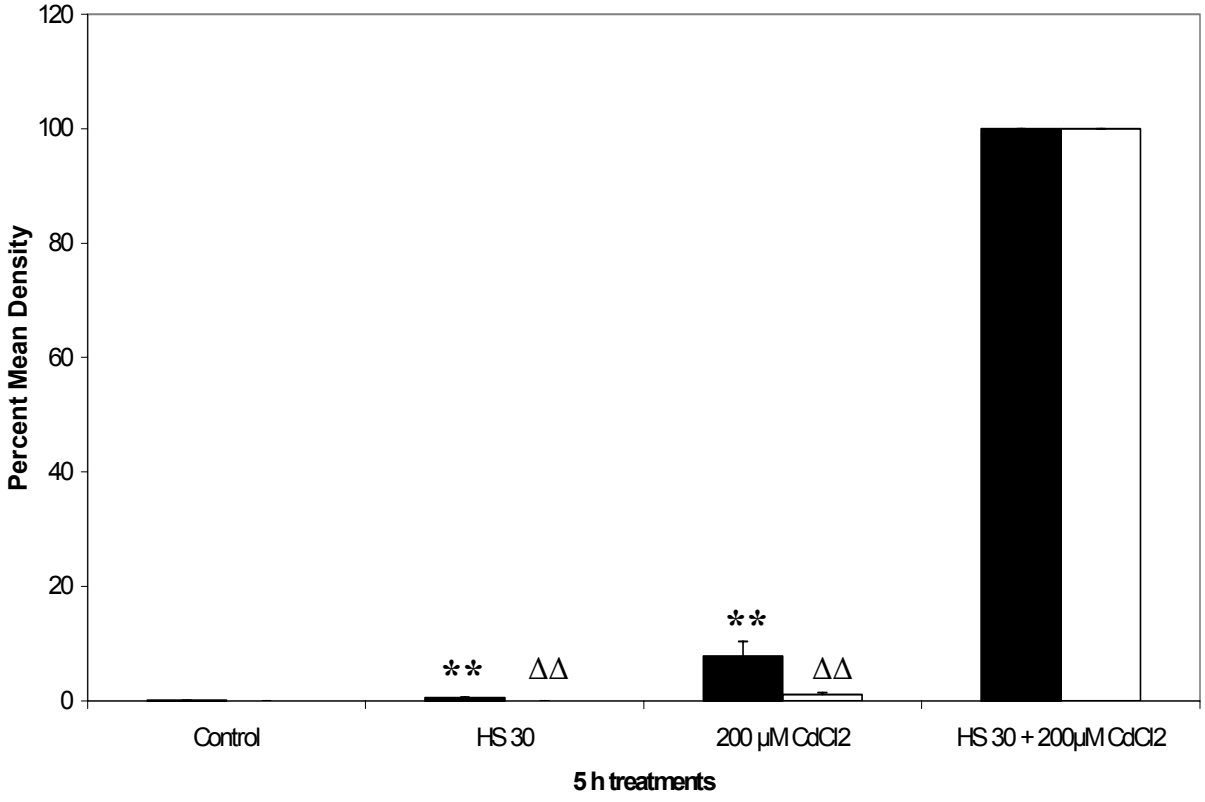
120
100
80
60
40
20
0
Percent Mean Density
**
ΔΔ
**
ΔΔ
Control
HS 30
200 µM CdCl2
HS 30 + 200µM CdCl2
5 h treatments

Figure 21. Concentration series showing accumulation of HSP30 and HSP70 protein in A6 cells after treatment with a mild heat shock plus cadmium. Cells were maintained at 22ºC (C) or subjected to either a 30ºC heat shock, a cadmium chloride treatment (10-100 μM) or a combination of two stressors. Cells were harvested and total protein was isolated. Total protein (20-40 μg) was analyzed by immunoblotting using HSP30 and HSP70 primary antibodies. The bottom panel shows a Ponceau-S reversible stain, which confirms equal loading and the quality of transfer.

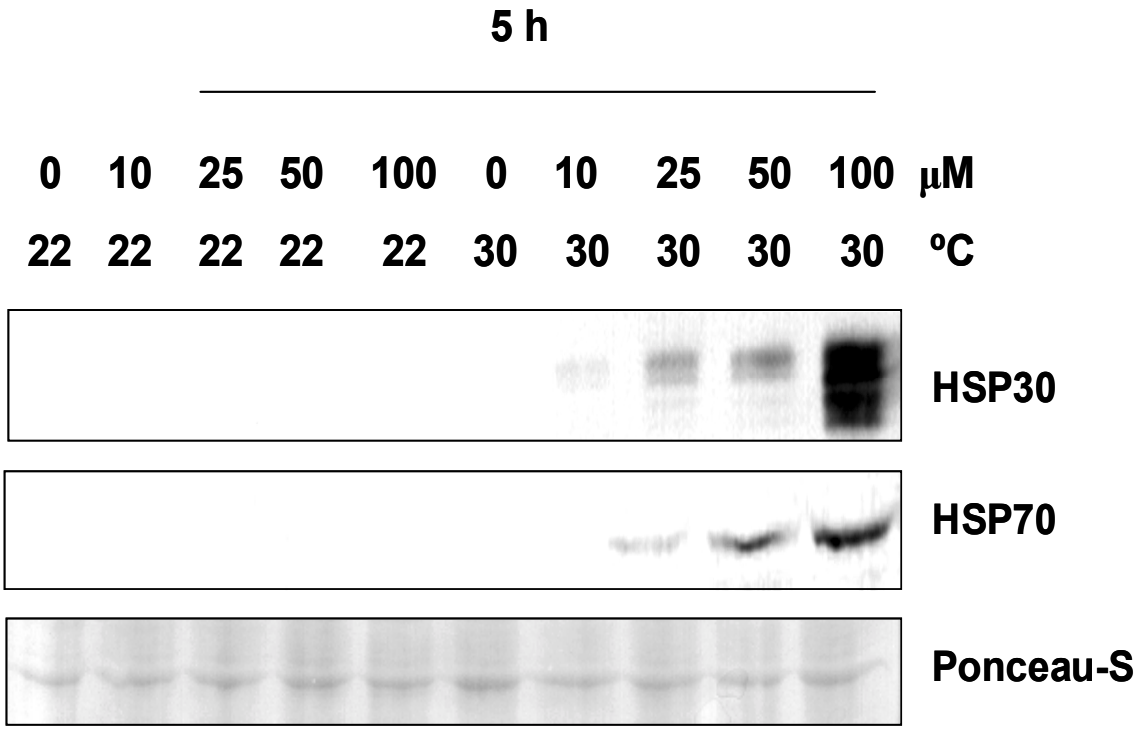
5 h
0 10 25 50 100 0 10 25 50 100 μM
22 22 22 22 22 30 30 30 30 30 ºC
HSP30
HSP70
Ponceau-S

Figure 22. Analysis of accumulation of HSP30 and HSP70 protein in A6 cells. Densitometric analysis was performed using ImageJ (1.38) software. Protein bands were analyzed from their respective western blots and the data for HSP30 (solid bars) and HSP70 (open bars) were expressed as a percentage of the maximum binding within each blot. Results were graphed with the standard error, which is represented as vertical error bars.

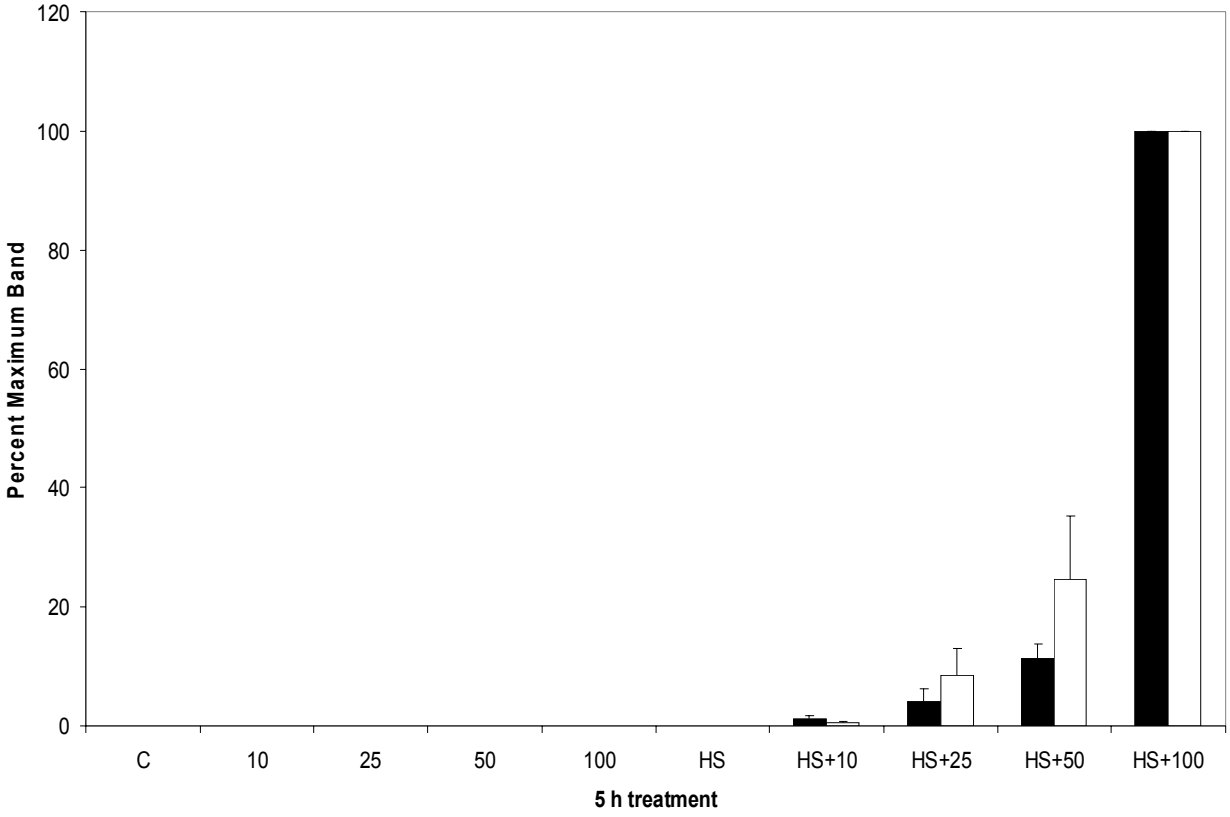
120
100
80
60
40
20
0
Percent Maximum Band
C
10
25
50
100
HS
HS+10
HS+25
HS+50
HS+100
5 h treatment

small accumulation of HSP30 (0.5% of the maximum band), whereas HSP70 protein was not detectable. Incubation of cells at 30ºC in the presence of 25 μM cadmium chloride for 5 h induced a small accumulation of HSP70 as well as a 3-fold increase in HSP30 compared to the 10 μM cadmium chloride plus a 30ºC heat shock treatment. Compared to the treatment that combined a heat shock at 30ºC with 25 μM, a heat shock in the presence of 50 μM showed a 3-fold increase in both HSP30 and HSP70 protein accumulation. A6 cells treated with 100 μM cadmium chloride with a 30ºC heat shock for 5 h resulted in greater enhanced levels of HSP30 and HSP70 protein (8- and 4-fold, respectively).

The next set of studies also examined the effects of combining two stressors, but in this case, the concentration of cadmium chloride was kept constant and the temperature of the heat shock was varied. Cells were maintained at 22ºC or treated with either a heat shock at 30ºC, 200 μM cadmium chloride or a combination of a mild heat shock (26, 28, 30ºC) plus the cadmium chloride treatment for 5 h. A 30ºC heat shock alone did not result in detectable amounts of HSP30 or HSP70, whereas treatment of cells with 200 μM cadmium chloride for 5 h resulted in a small accumulation of HSP30 (3% of the maximum band) but not HSP70 protein (Figure 23 and 24). Cells treated with a combination of the two stressors resulted in larger increases in the relative level of HSP30 and HSP70 protein. Both HSP30 and HSP70 protein accumulation increased with increasing temperature up to 30ºC. Compared to a heat shock at 26ºC with 200 μM cadmium chloride, treatment with 200 μM at 28ºC showed a 2-fold increase in both HSP30 and HSP70 protein, while treatment at 30ºC in the presence of cadmium chloride showed a 3-fold increase.

Figure 23. Effect of different temperatures on HSP30 and HSP70 protein accumulation in A6 cells exposed to 200 µM cadmium chloride. Cells were maintained at 22ºC (C) or treated with either a heat shock at 30ºC, 200 µM or a combination of mild heat shock (26, 28 or 30ºC) plus the cadmium treatment. Total protein was isolated and 20-40 µg was analyzed by immunoblotting using HSP30 and HSP70 antibodies. Equal loading and quality of transfer is confirmed via a reversible Ponceau-S stain.

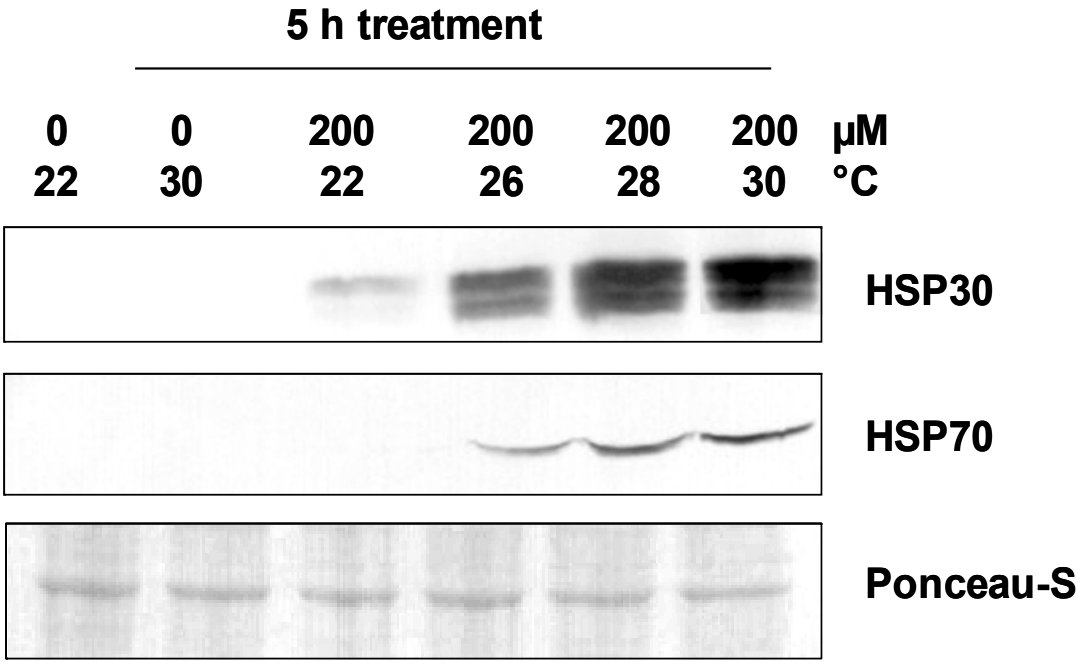
5 h treatment
0 0 200 200 200 200 µM
22 30 22 26 28 30 °C
HSP30
HSP70
Ponceau-S

Figure 24. Effect of temperature on cadmium-induced accumulation of HSP30 and HSP70 protein in A6 cells. ImageJ (1.38) software was used for densitometric analysis of HSP30 (solid bars) and HSP70 (open bars) protein on immunoblot images. Data were expressed as a percentage of the maximum binding within each blot and graphed. Vertical error bars represent the standard error.

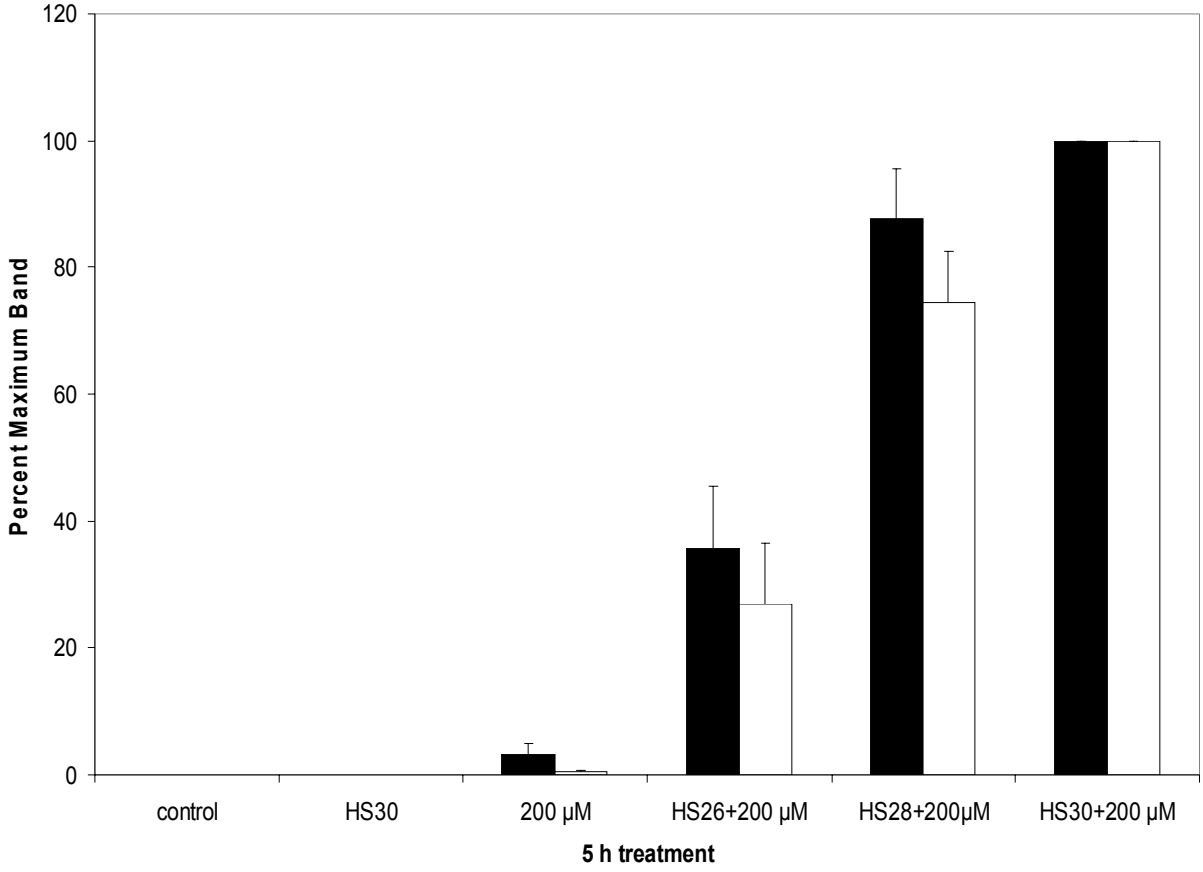
120
100
80
60
40
20
0
Percent Maximum Band
control
HS30
200 µM
HS26+200 µM
HS28+200µM
HS30+200 µM
5 h treatment

Immunocytochemistry and LSCM was then employed to examine the accumulation and localization of HSP30 in A6 cells treated with a mild heat shock plus cadmium. Cells were maintained at 22ºC or treated with either a heat shock at 30ºC, 200 µM cadmium chloride or a combination of the two for 5 h (Figure 25). HSP30 protein was not detectable in control cells (Figure 25, A-C) or cells incubated at 30ºC for 5 h (Figure 25, D-F). Cells treated with 200 µM cadmium chloride for 5 h resulted in low relative levels of HSP30 accumulation in the cytoplasm (Figure 25, G-I), whereas a combination of a mild heat shock and the cadmium treatment resulted in larger increases in HSP30 accumulation, as well as increased ruffled edges in areas of cell-to-cell contact (white asterisks) and actin disorganization (white arrows) (Figure 25, J-L). Further experiments examined the effect of cadmium chloride concentration in conjunction with a mild heat shock on HSP30 accumulation in A6 cells. Cells were maintained at 22ºC or 30ºC or treated with 10, 25 or 50 µM cadmium chloride for 5 h. Additionally, cells were heat shocked at 30ºC in the presence of either 10, 25 or 50 µM cadmium chloride for 5 h. HSP30 protein accumulation was not detectable in control cells (Figure 26, A-C), or in cells treated with 10 (Figure 26, D-F), 25 (Figure 26, G-I) or 50 µM (Figure 26, J-L) cadmium chloride alone. Further, cells incubated at 30ºC also did not result in HSP30 accumulation (Figure 26, M-O). However, treatment of A6 cells with a combination of stressors resulted in enhanced HSP30 levels. Incubation of cells at 30ºC in the presence of 10 µM cadmium chloride induced a small accumulation of HSP30 protein (Figure 26, P-R), whereas a larger increase in HSP30 accumulation was observed when cells were treated with 25 µM cadmium chloride plus heat shock at 30ºC (Figure 26, S-T). The abundance of HSP30 accumulation and proportion of cells exhibiting HSP30 accumulation increased with increasing cadmium chloride concentrations up to 50 µM (Figure 26, U-X).

Figure 25. Localization of HSP30 accumulation in A6 cells treated with a mild heat shock plus cadmium. Cells were grown on glass coverslips in L-15 media at 22 ºC. Cells were either maintained at 22ºC (A-C) or treated with a 30ºC heat shock (D-F), a 200 µM cadmium chloride treatment (G-I) or a combination of the two stressors (J-L) for 5 h. Actin and nuclei were detected directly by staining with TRITC (red) and DAPI (blue). HSP30 was indirectly detected with an anti-HSP30 antibody and Alexa-488 secondary antibody conjugate (green). Columns, from left to right, represent fluorescence detection channels for actin, HSP30 and merged images. HSP30 was not detected in cells heat shocked at 30ºC (D-F). Cells treated with 200 µM cadmium chloride (G-I) show low levels of HSP30 accumulation in the cytoplasm, as well as increased ruffling at cell edges (white asterisks). A combination of the two stressors (J-L) produced a relatively large increase of HSP30 accumulation in the cytoplasm. Further, actin fibers were disorganized (white arrows), cellular periphery showed ruffled edges in areas of cell-cell contact (white asterisks) and cells formed aggregates (J-L). The 10 µM white scale bar is indicated.

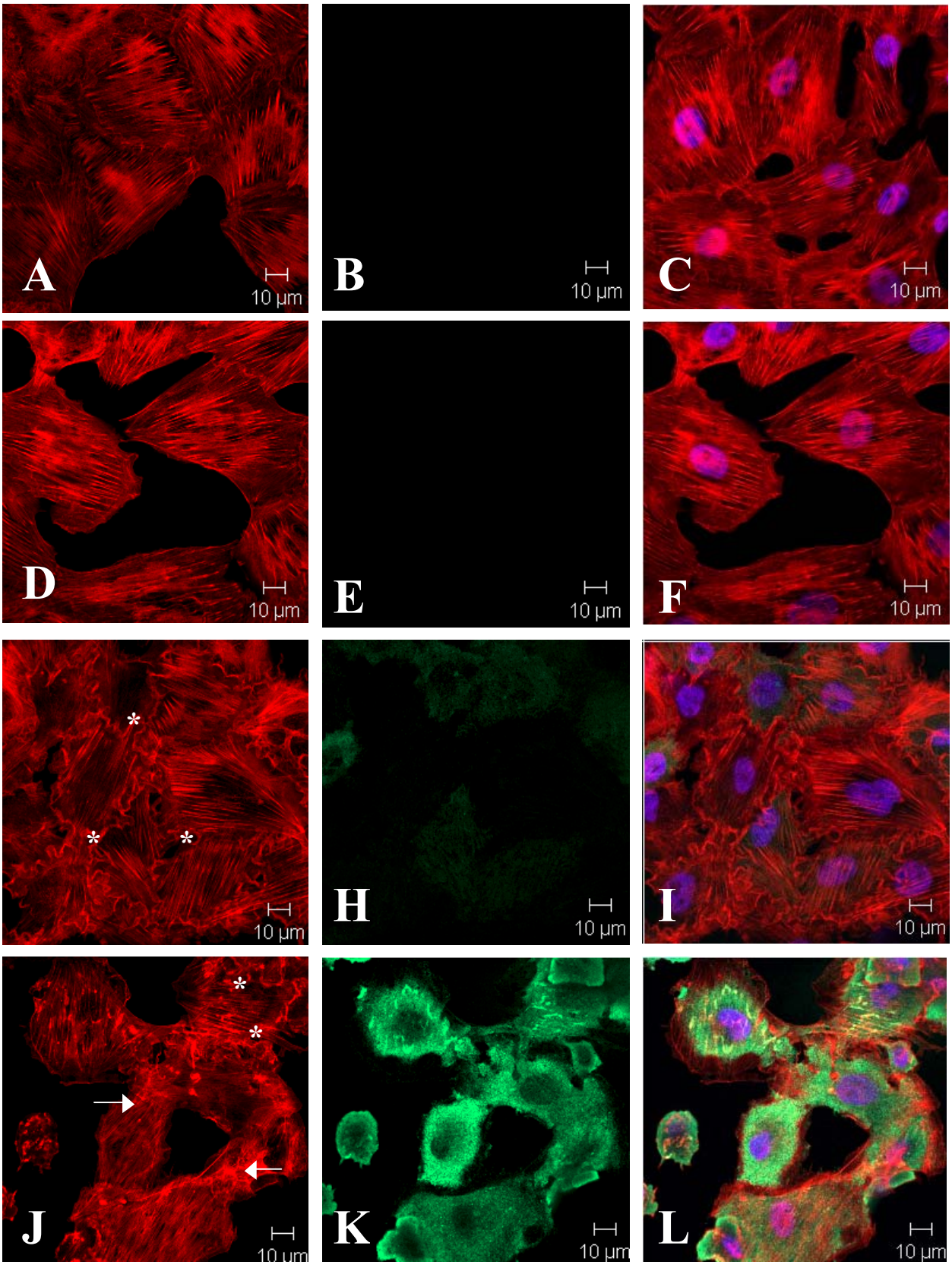
A
10 µm
B
10 µm
C
10 µm
D
10 µm
E
10 µm
F
10 µm
*
*
*
10 µm
H
10 µm
I
10 µm
*
*
J
10 µm
K
10 µm
L
10 µm

Figure 26. Accumulation of HSP30 in A6 cells treated with varying concentrations of cadmium plus a mild heat shock. Cells were grown on glass coverslips in L-15 media at 22 ºC. Cells were maintained at 22ºC (A-C) or treated with either 10 μM (D-F), 25 μM (G-I), 50 μM (J-L) cadmium chloride or a mild heat shock at 30ºC (M-O) for 5 h. Additionally, cells were heat shocked at 30ºC in the presence of either 10 μM (P-R), 25 μM (S-U) or 50 μM cadmium chloride (V-X). Actin and nuclei were directly stained with TRITC (red) and DAPI (blue), respectively. HSP30 was detected using an anti-HSP30 antibody and a secondary antibody conjugate, Alexa-488 (green). From left to right, columns show fluorescence detection channels for actin, HSP30 and merged channels with DAPI. Control cells (A-C), as well as cells treated with 10-50 μM cadmium chloride alone (D-L) did not result in the accumulation of HSP30. Cells treated with heat shock alone at 30ºC also did not display an accumulation of HSP30 (M-O). When the two stressors were combined, HSP30 accumulation was detected in low levels in cells treated with the lowest concentration of cadmium chloride (10 μM) (P-R). However, when cells were treated with higher concentrations of cadmium chloride (25 and 50 μM) in conjunction with a mild heat shock, enhanced HSP30 accumulation was observed in a concentration-dependent manner (S-X). Actin organization remained intact throughout control and experimental conditions (A-X). The 10 μM white scale bar is indicated.

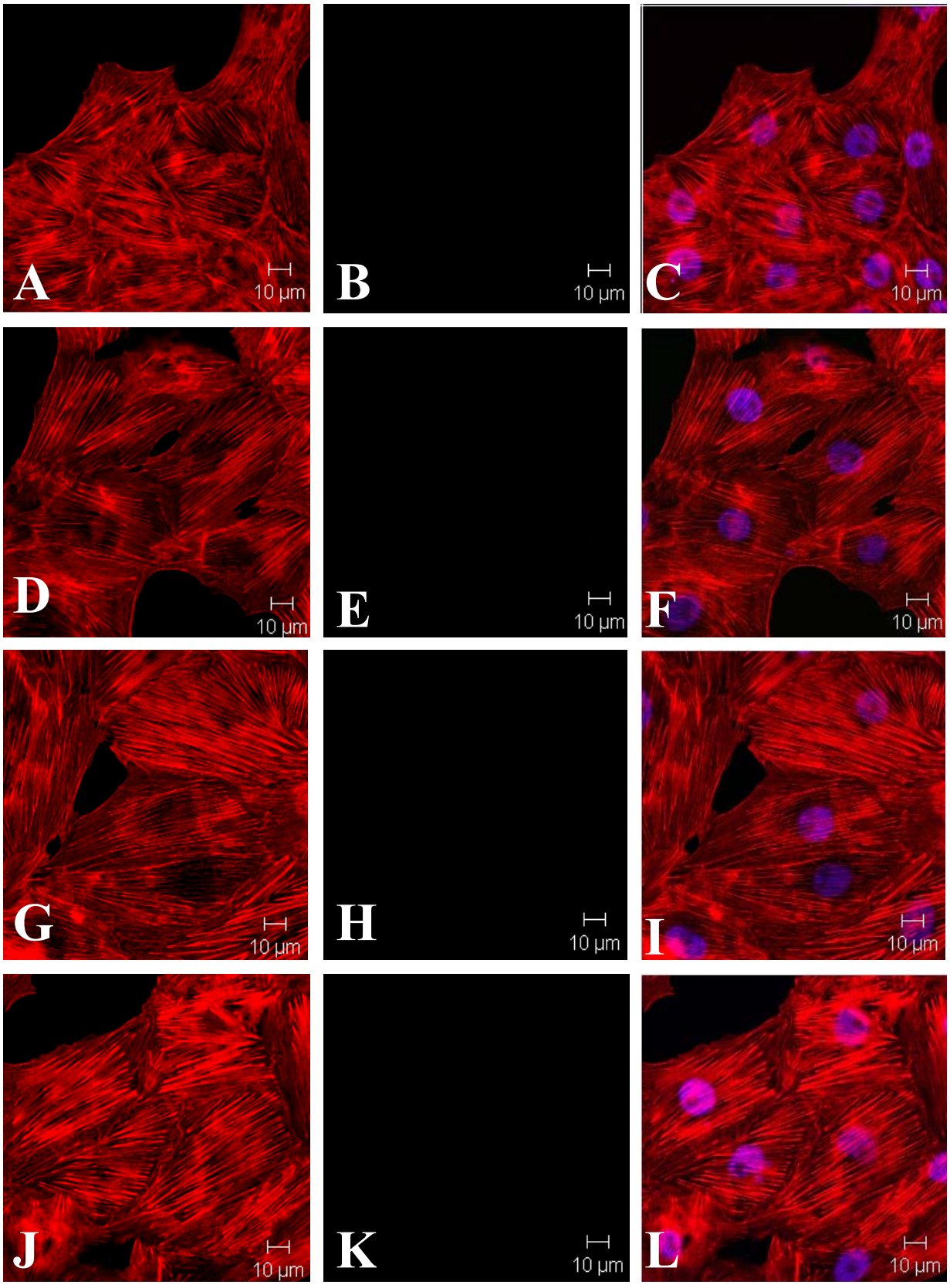
A
10 µm
B
10 µm
C
10 µm
D
10 µm
E
10 µm
F
10 µm
G
10 µm
H
10 µm
I
10 µm
J
10 µm
K
10 µm
L
10 µm

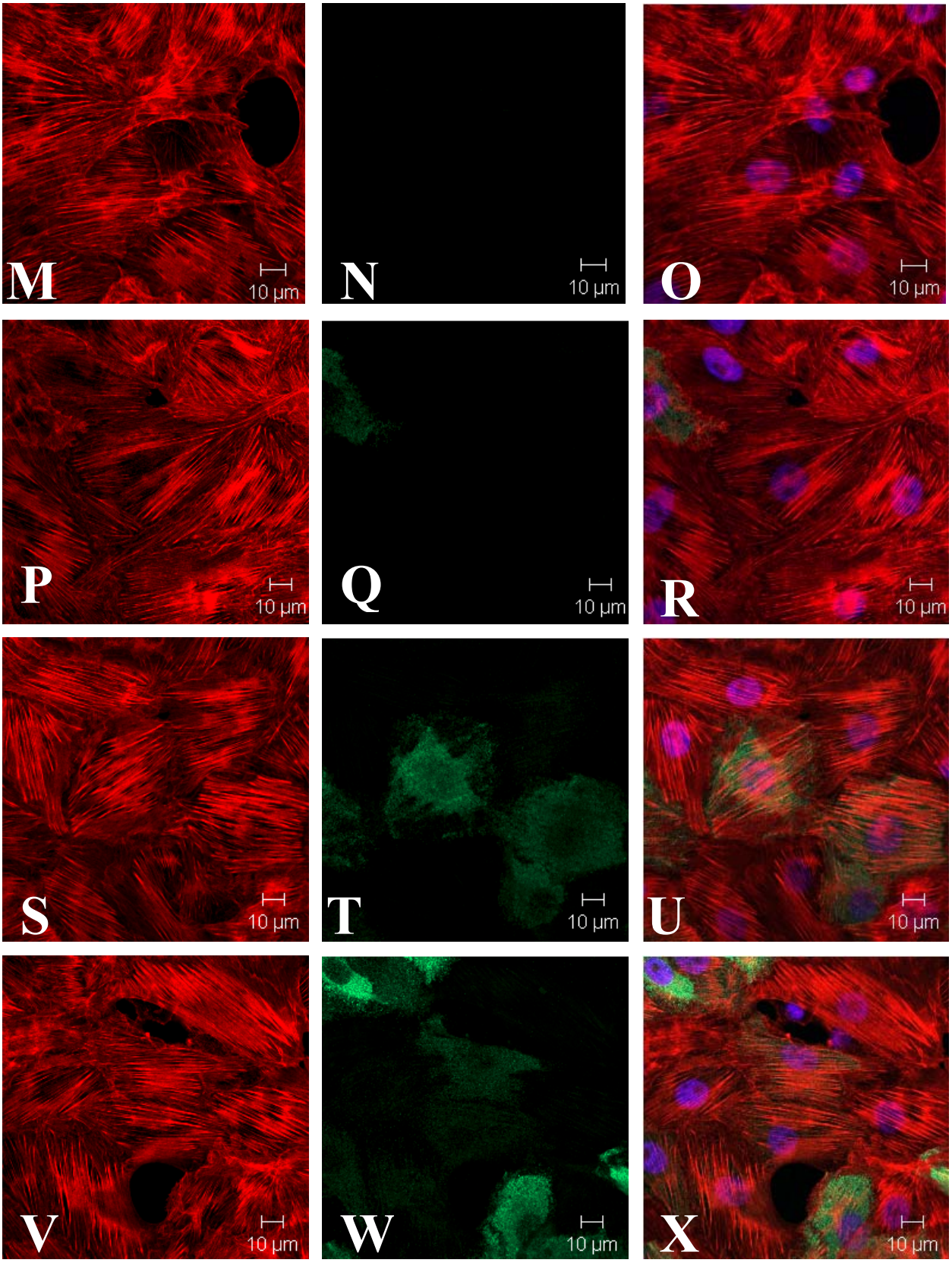
M
10 µm
N
10 µm
O
10 µm
P
10 µm
Q
10 µm
R
10 µm
S
10 µm
T
10 µm
U
10 µm
V
10 µm
W
10 µm
X
10 µm

A temperature profile of heat shock plus cadmium was then performed to observe its effects on HSP30 accumulation in A6 cells. Cells that were maintained at 22ºC (Figure 27, A-C) or incubated at 26ºC (Figure 27, D-F), 28ºC (Figure 27, G-I) or 30ºC (Figure 27, J-L) for 5 h did not result in HSP30 accumulation. A 5 h 100 μM cadmium chloride treatment induced the accumulation of HSP30 protein in some A6 cells (Figure 27, M-O). Cells treated with a combination of 100 μM plus a mild heat shock displayed a relatively large increase in HSP30 accumulation. HSP30 accumulation levels increased with increasing temperature when cells were heat shocked at 26, 28 or 30ºC in the presence of 100 μM cadmium chloride. While treatment of cells with 100 μM plus a 26ºC heat shock induced HSP30 (Figure 27, P-R), treatment of cells with 100 μM at 28ºC (Figure 27, S- U) or 30ºC (Figure 27, V-X) resulted in enhanced HSP30 levels. HSP30 remained localized to the cytoplasm, sometimes forming large granular structures (Figure 27, white arrows). Actin stress fibers remained intact when cells were subjected to one stress; however a combination of stressors resulted ruffled edges at the cellular periphery (Figure 27, white asterisks) and some actin disorganization (Figure 27, white triangles). Ruffled edges in areas of cell-cell contact and actin disorganization increased with increasing temperature during combination treatments.

Figure 27. Temperature profile of heat shock plus cadmium and its effects on HSP30 accumulation in A6 cells. Cells were grown on glass coverslips in L-15 media at 22 ºC. Control cells were maintained at 22ºC (A-C) or treated with either a heat shock at 26 ºC (D-F), 28 ºC (G-I), 30ºC (J-L) or 100 µM cadmium chloride (M-O) for 5 h. To examine the effects of more than one stressor on HSP30 accumulation, cells were also subjected to a combination of 100 µM with 26 ºC (P-R), 28 ºC(S-U) or 30ºC (V-X). TRITC (red) and DAPI (blue) were used to directly stain actin and nuclei, respectively. Secondary antibody conjugate Alexa-488 (green) was used with anti-HSP30 antibody to detect HSP30. From left to right, columns indicate fluorescence detection channels for actin, HSP30 and all three merged channels. As expected control cells were void of HSP30 (A-C). Cells heat shocked at 26, 28 and 30ºC also showed no accumulation of HSP30 (D-L). HSP30 was detected in low levels in cells treated with 100 µM cadmium chloride for 5 h (M-O). Enhanced accumulation was observed when cells were exposed to a combination of cadmium and a mild heat shock (P-X). HSP30 accumulation levels increased with increasing temperature (P-X). HSP30 remained localized to the cytoplasm and the formation of large structural granules (white arrows) was observed (P-X). Actin stress fibers remained intact when cells were subjected to one stress; however cells that experienced a combination of stressors displayed ruffled edges (asterisks) and some actin disorganization (white triangles) (P-X). Membrane ruffles and actin disorganization increased with increasing temperature (P-X). The 10 µM white scale bar is indicated.

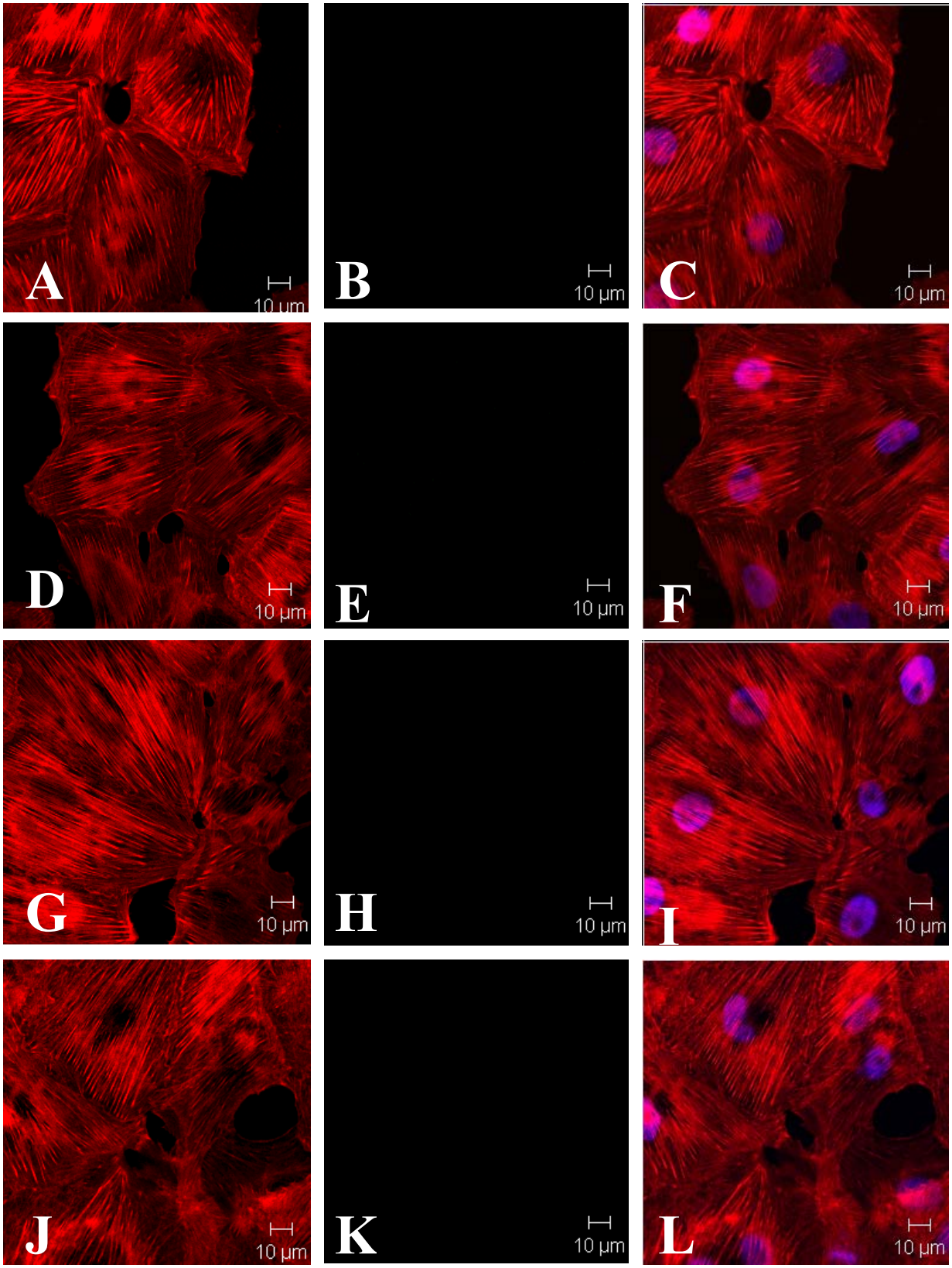
A
10 µm
B
10 µm
C
10 µm
D
10 µm
E
10 µm
F
10 µm
G
10 µm
H
10 µm
I
10 µm
J
10 µm
K
10 µm
L
10 µm

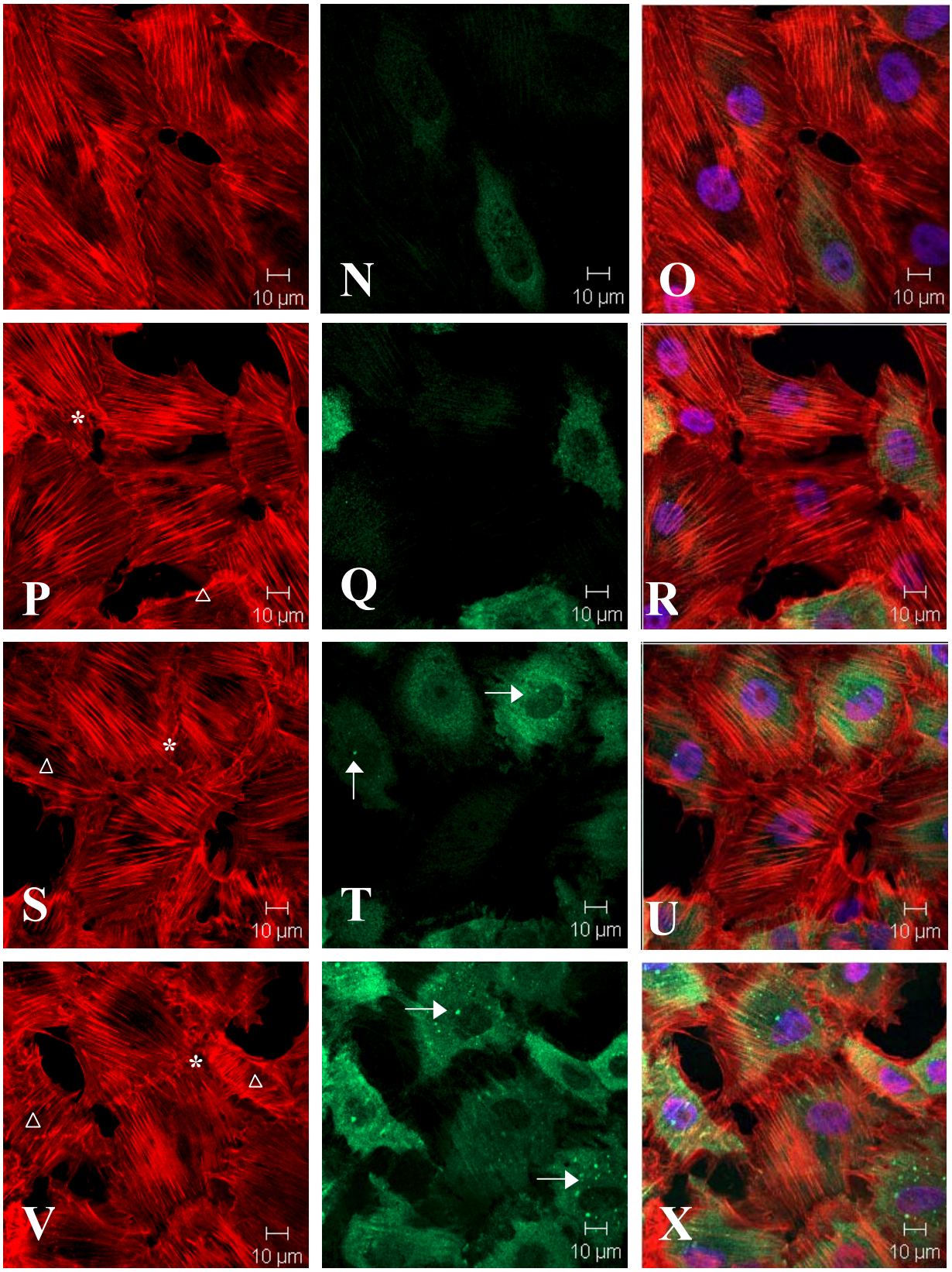
N
O
P
Q
R
S
T
U
V
X
10 µm

4 Discussion

The present study has characterized cadmium chloride-induced *hsp* gene expression in *Xenopus laevis* A6 cells. Initial studies demonstrated that treatment of A6 cells with cadmium chloride induced the accumulation of *hsp30* and *hsp70* mRNA. Relative levels of *hsp30* and *hsp70* transcripts increased with increasing concentrations of cadmium chloride. Also, both *hsp30* and *hsp70* mRNA accumulation increased with increasing duration of treatment to a maximum at 8 and 16h, respectively, which was followed by a decrease at 24 h. Preliminary studies also showed that treatment of A6 cells with cadmium chloride resulted in the accumulation of HSP30 and HSP70 protein. In time course studies, HSP30 was detected earlier than HSP70 accumulation; however, both reached maximum levels of accumulation at 14-16 h. These results are consistent with previously published results. In our laboratory, Gauley and Heikkila (2006) reported that a 200 μM cadmium chloride treatment for 5 h resulted in enhanced accumulation of both *hsp110* and *hsp70* mRNA in *Xenopus laevis* A6 cells. In other studies, a concentration-dependent increase in HSP27 and elevated HSP70 levels were detected in MDCK and LLC-PK1 renal epithelial cells treated with cadmium (Bonham *et al.,* 2003). Also, HSP70 induction in zebrafish was also found to be dependent on cadmium concentration (Hallare *et al.,* 2005).

Accumulation of stress-inducible HSPs is dependent on the activation of HSF1 and its subsequent binding to HSE, to initiate *hsp* gene expression. The specific interaction between HSF1 and HSE was shown to be enhanced in heat shocked *Xenopus laevis* embryos (Ovsenek and Heikkila, 1990). Also, Manwell and Heikkila (2007) demonstrated that KNK437, a HSF1 inhibitor which is known to inhibit HSF-HSE binding activity, reduced the heat shock-induced accumulation of *hsp30* in *Xenopus laevis* cultured cells. In the present study, it is probable that

cadmium induced *hsp* gene expression in A6 cells occurs through the activation of HSF1. Cadmium has been shown to induce HSE binding activity, resulting in the formation of an HSE/HSF-specific complex in *Xenopus laevis* oocytes (Gordon *et al.,* 1997). Also, Uenishi *et al.* (2006) demonstrated that HSF1 was activated by cadmium, resulting in the formation of HSF1/HSE complexes in HeLa cells. Although the mechanism by which a cell detects stress is unclear, it is thought that the presence of non-native or misfolded proteins triggers HSF1 activation, thereby initiating the heat shock response (Georgopoulos and Welch, 1993; Krebs and Feder, 1997; Morimoto, 1998; Pirkkala *et al.*, 2001). Cadmium has been shown to induce the generation of denatured or abnormal proteins by substituting for zinc in proteins or by reacting with vicinal thiol groups within cells (Waisberg *et al.,* 2003).

While both *hsp30* and *hsp70* mRNA and their respective proteins were induced by cadmium chloride, there were differences in the pattern of their expression and accumulation. For example, *hsp70* mRNA accumulation was detectable and reached its maximum several hours before *hsp30* mRNA. Dissimilarly, HSP30 protein was initially detected several hours earlier than HSP70 accumulation. Interestingly, a 14 h 400 μM cadmium chloride treatment resulted in a 60% decrease in relative levels of HSP70 protein, whereas HSP30 accumulation only decreased 8% from the maximum signal observed at 200 μM. Also, HSP30 protein levels did not decrease as rapidly as HSP70 protein during recovery from a cadmium chloride treatment. These results suggest that distinct patterns of *hsp30* and *hsp70* expression may be due to differences in regulation at the levels of transcription, translation and/or mRNA or protein stability. Differences in *hsp30* and *hsp70* mRNA levels during a recovery from heat shock have been previously noted (Darasch *et al.,* 1988). Further dissimilarities in expression between HSP30 and HSP70 protein may be caused by differences in sensitivity to stress or differences in demand, since HSP30 and

HSP70 have unique roles inside the cell. HSP30 and HSP70 are biologically different; HSP30 maintains proteins in a stable state, whereas HSP70 actively refolds proteins using ATP. Earlier studies have documented differences in expression patterns between HSPs with respect to stressor type, stage of development and tissue specificity (Bienz, 1984; Ali *et al.,* 1993; Lang *et al.,* 1999). It is also plausible that differences observed in HSP30 and HSP70 protein accumulation are a function of the binding efficiency of each antibody. However, it is important to note that *hsp30* and *hsp70* mRNA and their respective proteins are inducible by cadmium chloride, even if there is variation in their pattern of expression.

Recovery experiments demonstrated that *hsp* gene expression continued, even after the cadmium chloride treatment had been stopped. It was possible that A6 cells required additional time to recover from cellular damage produced by cadmium chloride. Cadmium was shown to produce reactive oxygen species, interfere with calcium signaling and cause DNA damage (Faurskov and Bjerregaard, 2002; Han *et al.,* 2007; Mouchet *et al.,* 2007). Continued expression of HSP30 may assist with returning cellular machinery back to a normal state. The decrease in the relative level of HSP30 accumulation 72 h after removal of the cadmium stressor could be an indication of the cells returning to normal conditions. Another possible explanation for the sustained level of HSP30 accumulation during recovery from cadmium chloride treatment, is that cadmium chloride is still present in the cells, even though the media were replaced. Cadmium is readily absorbed by the kidneys and has been shown to accumulate in the kidneys in amphibian species (Vogiatzis and Loumbourdis, 1997; Barbier *et al.,* 2004). Also, in *Xenopus laevis* embryos, it was found that cadmium uptake was directly related to the external cadmium concentration (Herkovits *et al.,* 1998). Furthermore, cadmium accumulation in the kidneys occurs in a time-dependent manner (Vogiatzis and Loumbourdis, 1998). If the intracellular

cadmium chloride in A6 cells was not excreted, it may still have exerted its adverse effects, thus requiring a continued accumulation of HSPs to manage this stress. In this instance, the decrease in HSP30 accumulation observed 72 h after removal of the cadmium stress could have been due to the breakdown of cellular machinery. However, A6 cells displayed normal morphology 72 h after the removal of cadmium chloride and the cadmium chloride treatment did not appear to inhibit cell growth or division, since cells were able to achieve normal confluency. If A6 cells retained cadmium chloride, it would have likely interfered with cell adherence and cell morphology would have been abnormal.

A synergistic increase in *hsp30* and *hsp70* mRNA levels and their respective proteins were observed when two stressors, which individually had a weak effect, were combined in A6 cells. This phenomenon was previously reported when a mild heat shock was combined with sodium arsenite in *Xenopus laevis* A6 cells (Heikkila *et al.,* 1987b). Also, a synergistic increase in the relative levels of *hsp30* and *hsp70* mRNA were observed in *Xenopus* A6 cells when heat shocked in the presence of herbimycin A or hydrogen peroxide (Briant *et al.,* 1997; Muller *et al.,* 2004). Further, enhanced synthesis of HSPs was demonstrated in mouse lymphocytes treated with elevated temperature plus ethanol (Rodenhiser *et al.,* 1986). The mechanism by which synergistic accumulation of HSPs was produced is not yet known; however, it could be explained by an increase in either the rate of transcription or stability of *hsp30* and *hsp70* mRNA, or stability of their proteins (Heikkila *et al.,* 1987b). It was also plausible that a combination of stressors caused a significant increase in denatured or misfolded protein, thereby increasing the magnitude of the heat shock response. This may be the case since heat and cadmium affect protein structure through different means.

The present study also examined the intracellular localization and accumulation of HSP30 in *Xenopus laevis* A6 cells after heat shock or cadmium chloride treatment. Immunocytochemistry and LSCM revealed that HSP30 accumulation was localized in the cytoplasm following cadmium chloride treatments, whereas HSP30 enrichment in the perinuclear region was observed following a heat shock at 35ºC for 2 h, with a 2 h recovery period. HSP30 may relocalize to the nucleus in A6 cells to protect target nuclear proteins; however the mechanism has yet to be described. Translocation of sHSPs from the cytosol to the nucleus during heat shock have been observed in *Drosophila* and mouse myoblasts (Beaulieu *et al.,* 1989; Adhikari *et al.,* 2004). A more detailed examination of HSP30 revealed the presence of large granular structures. HSP30 has been shown to form large multimeric structures in *Xenopus laevis* A6 cells (Ohan *et al.,* 1998b). An increase in molecular mass and the appearance of granules have been documented in other sHSP family members in response to stress (Leroux *et al., 1997*; Ehrnsperger *et al.,* 1997; Ehrnsperger *et al.,* 1999). The formation of a multimeric complex was imperative for sHSP chaperone function and prevention of protein aggregation (Leroux *et al.,* 1997; Ehrnsperger *et al*., 1997). Therefore, it is possible that the observed granules were a result of the formation of high molecular weight multimeric structures. A similar pattern of HSP30 expression was observed in *Xenopus laevis* A6 cells treated with sodium arsenite (Gellalchew and Heikkila, 2005).

While cadmium chloride treatments at low concentrations or durations did not induce a detectable alteration in A6 cell shape or F-actin structure, incubation of cells at higher cadmium concentrations resulted in localized areas of F-actin disorganization and ruffled edges at the cellular periphery, especially when cells were heat shocked in the presence of cadmium. Physiological stress results in alterations in cytoskeletal organization, such as the aggregation,

fragmentation or collapse of microfilaments, intermediate filaments and microtubules (Welch and Suhan, 1985; Wiegant *et al.,* 1987; Head and Goldman, 2000). The presence of HSPs has been implicated in the development of thermotolerance in the cytoskeleton, likely by protecting cytoskeletal proteins and maintaining the integrity of filaments (Wiegant *et al.,* 1987; Lavoie *et al.,* 1993; Mairesse *et al.,* 1996; Mounier and Arrigo, 2002).

Cells that experienced the most intense stressors resulted in the formation of cellular aggregates and/or cell rounding. The addition of cadmium chloride affected the settling and adherence of A6 cells, thereby inhibiting the development of confluent epithelia in *Xenopus laevis* (Bjerregaard, 2007). Cadmium specifically damages cadherin-dependent junctions between epithelial cells, which coincides with the loss of cell-to-cell contacts (Prozialeck *et al.,* 2003). Calcium-dependent cell adhesion molecules are an essential structural component of adherens junctions. Studies have suggested that cadmium may disrupt intercellular junctions by mimicking calcium (Prozialeck and Niewenhuis, 1991a; Prozialeck and Edwards, 2007). Also, cadmium caused time and concentration dependent changes in cell adherence, which resulted in complete separation of renal epithelial cells (Prozialeck and Niewenhuis, 1991b). In the present study, it is possible that cadmium chloride damaged or altered cadherin-dependent junctions, and disrupted actin filaments, resulting in a loss of adherence of A6 cells.

In summary, the present study has shown that cadmium chloride is an inducer of *hsp30* and *hsp70* gene expression in A6 cells. In future studies, it would be beneficial to examine the effects of cadmium chloride on the expression of other stress response genes, such as other HSP family members and the metallothioneins in A6 cells. As well, it would be valuable to characterize the pattern of *hsp* gene expression during development by exposing *Xenopus laevis* embryos to cadmium chloride. It was demonstrated that *Xenopus* embryos grown in media

containing cadmium chloride exhibited a concentration-dependent mortality and a concentration-related pattern of malformations (Sunderman *et al.,* 1991). Also, cadmium induced an increase *hsp70* and metallothionein gene expression in *Xenopus laevis* larvae (Mouchet *et al.,* 2006). However, it is not known if cadmium induces a tissue-specific enrichment of *hsp* gene expression during *Xenopus* development. Interestingly, an increase in cadmium resistance was noted in the late embryonic stage (hindlimb bud distinct) of *Xenopus*, which may be correlated with an enhancement of *hsp* gene expression (Herkovits *et al.,* 1998).

Future studies should also examine the effect of cadmium chloride on cell proliferation and cell death. Previously, it was demonstrated that cadmium chloride inhibited cell division, by inducing a dose-dependent increase in the proportion of G1 phase A6 cells in *Xenopus laevis* (Bjerregaard, 2007). Studies have also reported that cadmium induces apoptosis, likely through activating pathways that lead to cytochrome C release (Waisberg *et al.*, 2003; Wätjen and Beyersmann, 2004). Thus, it would be interesting to determine whether cadmium is able to induce apoptosis in the A6 cell, as well as in whole embryos.

HSP30 and HSP70 protein accumulation has been correlated with the acquisition of thermotolerance in *Xenopus* embryos and A6 cells (Heikkila *et al.,* 1985; Phang *et al.,* 1999). In Reuber H35 rat hepatoma cells, it was found that an initial cadmium exposure was followed by development of tolerance towards a second cadmium treatment, as well as additional increases in HSP accumulation (Wiegant *et al.,* 1997). Since cadmium chloride induces the accumulation of HSP30 and HSP70 in A6 cells, it would be interesting to examine its role in conferring thermotolerance or stress resistance.

The discovery of cadmium as an HSP inducer has proved to be a valuable biomarker for aquatic organisms. The synergistic effects of cadmium plus elevated temperatures may also be

beneficial, given aquatic organisms are often subjected to more than one stressor in their natural environments. In humans, the present findings may be important given that febrile states are often associated with kidney disease. Therefore, it is important to further characterize *hsp* gene expression so we can have a better understanding of how cells cope with cadmium stress.

References

Abdulle R, Mohindra A, Fernando P, Heikkila JJ. 2002. *Xenopus* small heat shock proteins, Hsp30C and Hsp30D, maintain heat- and chemically denatured luciferase in a folding-competent state. *Cell Stress and Chaperones*. 7(1): 6-16.

Adhikari AS, Sridhar Rao K, Rangaraj N, Parnaik VK, Mohan Rao Ch. 2004. Heat stress-induced localization of small heat shock proteins in mouse myoblasts: intranuclear lamin A/C speckles as target for alphaB-crystallin and Hsp25. *Exp Cell Res*. 299(2): 393-403.

Agnello M, Filosto S, Scudiero R, Rinaldi AM, Roccheri MC. 2007. Cadmium induces an apoptotic response in sea urchin embryos. *Cell Stress Chaperones*. 12(1): 44-50.

Ali A, Krone P, Heikkila JJ. 1993. Expression of the endogenous and microinjected *hsp30* genes in early *Xenopus laevis* embryos. *Dev. Gen*. 14: 42-50.

Ali A, Salter-Cid L, Flajnik MF, Heikkila JJ. 1996a. Isolation and characterization of a cDNA encoding a *Xenopus* 70-kDa heat shock cognate protein, Hsc70.I. *Comp Biochem Physiol B Biochem Mol Biol*. 113(4): 681-687.

Ali A, Salter-Cid L, Flajnik MF, Heikkila JJ. 1996b. Molecular cloning of a cDNA encoding a *Xenopus laevis* 70-kDa heat shock cognate protein, hsc70.II. *Biochim Biophys Acta*. 1309(3): 174-178.

Ali A, Fernando P, Smith WL, Ovsenek N, Lepock JR, Heikkila JJ. 1997. Preferential activation of HSF-binding activity and *hsp70* gene expression in *Xenopus* heart after mild hyperthermia. *Cell Stress Chaperones*. 2(4): 229-237.

Ali A, Bharadwaj S, O'Carroll R, Ovsenek N. 1998. HSP90 interacts with and regulates the activity of heat shock factor 1 in Xenopus oocytes. *Mol Cell Biol*. 18(9): 4949-4960.

Ananthan J, Goldberg AL, Voellmy R. 1986. Abnormal proteins serve as eukaryotic stress signals and trigger the activation of heat shock genes. *Science*. 232(4749): 522-524.

Arrigo AP. 2000. sHSPs as novel regulators of programmed cell death and tumorigenicity. *Pathol Biol (Paris)* 48: 280-288.

Audry S, Blanc G, Schäfer J. 2004. Cadmium transport in the Lot-Garonne River system (France) - temporal variability and a model for flux estimation. *Sci Total Environ*. 319(1-3): 197-213.

Barbe MF, Tytell M, Gower DH, Welch WJ. 1988. Hyperthermia protects against light damage in the rat retina. *Science*. 241: 1817-1820.

Barbier O, Jacquillet G, Tauc M, Poujeol P, Cougnon M. 2004. Acute study of interaction among cadmium, calcium, and zinc transport along the rat nephron in vivo.*Am J Physiol Renal Physiol.* 287(5): 1067-1075.

Beaulieu JF, Arrigo AP, Tanguay RM. 1989. Interaction of Drosophila 27,000 Mr heat-shock protein with the nucleus of heat-shocked and ecdysone-stimulated culture cells. *J Cell Sci.* 92(Pt 1): 29-36.

Beckman RP, Mizzen LE, Welch WJ. 1990. Interaction of Hsp 70 with newly synthesized proteins: implications for protein folding and assembly. *Science*. 248(4957): 850-854.

Bharadwaj S, Hnatov A, Ali A, Ovsenek N. 1998. Induction of the DNA-binding and transcriptional activities of heat shock factor 1 is uncoupled in Xenopus oocytes.
Biochim Biophys Acta. 1402(1):79-85.

Bienz M. 1984a. Xenopus hsp 70 genes are constitutively expressed in injected oocytes. *EMBO J*. 3(11): 2477-2483.

Bienz M. 1984b. Developmental control of the heat shock response in Xenopus. *Proc Natl Acad Sci U S A*. 81(10): 3138–3142.

Bjerregaard H. 2007. Effects of cadmium on differentiation and cell cycle progression in cultured Xenopus kidney distal epithelial (A6) cells. *Altern Lab Anim*. 35(3): 343-348.

Bonham RT, Fine MR, Pollock FM, Shelden EA. 2003. Hsp27, Hsp70 and metallothionein in MDCK and LLC-PK1 renal epithelial cells: effects of prolonged exposure to cadmium. *Toxicology and Applied Pharmacology*. 191: 63-73.

Bova MP, Yaron O, Huang Q, Ding L, Haley DA, Stewart PL, Horwitz J. 1999. Mutation R120G in alphaB-crystallin, which is linked to a desmin-related myopathy, results in an irregular structure and defective chaperone-like function. *Proc Natl Acad Sci U S A*. 96 (11): 6137-6142.

Briant D, Ohan N, Heikkila JJ. 1997. Effect of herbimycin A on hsp30 and hsp70 heat shock protein gene expression in *Xenopus* cultured cells. *Biochem Cell Bio*. 75: 777-782.

Bruce JL, Price BD, Coleman N, Calderwood SK. 1993. Oxidant injury rapidly activates the heat shock transcription factor but fails to increase levels of heat shock proteins. *Cancer Res.* 53: 12-15.

Cao X-J, Chen R, Li A-P, Zhou J-W. 2007. *JWA* gene is involved in cadmium-induced growth inhibition and apoptosis in HEK-293T cells. *Journal of Toxicology and Environmental Health, Part A*. 70: 931-937.

Choudhuri S, McKim JM Jr, Klaassen CD. 1993. Differential expression of the metallothionein gene in liver and brain of mice and rats. *Toxicol Appl Pharmacol*. 119 (1): 1-10.

Ciocca DR, Adams DJ, Edwards DP, Bjercke RJ, McGuire WL. 1983. Distribution of an estrogen-induced protein with a molecular weight of 24,000 in normal and malignant human tissues and cells. *Cancer Res*. 43(3) :1204-1210.

Ciocca DR, Oesterreich S, Chamness GC, McGuire WL, Fuqua SAW. 1993. Biological and clinical implications of heat shock protein 27000 (Hsp27): a review. *Journal of the National Cancer Institute*. 85(19): 1558-1570.

Darasch S, Mosser DD, Bols NC, Heikkila JJ. 1988. Heat shock gene expression in *Xenopus laevis* A6 cells in response to heat shock and sodium arsenite treatments. *Biochem. Cell Biol*. 66: 862-868.

Daugaard M, Rohde M, Jäättelä. 2007. The heat shock protein 70 family: highly homologous proteins with overlapping and distinct functions. *FEBS Letters*. 581: 3702-3710.

Davis RE, King ML. 1989. The developmental expression of the heat-shock response in *Xenopus laevis*. *Development.* 105: 213-222.

Djabali K, de Nechaud B, Landon F, Portier M-M. 1997. aB-crystallin interacts with intermediate filaments in response to stress. *J Cell Sci.* 110: 2759-2769.

Ehrnsperger M, Gräber S, Gaestel M, Buchner J. 1997. Binding of non-native protein to Hsp25 during heat shock creates a reservoir of folding intermediates for reactivation. *The EMBO Journal*. 16(2): 221-229.

Ehrnsperger M, Lilie H, Gaestel M, Buchner J. 1999. The dynamics of Hsp25 quaternary structure. *J Biol Chem.* 274(21): 14867-14874.

Fang MZ, Mar W, Cho MH. 2002. Cadmium affects genes involved in growth regulation during two-stage transformation of Balb/3T3 cells. *Toxicology.* 177(2-3): 253-265.

Farkas T, Kutskova YA, Zimarino V. 1998. Intramolecular repression of mouse heat shock factor 1. *Mol Cell Biol*. 18(2): 906-918.

Faurskov B, Bjerregaard HF. 2002. Evidence for cadmium mobilization of intracellular calcium through a divalent cation receptor in renal distal epithelial A6 cells. *Pflugers Arch - Eur J Physiol.* 445: 40–50

Fernando P, Heikkila JJ. 2000. Functional characterization of *Xenopus* small heat shock protein, Hsp30C: the carboxyl end is required for stability and chaperone activity. *Cell Stress and Chaperones*. 5(2): 148-159.

Fernando P, Abdulle R, Mohindra A, Guillemette JG, Heikkila JJ. 2002. Mutation or deletion of the C-terminal tail affects function and structure of *Xenopus laevis* small heat shock protein, hsp30. *Comparative Biochemistry and Physiology. Part B.* 133: 95-103.

Fernando P, Megeny LA, Heikkila JJ. 2003. Phosphorylation-dependent structural alterations in the small hsp30 chaperone are associated with cellular recovery. *Experimental Cell Research.* 286: 175-185.

Fort DJ, Stover EL, Bantle JA, Dumont JN, Finch RA. 2001. Evaluation of reproductive toxicity assay using *Xenopus laevis*: boric acid, cadmium and ethylene glycol monomethyl ether. *Journal of Applied Toxicology*. 21: 41-52.

Freeman BC, Morimoto RI. 1996. The human cytosolic molecular chaperones hsp90, hsp70 (hsc70) and hdj-1 have distinct roles in recognition of a non-native protein and protein refolding. *EMBO J.* 15(12): 2969-2979.

Freeman BC, Myers MP, Schumacher R, Morimoto RI. 1995. Identification of a regulatory motif in Hsp70 that affects ATPase activity, substrate binding and interaction with HDJ-1. *EMBO J.* 14(10): 2281-2292.

Ganea E. 2001. Chaperone-like activity of α-crystallin and other small heat shock proteins. *Current Protein and Peptide Science*. 2: 205-225.

Gauley J, Heikkila JJ. 2006. Examination of the expression of the heat shock protein gene, hsp110, in Xenopus laevis cultured cells and embryos. *Comp Biochem Physiol A Mol Integr Physiol*. 145(2) :225-234.

Gellalchew M, Heikkila JJ. 2005. Intracellular localization of *Xenopus* small heat shock protein, hsp30, in A6 kidney epithelial cells. *Cell Biology International*. 29: 221-227.

Georgopoulous C, Welch WJ. 1993. Role of the major heat shock proteins as molecular chaperones. *Annu. Rev. Cell Biol*. 9: 601-634.

Giffard RG, Xu L, Zhao H, Carrico W, Ouyang Y, Qiao Y, Sapolsky R, Steinberg G, Hu B, Yenari MA. 2004. Chaperones, protein aggregation, and brain protection from hypoxic/ischemic injury. *J Exp Biol.* 207: 3213-3220.

Goloubinoff P, De Los Rios P. 2007. The mechanism of Hsp70 chaperones: (entropic) pulling the models together. *TRENDS in Biochemical Sciences.* 32(8): 372-380.

Goodson ML, Park-Sarge OK, Sarge KD. 1995. Tissue-dependent expression of heat shock factor 2 isoforms with distinct transcriptional activities. *Mol Cell Biol.* 15(10): 5288-5293.

Gordon S, Bharadwaj S, Hnatov A, Ali A, Ovsenek N. 1997. Distinct stress-inducible and developmentally regulated heat shock transcription factors in Xenopus oocytes. *Dev Biol.* 181(1): 47-63.

Hallare AV, Schirling M, Luckenbach T, Kohler H-R, Triebskorn R. 2005. Combined effects of temperature and cadmium on developmental parameters and biomarker responses in zebrafish (*Danio rerio*) embryos. *Journal of Thermal Biology*. 30: 7-17.

Han SG, Castranova V, Vallyathan V. 2007. Comparative cytotoxicity of cadmium and mercury in a human bronchial epithelial cell line (BEAS-2B) and its role in oxidative stress and induction of heat shock protein 70. *Journal of Toxicology and Environmental Health, Part A*. 70: 852-860.

Haslbeck M. 2002. sHsps and their role in the chaperone network. *Cell. Mol. Life Sci.* 59: 1649-1657.

Head MW, Goldman JE. 2000. Small heat shock proteins, the cytoskeleton, and inclusion body formation. *Neuropathol Appl Neurobiol*. 26(4): 304-312.

Heikkila JJ, Kloc M, Bury J, Schultz GA, Browder LW. 1985. Acquisition of the heat-shock response and thermotolerance during early development of *Xenopus laevis*. *Developmental Biology*. 107: 483-489.

Heikkila JJ, Ovsenek N, Krone PH. 1987a. Examination of heat shock protein mRNA accumulation in early *Xenopus laevis* embryos. *Biochm. Cell Biol*. 65: 87-94.

Heikkila JJ, Darasch SP, Mosser DD, Bols NC. 1987b. Heat and sodium arsenite act synergistically on the induction of heat shock gene expression in *Xenopus laevis* A6 cells. *Biochem Cell Biol*. 65: 310-316.

Heikkila JJ, Ohan N, Tam Y, Ali A. 1997. Heat shock protein gene expression during *Xenopus* development. *Cellular and Molecular Life Sciences*. 53: 114-121.

Heikkila JJ. 1990. Expression of cloned genes and translation of messenger RNA in microinjected Xenopus oocytes. *Int J Biochem*. 22(11): 1223-1228.

Heikkila JJ. 2003. Expression and function of small heat shock protein genes during *Xenopus* development. *Seminars in Cell and Developmental Biology*. 14: 259-266.

Heikkila JJ. 2004. Regulation and function of small heat shock protein genes during amphibian development. *Journal of Cellular Biology*. 93: 672-680.

Herkovits J, Cardellini P, Pavanati C, Pérez-Coll CS. 1998. Cadmium uptake and bioaccumulation in *Xenopus laevis* embryos at different developmental stages. *Ecotoxicology and Environmental Safety*. 39: 21-26.

Herrin DL, Schmidt GW. 1988. Rapid, reversible staining of northern blots prior to hybridization. *Biotechniques*. 6(3): 196-197, 199-200.

Hitotsumatsu T, Iwaki T, Fukui M, Tateishi J. 1996. Distinctive immunohistochemical profiles of small heat shock proteins (heat shock protein 27 and alpha B-crystallin) in human brain tumors. *Cancer*. 77(2): 352-361.

Jäättelä M. 1995. Over-expression of hsp70 confers tumorigenicity to mouse fibrosarcoma cells. *Int J Cancer*. 60(5) :689-93.

Jin T, Lu J, Nordberg M. 1998. Toxicokinetics and biochemistry of cadmium with special emphasis on the role of metallothionein. *Neurotoxicology*. 19(4-5): 529-535.

Kim YK, Jang SK. 2002. Continuous heat shock enhances translational initiation directed by internal ribosomal entry site. *Biochem Biophys Res Commun*. 297(2): 224-231.

Klemenz R, Andrews A-C, Fröhli E, Schäfer R, Aoyama A. 1993. Expression of the murine small heat shock proteins hsp25 and αB crystalline in the absence of stress. *The Journal of Cell Biology*. 120(3): 639-645.

Krebs RA, Feder ME. 1997. Tissue-specific variation in Hsp70 expression and thermal damage in *Drosophila melanogaster* larvae. *The Journal of Experimental Biology*. 200: 2007-2015.

Kregel KC. 2002. Heat shock proteins: modifying factors in physiological stress responses and acquired thermotolerance. *J Appl Physiol*. 92: 2177-2186.

Krone PH, Snow A, Ali A, Pasternak JJ, Heikkila JJ. 1992. Comparison of the regulatory and structural regions of *Xenopus laevis* small heat-shock protein-encoding gene family. *Gene*. 110: 159-166.

Kundu M, Sen PC, Das KP. 2007. Structure, stability, and chaperone function of alpha A-crystallin: role of N-terminal region. *Biopolymers*. 86(3): 177-192.

Lambert H, Charette SJ. Bernier AF, Guimond A, Landry J. 1999. HSP27 multimerization mediated by phosphorylation-sensitive intermolecular interactions at the amino terminus. *J Biol Chem.* 274(14): 9378-9385

Lang L, Miskovic D, Fernando P, Heikkila JJ. 1999. Spatial pattern of constitutive and heat shock-induced expression of the small heat shock protein gene family hsp30, in *Xenopus laevis* tailbud embryos. *Dev Genet*. 25(4): 365-374.

Lang L, Miskovic D, Lo M, Heikkila JJ. 2000. Stress-induced, tissue-specific enrichment of hsp70 mRNA accumulation in Xenopus laevis embryos. *Cell Stress and Chaperones*. 5(1): 36-44.

Lavoie JN, Gingras-Breton G, Tanguay RM, Landry J. 1993. Induction of Chinese hamster HSP27 gene expression in mouse cells confers resistance to heat shock. HSP27 stabilization of the microfilament organization. *J Biol Chem*. 268(5): 3420-3429.

Lentze N, Studer S, Narberhaus F. 2003. Structural and functional defects caused by point mutations in the alpha-crystallin domain of a bacterial alpha-heat shock protein.
J Mol Biol. 328(4): 927-937.

Leroux MR, Melki R, Gordon B, Batelier G, Candido EPM. 1997. Structure-function studies on small heat shock protein oligomeric assembly and interaction with unfolded polypeptides. *J Biol Chem*. 272(39): 24646-24656.

Lienesch LA, Dumont JN, Bantle JA. 2000. The effect of cadmium on oogenesis on *Xenopus laevis*. *Chemosphere*. 41: 1651-1658.

Lindquist S. 1986. The heat shock response. *Ann. Rev. Biochem*. 55: 1151-1191.

Liu F, Inageda K, Nishitai G, Matsuoka M. 2006. Cadmium induces the expression of Grp78, an endoplasmic reticulum molecular chaperone, in LLC-PK1 renal epithelial cells. *Environmental Health Persepectives*. 114(6): 859-864.

Lohiya NK. 1976. Effects of cadmium chloride on the testis and sex accessory glands of the Indian palm squirrel, Funambulus pennanti (Wroughthon). *Acta Eur Fertil*. 7(3): 257-265.

Loumbourdis NS. 2005. Hepatotoxic and nephrotoxic effects of cadmium in the frog *Rana ridibunda*. *Arch Toxicol*. 79: 434-440.

MacRae TH. 2000. Structure and function of small heat shock/α-crystallin proteins: established concepts and emerging ideas. *Cell. Mol. Life Sci*. 57: 899-913.

Mairesse N, Horman S, Mosselmans R, Galand P. 1996. Antisense inhibition of the 27 kDa heat shock protein production affects growth rate and cytoskeletal organization in MCF-7 cells. *Cell Biol Int.* 20(3): 205-212.

Manwell LA, Heikkila JJ. 2007. Examination of KNK437- and quercetin-mediated inhibition of heat shock-induced heat shock protein gene expression in Xenopus laevis cultured cells. *Comp Biochem Physiol A Mol Integr Physiol*. 148(3): 521-530.

Martins RJ, Pardo R, Boaventura RA. 2004. Cadmium(II) and zinc(II) adsorption by the aquatic moss Fontinalis antipyretica: effect of temperature, pH and water hardness. *Water Res*. 38(3): 693-699.

Mendez-Armenta M, Rios C. 2007. Cadmium neurotoxicity. *Environmental Toxicology and Pharmacology*. 23: 350-358.

Mercier PA, Winegarden NA, Westwood JT. 1999. Human heat shock factor 1 is predominantly a nuclear protein before and after heat stress. *J Cell Sci*. 112(Pt 16): 2765-2774.

Miskovic D, Heikkila JJ. 1999. Constitutive and stress-inducible expression of the endoplasmic reticulum heat shock protein 70 gene family member, immunoglobulin-binding protein (BiP), during Xenopus laevis early development. *Dev Genet*. 25(1): 31-39.

Morimoto RI. 1998. Regularion of the heat shock transcriptional response: cross talk between a family of heat shock factors, molecular chaperones and negative regulators. *Genes and Development*. 12: 3788-3796.

Mosser DD, Caron AW, Bourget L, Denis-Larose C, Massie B. 1997. Role of the human heat shock protein hsp70 in protection against stress-induced apoptosis. *Mol Cell Biol*. 17(9): 5317-5327.

Mouchet F, Baudrimont M, Gonzalez P, Cuenot Y, Bourdineaud JP, Boudou A, Gauthier L. 2006. Genotoxic and stress inductive potential of cadmium in *Xenopus laevis* larvae. *Aquatic Toxicology*. 78: 157-166.

Mouchet F, Gauthier L, Baudrimont M, Gonzalez P, Mailhes C, Ferrier V, Devaux A. 2007. Comparative evaluation of the toxicity and genotoxicity of cadmium in amphibian larvae (*Xenopus laevis* and *Pleurodeles waltl*) using the comet assay and the micronucleus test. *Environmental Toxicology*. 22: 422-435.

Mounier N, Arrigo AP. 2002. Actin cytoskeleton and small heat shock proteins: how do they interact? *Cell Stress Chaperones*. 7(2): 167-176.

Muller M, Gauley J, Heikkila JJ. 2004. Hydrogen peroxide induces heat shock protein and *proto-oncogene* mRNA accumulation in *Xenopus laevis* A6 kidney epithelial cells. *Can. J. Physiol. Pharamcol*. 82: 523-529.

Munro S, Pelham HR. 1986. An Hsp70-like protein in the ER: identity with the 78 kd glucose-regulated protein and immunoglobulin heavy chain binding protein. *Cell*. 46(2): 291-300.

Munro S, Pelham HR. 1987. A C-terminal signal prevents secretion of luminal ER proteins. *Cell*. 48(5): 899-907.

Nakai A, Kawazoe Y, Tanabe M, Nagata K, Morimoto RI. 1995. The DNA-binding properties of two heat shock factors, HSF1 and HSF3, are induced in the avian erythroblast cell line HD6. *Mol Cell Biol*. 15(10): 5268-5278.

Nakai A, Tanabe M, Kawazoe Y, Inazawa J, Morimoto RI, Nagata K. 1997. HSF4, a new member of the human heat shock factor family which lacks properties of a transcriptional activator. *Mol Cell Biol*. 17(1): 469-481.

Newton EM, Knauf U, Green M, Kingston RE. 1996. The regulatory domain of human HSF1 is sufficient to sense heat stress. *Mol Cell Biol*. 16: 839-846

Njemini R, Lambert M, Demanet C, Kooijman R, Mets T. 2007. Basal and infection-induced levels of heat shock proteins in human aging. *Biogerontology*. 8(3): 353-364.

Nollen EA, Morimoto RI. 2002. Chaperoning signaling pathways: molecular chaperones as stress-sensing 'heat shock' proteins. *J Cell Sci*. 115(Pt 14): 2809-2816.

Nowak TS Jr, Bond U, Schlesinger MJ. 1990. Heat shock RNA levels in brain and other tissues after hyperthermia and transient ischemia. *J Neurochem*. 54(2): 451-458.

Ohan NW, Heikkila JJ. 1995. Involvement of differential gene expression and mRNA stability in the developmental regulation of the hsp 30 gene family in heat-shocked Xenopus laevis embryos. *Developmental Genetics*. 7(2): 176-84.

Ohan NW, Tam Y, Fernando P, Heikkila JJ. 1998a. Characterization of a novel group of basic small heat shock proteins in *Xenopus laevis* A6 kidney epithelial cells. *Biochem. Cell Biol*. 76:665-671.

Ohan NW, Tam Y, Heikkila JJ. 1998b. Heat-shock-induced assembly of Hsp30 family members into high molecular weight aggregates in Xenopus laevis cultured cells. *Comp Biochem Physiol B Biochem Mol Biol*. 119(2): 381-9.

Othumpangat S, Kashon M, Pius J. 2005. Eukaryotic translation initiation factor 4E is a cellular target for toxicity and death due to exposure to cadmium chloride. *The Journal of Biological Chemistry*. 280(26): 25162-25169.

Ovelgönne JH, Souren JE, Wiegant FA, Van Wijk R. 1995. Relationship between cadmium-induced expression of heatshock genes, inhibition of protein synthesis and cell death. *Toxicology*. 99(1-2): 19-30.

Ovsenek N, Heikkila JJ. 1990. DNA sequence-specific binding activity of the heat-shock transcription factor is heat-inducible before the midblastula transition of early *Xenopus* development. *Development*. 100: 427-433.

Palleros DR, Welch WJ, Fink AL. 1991. Interaction of hsp70 with unfolded proteins: effects of temperature and nucleotides on the kinetics of binding. *Proc Natl Acad Sci USA*. 88: 5719-5723.

Pedersen TV, Bjerregaard P. 2000. Cadmium influx and efflux across perfused gills of the shore crab, Carcinus maenas. *Aquat Toxicol*. 48(2-3): 223-231.

Phang D, Joyce EM, Heikkila JJ. 1999. Heat shock-induced acquisition of thermotolerance at the levels of cell survival and translation in *Xenopus*A6 kidney epithelial cells. *Biochem. Cell Biol*. 77: 141-151.

Pirkkala L, Nykanen P, Sistonen L. 2001. Roles of the heat shock transcription factors in regulation of the heat shock response and beyond. *FASEB J*. 15: 1118-1131.

Préville X, Salvemini F, Giraud S, Chaufour S, Paul C, Stepien G, Ursini MV, Arrigo AP. 1999. Mammalian small stress proteins protect against oxidative stress through their ability to increase glucose-6-phosphate dehydrogenase activity and by maintaining optimal cellular detoxifying machinery. *Exp Cell Res*. 247(1): 61-78.

Prozialeck WC, Niewenhuis RJ. 1991a. Cadmium (Cd2+) disrupts Ca(2+)-dependent cell-cell junctions and alters the pattern of E-cadherin immunofluorescence in LLC-PK1 cells. *Biochem Biophys Res Commun*. 181(3): 1118-1124.

Prozialeck WC, Niewenhuis RJ. 1991b. Cadmium (Cd2+) disrupts intercellular junctions and actin filaments in LLC-PK1 cells. *Toxicol Appl Pharmacol*. 107(1): 81-97.

Prozialeck WC, Lamar PC, Lynch SM. 2003. Cadmium alters the localization of N-cadherin, E-cadherin, and beta-catenin in the proximal tubule epithelium.
Toxicol Appl Pharmacol. 189(3): 180-195.

Prozialeck WC, Edwards JR. 2007. Cell adhesion molecules in chemically-induced renal injury. *Pharmacol Ther*. 114(1): 74-93.

Rabindran SK, Giorgi G, Clos J, Wu C. 1991. Molecular cloning and expression of a human heat shock factor, HSF1. *Proc Natl Acad Sci U S A*. 88(16): 6906-1690.

Rafferty KA. 1969. Mass culture of amphibian cells: methods and observations concerning stability of cell type. In *Biology of Amphibian Tumors* (ed. M Mizzel), pp. 52-81. New York, NY, USA: Springer Verlag.

Renkawek K, Stege GJ, Bosman GJ. 1999. Dementia, gliosis and expression of the small heat shock proteins hsp27 and alpha B-crystallin in Parkinson's disease. *Neuroreport*. 10(11): 2273-2276.

Ritossa F 1962 A new puffing pattern induced by temperature shock and DNP in *Drosophila; Experientia.* 18**:** 571–573.

Rodenhiser DI, Jung JH, Atkinson BG. 1986. The synergistic effect of hyperthermia and ethanol on changing gene expression of mouse lymphocytes. *Can J Genet Cytol*. 28(6): 1115-1124.

Rüdiger S, Buchberger A, Bukau B. 1997. Interaction of Hsp70 chaperones with substrates. *Nat Struct Biol*. 4(5): 342-349.

Sambrook J, Russell DW. 2001. Molecular *cloning: A Laboratory* Manual. 3rd Edition. Cold Spring Harbour Laboratory Press. Cold Spring Harbor, NY.

Samelman TR. 2000. Heat shock protein expression is increased in cardiac and skeletal muscles of Fischer 344 rats after endurance training. *Exp Physiol*. 85: 92-102.

Sarge KD, Murphy SP, Morimoto RI. 1993. Activation of heat shock gene transcription by heat shock factor 1 involves oligomerization, acquisition of DNA-binding activity, and nuclear localization and can occur in the absence of stress. *Mol Cell Biol*. 13(3): 1392-1407.

Satyal SH, Chen D, Fox SG, Kramer JM, Morimoto RI. 1998. Negative regulation of the heat shock transcriptional response by HSBP1. *Genes Dev*. 12(13) :1962-1974.

Schlesinger MJ. 1990. Heat shock proteins. *The Journal of Biological Chemistry*. 265(21): 1211-12114.

Schuetz TJ, Gallo GJ, Sheldon L, Tempst P, Kingston RE. 1991. Isolation of a cDNA for HSF2: evidence for two heat shock factor genes in humans. *Proc Natl Acad Sci U S A*. 88(16): 6911-6915.

Shi Y, Mosser DD. Morimoto RI. 1998. Molecular chaperones as HSF1-specific transcriptional repressors. *Genes and Development*. 12: 654-666.

Singh K, Zewge D, Groth-Vasselli B, Farnsworth PN. 1996. A comparison of structural relationships among alpha-crystallin, human Hsp27, gamme-crystallins and beta B2-crystallin. *Int J Biol Macromol*. 19(4): 227-233.

Singh D, Raman B, Ramakrishna T, Rao ChM. 2006. The cataract-causing mutation G98R in human alphaA-crystallin leads to folding defects and loss of chaperone activity.
Mol Vis. 12: 1372-1379.

Smulders RH, de Jong WW. 1997. The hydrophobic probe 4,4'-bis(1-anilino-8-naphthalene sulfonic acid) is specifically photoincorporated into the N-terminal domain of alpha B-crystallin. *FEBS Lett*. 409(1): 101-104.

Sunderman FW Jr, Plowman MC, Hopfer SM. 1992. Teratogenicity of cadmium chloride in the South African frog *Xenopus laevis. IARC Sci Publ*. 118: 249-256.

Tam Y, Heikkila JJ. 1995. Identification of members of the HSP30 small heat shock protein family and characterization of their developmental regulation in heat-shocked *Xenopus laevis* embryos. *Developmental Genetics*. 17: 331-339.

Uenishi R, Gong P, Suzuki K, Koizumi S. 2006. Cross talk of heat shock and heavy metal regulatory pathways. *Biochemical and Biophysical Research Communications*. 341: 1072-1077.

Uriu K, Kaizu K, Qie YL, Ito A, Takagi I, Suzuka K, Inada Y, Hashimoto O, Eto S. 2000. Long-term oral intake of low-dose cadmium exacerbates age-related impairment of renal functional reserve in rats. *Toxicol Appl Pharmacol*. 169(2): 151-158.

Vargas-Roig LM, Gago, FE, Tello O, Aznar JC, Ciocca DR. 1998. Heat shock protein expression and drug resistance in breast cancer patients treated with induction chemotherapy. *Int J Cancer*. 79: 468-475.

Vogiatzis AK, Loumbourdis NS. 1997. Uptake, tissue distribution and depuration of cadmium (Cd) in the frogs *Rana ridibunda*. *Bull. Environ. Contam. Toxicol.* 59: 770–777.

Voellmy R. 2004. On mechanisms that control heat shock transcription factor activity in metazoan cells. *Cell Stress Chaperones.* 9(2): 122-33.

Waisberg M, Pius J, Hale B, Beyersmann D. 2003. Molecular and cellular mechanisms of cadmium carcinogenesis. *Toxicology*. 192: 95-117.

Waalkes MP, Anver MR, Diwan BA. 1999. Chronic toxic and carcinogenic effects of oral cadmium in the Noble (NBL/Cr) rat: induction of neoplastic and proliferative lesions of the adrenal, kidney, prostate, and testes. *J Toxicol Environ Health A.* 58(4): 199-214.

Wang K, Spector A. 2000. Alpha-crystallin prevents irreversible protein denaturation and acts cooperatively with other heat-shock proteins to renature the stabilized partially denatured protein in an ATP-dependent manner. *Eur J. Biochem*. 267(15): 4705-4712.

Wang X, Klevitsky R, Huang W, Glasford J, Li F, Robbins J. 2003. AlphaB-crystallin modulates protein aggregation of abnormal desmin. *Circ Res*. 93(10): 998-1005.

Wätjen W, Beyersmann D. 2004. Cadmium-induced apoptosis in C6 glioma cells: influence of oxidative stress. *Biometals.* 17(1): 65-78.

Weitzel G, Pilatus U, Rensing L. 1985. Similar dose response of heat shock protein synthesis and intracellular pH change in yeast. *Exp Cell Res*. 159: 252-256.

Welch WJ. 1985. Phorbol ester, calcium ionophore, or serum added to quiescent rat embryo fibroblast cells all result in the elevated phosphorylation of two 28,000-dalton mammalian stress proteins. *J Biol Chem*. 260(5) :3058-3062.

Welch WJ, Suhan JP. 1985. Morphological study of the mammalian stress response: characterization of changes in cytoplasmic organelles, cytoskeleton, and nucleoli, and appearance of intranuclear actin filaments in rat fibroblasts after heat-shock treatment. *J Cell Biol.* 101(4): 1198-1211.

Wiegant FA, van Bergen en Henegouwen PM, van Dongen G, Linnemans WA. 1987. Stress-induced thermotolerance of the cytoskeleton of mouse neuroblastoma N2A cells and rat Reuber H35 hepatoma cells. *Cancer Res*. 47(6): 1674-1680.

Wiegant FA, van Rijn J, van Wijk R. 1997. Enhancement of the stress response by minute amounts of cadmium in sensitized Reuber H35 hepatoma cells. *Toxicology*. 116(1-3): 27-37.

Wilhelmus MMM, Otte-Höller I, Wesseling P, de Waal RMW, Boelens WC, Verbeek MM. 2006. Specific association of small heat shock proteins with the pathological hallmarks of Alzheimer's disease brains. *Neuropathology and Applied Neurobiology*. 32: 119-130.

Wistow G. 1985. Domain structure and evolution in alpha-crystallins and small heat-shock proteins. *FEBS Lett.* 181(1): 1-6.

Wu BJ, Kingston RE, Morimoto RI. 1986. Human HSP70 promoter contains at least two distinct regulatory domains. *Proc Natl Acad Sci USA*. 83: 629-633.

Xie J, Shaikh ZA. 2006. Cadmium induces cell cycle arrest in rat kidney epithelial cells in G2/M phase. *Toxicology*. 224(1-2): 56-65.

Yokouchi M, Hiramatsu N, Hayakawa K, Kasai A, Takano Y, Yao J, Kitamura M. 2007. Atypical, bidirectional regulation of cadmium-induced apoptosis via distinct signalling of unfolded protein response. *Cell Death and Differentiation*. 14: 1467-1474.

Yu Z, Magee WE, Spotila JR. 1994. Monoclonal antibody ELISA test indicates that large amounts of constitutive hsp70 are present in salamanders, turtle and fish. *J Therm Biol*. 19: 41-53.

Zimmermann R, Müller L, Wullich B. 2006. Protein transport into the endoplasmic reticulum: mechanisms and pathologies. *Trends Mol Med*. 12(12): 567-573.

Zou J, Guo Y, Guettouche T, Smith DF, Voellmy R. 1998. Repression of heat shock transcription factor HSF1 activation by HSP90 (HSP90 complex) that forms a stress-sensitive complex with HSF1. *Cell*. 94(4): 471-480.